

Functional characterization of white spot syndrome virus-responsive miR-750 in black
tiger shrimp *Penaeus monodon*



A Thesis Submitted in Partial Fulfillment of the Requirements
for the Degree of Master of Science in Biochemistry and Molecular Biology

Department of Biochemistry

Faculty of Science

Chulalongkorn University

Academic Year 2018

Copyright of Chulalongkorn University



จุฬาลงกรณ์มหาวิทยาลัย
CHULALONGKORN UNIVERSITY

ลักษณะสมบัติเชิงหน้าที่ของไมโครอาร์เอ็นเอ-750 ที่ตอบสนองต่อเชื้อไวรัสตัวแดงดวงขาวในกิ้ง
กฤดาำ *Penaeus monodon*



วิทยานิพนธ์นี้เป็นส่วนหนึ่งของการศึกษาตามหลักสูตรปริญญาวิทยาศาสตรมหาบัณฑิต
สาขาวิชาชีวเคมีและชีววิทยาโมเลกุล ภาควิชาชีวเคมี
คณะวิทยาศาสตร์ จุฬาลงกรณ์มหาวิทยาลัย
ปีการศึกษา 2561
ลิขสิทธิ์ของจุฬาลงกรณ์มหาวิทยาลัย

Thesis Title	Functional characterization of white spot syndrome virus-responsive miR-750 in black tiger shrimp <i>Penaeus monodon</i>
By	Miss Nichaphat Kanoksinwuttipong
Field of Study	Biochemistry and Molecular Biology
Thesis Advisor	Associate Professor KUNLAYA SOMBOONWIWAT, Ph.D.

Accepted by the Faculty of Science, Chulalongkorn University in Partial Fulfillment of the Requirement for the Master of Science

..... Dean of the Faculty of Science
(Professor POLKIT SANGVANICH, Ph.D.)

THESIS COMMITTEE

..... Chairman
(Assistant Professor RATH PICHYANGKURA, Ph.D.)

..... Thesis Advisor
(Associate Professor KUNLAYA SOMBOONWIWAT, Ph.D.)

..... Examiner
(Associate Professor SUPAART SIRIKANTARAMAS, Ph.D.)

..... External Examiner
(Associate Professor Chalernporn Ongvarrasopone, Ph.D.)

นิชาพัฒน์ กนกสินวุฒิมิพงค์ : ลักษณะสมบัติเชิงหน้าที่ของไมโครอาร์เอ็นเอ-750 ที่ตอบสนองต่อเชื้อไวรัสตัวแดงดวงขาวในกุ้งกุลาดำ *Penaeus monodon*. (Functional characterization of white spot syndrome virus-responsive miR-750 in black tiger shrimp *Penaeus monodon*) อ.ที่ปรึกษาหลัก : รศ. ดร.กุลยา สมบูรณ์วิวัฒน์

ในกระบวนการ RNA interference (RNAi) มี RNA ขนาดเล็กที่เรียกว่า microRNA (miRNA) ทำหน้าที่ในการควบคุมการแสดงออกของยีนโดยเป็นตัวนำโปรตีนเชิงซ้อน RNA-induced silencing complexes (RISCs) ที่มีโปรตีน Argonaute (Ago) เป็นองค์ประกอบ ไปยัง mRNA เป้าหมาย จากงานวิจัยก่อนหน้านี้พบว่า miR-750 ของกุ้งกุลาดำมีการแสดงเพิ่มขึ้นในกระเพาะอาหารหลังจากติดเชื้อไวรัสตัวแดงดวงขาว (WSSV) โดยในงานวิจัยนี้ใช้เทคนิค 2D Gel Electrophoresis (2-DE) และโปรแกรมคอมพิวเตอร์ในการระบุเป้าหมายของ miRNA จากผลการวิเคราะห์ยีนเป้าหมายด้วยวิธีการคำนวณทางคอมพิวเตอร์ พบว่ายีน ubiquitin-conjugating enzyme E2 Q1 gene (*UbcQ1*) Sarcoplasmic calcium-binding protein (*Scp*) และ Actin1 (*Act1*) น่าจะเป็นยีนเป้าหมายของ miR-750 จากผลการเพิ่มปริมาณ miR-750 ในกุ้งกุลาดำและตรวจสอบการแสดงออกของโปรตีนในกระเพาะอาหารและระบุเป้าหมายของ miR-750 ด้วยเทคนิค 2-DE พบจุดโปรตีน 5 จุดที่มีการแสดงออกลดลงซึ่งสามารถระบุชนิดของโปรตีนได้ 4 ชนิด คือ actin1 (*Act1*) hemocyanin (*Hc*) sarcoplasmic calcium-binding protein (*Scp*) และ tropomyosin (*Tpm*) ในขณะที่จุดโปรตีนที่มีการแสดงออกเพิ่มขึ้นเมื่อเพิ่มปริมาณ miR-750 จำนวน 8 จุดซึ่งสามารถระบุชนิดของโปรตีนได้ 3 ชนิด คือ actin1 (*Act1*) chymotrypsin (*Ctr*) และ hemocyanin (*Hc*) เมื่อวิเคราะห์ระดับการแสดงออกของยีน *Scp* ในกระเพาะอาหารของกุ้งกุลาดำที่ติดเชื้อ WSSV ด้วยเทคนิค qRT-PCR พบว่ายีน *Scp* มีรูปแบบการแสดงออกแบบแปรผันกับ miR-750 จากการยืนยันปฏิสัมพันธ์ระหว่าง miR-750 กับยีนเป้าหมาย *Scp* ด้วยเทคนิค dual luciferase reporter assay พบว่า miR-750 สามารถลด luciferase activities ลงได้ 20% จากผลข้างต้นจึงสรุปได้ว่า *Scp* เป็นยีนเป้าหมายของ miR-750 นอกจากนี้จากพื้นฐานความรู้ที่กลุ่มโปรตีน Ago สามารถจับกับ miRNA ในระหว่างวิถีการผลิต miRNA เกิดเป็น miRNA-RISC complex (miRISC) และจับกับเป้าหมายได้ ดังนั้นกลุ่มโปรตีน Ago จึงมีความสำคัญในการควบคุมการแสดงออกของยีนเป้าหมายของ miRNA เนื่องจากว่ายังไม่มียางานหน้าที่ที่จำเพาะของ Ago ที่เกี่ยวข้องกับวิถีการผลิต miRNA ในการศึกษาวิถีการผลิต miRNA ในกระเพาะอาหารของกุ้งกุลาดำด้วยเทคนิค RNAi พบว่า *PmAgo3* เกี่ยวข้องกับวิถีการผลิต miR-750 นอกจากนี้ยังศึกษาผลของการให้ miR-750 ที่มีปริมาณมากเกินไปกับกุ้งกุลาดำและยับยั้ง miR-750 ต่อจำนวนไวรัส WSSV การแสดงออกของยีน *Scp* และการแสดงออกของยีนที่เกี่ยวข้องกับระบบภูมิคุ้มกันของกุ้งหลังติดเชื้อไวรัส WSSV พบว่าเมื่อมีการเพิ่มปริมาณ miR-750 ยีน *Scp* มีการแสดงออกลดลง ไวรัส WSSV มีจำนวนเพิ่มขึ้นและยีน *Pen5* *PmCasp* และ *PmCaspase* มีการแสดงออกลดลง สรุปได้ว่า miR-750 ที่มีการแสดงออกเพิ่มขึ้นระหว่างการติดเชื้อ WSSV จะจับกับยีน *Scp* ส่งผลให้ยีนเพปไทด์ต้านจุลชีพและยีนในกระบวนการ apoptosis มีการแสดงออกเปลี่ยนแปลงไปโดยมีผลทำให้เกิดการติดเชื้อไวรัส WSSV ในกุ้งมากขึ้น

จุฬาลงกรณ์มหาวิทยาลัย
CHULALONGKORN UNIVERSITY

สาขาวิชา ชีวเคมีและชีววิทยาโมเลกุล
ปีการศึกษา 2561

ลายมือชื่อนิสิต
ลายมือชื่อ อ.ที่ปรึกษาหลัก

5871959723 : MAJOR BIOCHEMISTRY AND MOLECULAR BIOLOGY

KEYWORD: miRNA, White spot syndrome virus, 2-D gel electrophoresis, Sarcoplasmic calcium-binding protein
 Nichaphat Kanoksinwuttipong : Functional characterization of white spot syndrome virus-responsive miR-750
 in black tiger shrimp *Penaeus monodon*. Advisor: Assoc. Prof. KUNLAYA SOMBOONWIWAT, Ph.D.

In the RNA interference (RNAi) process, small RNAs called microRNAs (miRNAs) modulate gene expression post-transcriptionally by acting as guides to direct Argonaute (Ago)-containing RNA-induced silencing complexes (RISCs) to targeted mRNAs. The *Penaeus monodon* miR-750 was previously reported as the highly upregulated miRNA during white spot syndrome virus (WSSV) infection. In this study, the computational program and 2D gel electrophoresis technique were used to identify miR-750 target genes. Bioinformatic analysis suggested that the predicted target mRNAs of miR-750 were ubiquitin-conjugating enzyme E2 Q1 gene (*UbcQ1*), Actin1 (*Act1*) and Sarcoplasmic calcium-binding protein (*Scp*). Furthermore, the alteration of protein expression in the stomach as a result of introducing the miR-750 was investigated by 2-DE technique. The 5 downregulated protein spots upon enhancing of miR-750 mimic were identified as 4 types of protein including actin1 (*Act1*), hemocyanin (*Hc*), sarcoplasmic calcium-binding protein (*Scp*) and tropomyosin (*Tpm*) whereas the 8 upregulated protein spots were identified as 3 types of proteins such as actin1 (*Act1*), chymotrypsin (*Ctr*) and hemocyanin (*Hc*). The gene expression level of only *Scp* determined in WSSV-infected *P. monodon* stomach by qRT-PCR showed negative correlation to miR-750 expression. The dual luciferase reporter assay for miR-750 and *Scp* target sequences showed the reduced luciferase activities about 20%, respectively. From the above results, we could identify the miR-750 target as *Scp*. It is known that miRNA is loaded into the Ago family of proteins during miRNA biogenesis and then the miRNA-RISC complex (miRISC) binds complementarily to the target. Therefore, Ago contributes to the robustness of miRNA-mediated gene regulation. So far, there is no report about Ago function associated with miRNA biogenesis. We showed that *PmAgo3* was involved in miR-750 biogenesis. The effect of introducing miR-750 mimic and miR-750 anti-miRNA oligonucleotide (AMO) into shrimp on the WSSV copy number, *Scp* gene expression and the expression of shrimp immune-related genes in stomach of WSSV-infected *P. monodon* was investigated. Overexpression of miR-750 led to low level of *Scp* gene expression and the significantly high level of WSSV copy number in WSSV-infected shrimp. During WSSV infection, overexpression of miR-750 led to the decrease in *Pen5*, *PmCasp*, and *PmCaspase* gene expression when compared with that of the control WSSV-infected group. Taken together, we can conclude that during WSSV infection, the upregulated miR-750 targets *Scp* led to alteration in expression of antimicrobial peptide and apoptosis genes and promoting viral infection.

Field of Study: Biochemistry and Molecular Biology Student's Signature

Academic Year: 2018 Advisor's Signature

ACKNOWLEDGEMENTS

I would like to express my deepest sincere gratitude to Associate Professor Dr. Kunlaya Somboonwiwat, who is not only the thesis advisor but also a role model for my scientific career, for her kindness, excellent guidance, and valuable suggestions.

My appreciation is also to the thesis committee, Assistant Professor Dr. Rath Pichyangkura, Associate Professor Dr. Supaart Sirikantaramas and Associate Professor Dr. Chalernporn Ongvarrasopone for giving me your precious time on being my thesis defense committee and for their valuable comments and useful suggestions.

It is a pleasure to thank Professor Dr. Anchalee Tassanakajon, Professor Dr. Vichien Rimpanitchayakit and Assistant Professor Dr. Nuchanat Wutipraditkul for their kindness and helpful advice. Additionally, my special thanks are extended to all members of the Center of Excellence for Molecular Biology and Genomics of Shrimp CEMs laboratory for their help and wonderful friendship.

My sincere thank is also expressed to Graduate School, The Chulalongkorn University Graduate Scholarship to commemorate the 72nd Anniversary of His Majesty King Bhumibol Adulyadej and The 90th Anniversary of Chulalongkorn University Fund grant for the scholarship.

Finally, indispensable persons and my gratefulness are my parents and all members in my family for their guidance, understanding, encouragement, endless love, and support along my education.

Nichaphat Kanoksinwuttipong

TABLE OF CONTENTS

	Page
.....	iii
ABSTRACT (THAI).....	iii
.....	iv
ABSTRACT (ENGLISH).....	iv
ACKNOWLEDGEMENTS.....	v
TABLE OF CONTENTS.....	vi
LIST OF TABLES.....	xi
LIST OF FIGURES.....	xii
CHAPTER I.....	1
INTRODUCTION.....	1
1.1 Shrimp aquaculture.....	1
1.2 White spot syndrome virus (WSSV).....	3
1.3 Shrimp immunity.....	4
1.4 RNA interference.....	9
1.4.1 miRNA biogenesis and function.....	10
1.4.2 miRNA target identification.....	13
1.4.2.1 Computational prediction program.....	13
1.4.2.2 2D gel electrophoresis.....	13
1.5 Purpose of the thesis.....	15
CHAPTER II.....	16
MATERIALS AND METHODS.....	16

2.1 Materials.....	16
2.1.1 Equipments	16
2.1.2 Chemicals and Reagents	17
2.1.3 Kits.....	19
2.1.4 Enzymes.....	19
2.1.5 Antibiotics.....	20
2.1.6 Bacterial, yeast and virus strains.....	20
2.1.7 Software.....	20
2.2 General technique for molecular cloning.....	20
2.2.1 Competent cell preparation.....	20
2.2.2 Transformation by heat shock method	21
2.2.3 Colony PCR technique.....	21
2.2.4 Recombinant plasmid extraction.....	21
2.3 Identification of miR-750 target gene.....	22
2.3.1 Target gene prediction using computational program.....	22
2.3.2 Identification of the full-length gene by RACE technique.....	23
2.3.3 2D gel electrophoresis.....	24
2.4 Determination of miRNA and target gene expression	28
2.4.1 Sample preparation.....	28
2.4.2 Quantitative real-time PCR (qRT-PCR) and data analysis.....	30
2.5 Confirmation of interaction between miR-750 and its target gene	32
2.5.1 Construction of the luciferase reporter plasmid.....	32
2.5.2 HEK293-T cell culture	35
2.5.3 Transfection of miR-750 and pmiR-target gene vector	35

2.5.4 Luciferase activity	37
2.6 Study of miR-750 biogenesis using RNAi assay.....	38
2.6.1 Construction of dsRNA expression vector	38
2.6.2 dsRNA production in <i>E. coli</i> HT115	40
2.6.2 Knockdown dsRNA-Ago.....	40
2.7 Study of miR-750 function against WSSV-infected shrimp	41
2.7.1 Overexpression of miR-750 in WSSV-infected shrimp.....	41
2.7.2 Genomic extraction	42
2.7.3 Determination of WSSV copy number	42
2.7.4 Determination of miR-750, target genes and WSSV immune related-gene expression	42
CHAPTER III	45
RESULTS.....	45
3.1 Identification of miR-750 target gene.....	45
3.1.1 Identification of miR-750 target gene by computational analysis	45
3.1.1.1 miRNA target prediction using computational program with the criteria of seed sequence perfect complementary	45
3.1.1.2 Expression analysis of predicted miR-750 target genes.....	48
3.1.1.3 Identification of the full-length UbcQ1.....	49
3.1.1.4 Confirmation of interaction between miR-750 and UbcQ1 by luciferase reporter system.....	51
3.1.1.5 miRNA target prediction using computational program with the criteria that allow 1 seed sequence mismatch	52
3.1.2 Identification of miR-750 target protein by 2-D gel electrophoresis.....	55
3.1.2.1 Optimization of miRNA mimic dosage.....	55

3.1.2.2 Differentially expressed proteins in stomach of mimic miR-750- injected shrimp.....	56
3.1.2.3 Protein spot identification	61
3.1.2.4 RNA hybrid prediction of candidate miR-750 target gene	64
3.1.2.5 Transcriptional analysis of selected differentially expressed genes	66
3.1.2.6 Confirmation of interaction between miR-750 and 4 candidate miR-750 target genes by luciferase reporter system	67
3.1.2.6.1 Construction of the luciferase reporter plasmid	67
3.1.2.6.2 Luciferase activity	69
3.2 Study of miR-750 biogenesis.....	71
3.2.1 Construction of dsRNA expression vector	71
3.2.2 The dsRNA- <i>PmAgo</i> preparation.....	72
3.2.3 Silencing of <i>PmAgo</i> genes using specific dsRNAs	73
3.3 Study of miR-750 function against WSSV-infected shrimp	75
3.3.1 miR-750 overexpression or silencing in WSSV-infected shrimp.....	75
3.3.1 The effect of miR-750 overexpression and suppression on shrimp immune gene expression.....	79
CHAPTER IV	84
DISCUSSION.....	84
CHAPTER IV	94
CONCLUSIONS	94
REFERENCES	96
VITA.....	112

LIST OF TABLES

Table 1 Primers used for the RACE technique.....	24
Table 2 miRNA mimic sequences.....	26
Table 3 The list of primers for analyzation of miR-750 and target genes expression	31
Table 4 The list of primers for cloning miR-750 and target genes into pmiRGLO vector	33
Table 5 The transfection components of miRNA mimic and pmiR-miR-750 target cassette into HEK293-T cells.....	36
Table 6 The list of primers for cloning <i>PmAgo</i> genes into pET-17b vector	39
Table 7 The list of <i>PmAgo</i> genes primers for RT-PCR.....	41
Table 8 The list of primers for determination of immune genes.....	43
Table 9 Predicted target genes using CU-Mir software with 1 mismatch at seed sequence.....	53
Table 10 The differentially expressed protein spots from stomach of <i>P. monodon</i> challenged with miR-750 mimic, miR-750 scramble. miR-750 AMO and miR-750 AMO scramble.....	58
Table 11 The %intensity of differentially expressed protein spots.....	61
Table 12 The selected differentially expressed protein spots from stomach of mimic miR-750-challenged <i>P. monodon</i> resolved by 2-DE and identified by LC-nano ESI- MS/MS.....	63
Table 13 Prediction of miRNA-target-mRNA duplex structure using RNAhybrid software.....	64

LIST OF FIGURES

Figure 1 Main producer countries of <i>Penaeus monodon</i>	2
Figure 2 Top Issues & Challenges in Shrimp Aquaculture of Asia and America.	2
Figure 3 The production of Shrimp Aquaculture in Asia: 2011 – 2018.....	2
Figure 4 WSSV infection in black tiger shrimp (<i>P. monodon</i>)	4
Figure 5 A schematic model of the shrimp immune system	5
Figure 6 Penaeid shrimp Toll and Imd signaling pathways	7
Figure 7 A model of the apoptotic interactions between a shrimp host cell and WSSV	8
Figure 8 The model of miRNA biogenesis and function	11
Figure 9 miRNA target identification CU-Mir software	23
Figure 10 MASCOT MS/MS Ions Search form Matrix Science.....	27
Figure 11 Galaxy software.....	28
Figure 12 The pmirGLO Dual-Luciferase miRNA Target Expression Vector	34
Figure 13 Diagram of pET17b-dsPmAgo constructs and double-stranded RNA product after RNase A digestion.....	39
Figure 14 Biological process Go term distribution of miR-750 predicted target gene form CU-Mir with the perfect complementary at seed sequence criteria.	46
Figure 15 The prediction of <i>P. monodon</i> genes targeted by miR-750. The 3'-UTR of <i>UbcQ1</i> and ORF of <i>VPS53</i> could be targeted by miR-750.....	46
Figure 16 The miRNA/target mRNA duplexes between miR-750 and target genes (A) <i>UbcQ1</i> (B) <i>VPS53</i> using RNAhybrid software or BiBiserv.	47
Figure 17 Expression analysis of the predicted miR-750 target gene.	48
Figure 18 Nucleotide and deduced amino acid sequences of <i>UbcQ1</i> from <i>P. monodon</i> identified by 5' - and 3' -RACE technique.....	51

Figure 19 In vitro miRNA/target interaction analysis of miR-750 and <i>UbcQ1</i>	52
Figure 20 Biological process Go term distribution of miR-750 predicted target genes form CU-Mir with 1 mismatch criteria.	54
Figure 21 Determination of the dosage of miRNA mimic used to overexpress miR-750 in <i>P. monodon</i>	55
Figure 22 Effect of miR-750 on stomach protein expression profile of <i>P. monodon</i> ..	57
Figure 23 qRT-PCR analysis of candidate miR-750 target genes identified by 2-DE.....	66
Figure 24 Colony PCR of recombinant plasmid pmiR_target genes.	68
Figure 25 Verification of luciferase reporter pmiR_target genes constructs.....	69
Figure 26 The interaction of miR-750 and target genes by luciferase reporter assay.	70
Figure 27 The purified PCR products of section A and section B of <i>PmAgo1-4</i> genes.	72
Figure 28 Double-stranded RNA of the <i>PmAgo1-4</i> genes produced by in vivo expression in bacteria.....	72
Figure 29 Knockdown of <i>PmAgo3</i> gene in <i>P. monodon</i> stomach at 24- and 48-h post dsRNA- <i>PmAgo3</i> infection.....	73
Figure 30 The relative gene expression of miR-750 target gene upon <i>PmAgo3</i> silencing in <i>P. monodon</i>	74
Figure 31 The relative miR-750 expression in WSSV challenge-shrimp stomach at 24 and 48 hpi.	76
Figure 32 The influence of miR-750 overexpression or silencing on WSSV copy number.	78
Figure 33 The effect of miR-750 overexpression and suppression in WSSV-infected shrimp on immune-related genes expression.	80

CHAPTER I

INTRODUCTION

1.1 Shrimp aquaculture

Shrimp aquaculture industry, which is the most important seafood product traded internationally, is very important to the Thai economy. The black tiger shrimp (*Penaeus monodon*; *P. monodon*) culture was widespread around the world including Thailand (Figure 1). Thailand's *P. monodon* industry was started in 1975. During the period of 1987–1991, the shrimp farming was widespread intensification and by 1994, 80% of the shrimp farms in Thailand were intensive (Dierberg and Kiattisimkul, 1996).

However, Taiwan's shrimp farming industry collapsed as a result of disease, reduced resistance from overuse of antibiotics, incorrectly processed food, overstocking and the overexploitation of groundwater (Gronski, 2000). This created a niche in the market that Thailand quickly filled, and Thailand became the world's leading shrimp producer (Nils Kautsky and Troell, 2000). However, since 1995 Thailand's yields have been dropping due to the outbreaks of bacterial and viral disease such as *Vibrio parahaemolyticus*, yellow head virus (YHV) covert mortality nodavirus (CMNV), white spot syndrome virus (WSSV) and Laem Singh virus (LSNV) (Mohan et al., 1998; Thitamadee et al., 2016) which extremely important issues in both Asia and America (Figure 2) lead to large economic loss of the shrimp aquaculture industry in Thailand. In 2018, the production of Thailand's shrimp farming was ranked 5th in Asia, after China, Vietnam, Indonesia and India (Figure 3).

Due to the shrimp farming problem from disease outbreak is important, the research of shrimp immunity should be intensively studied to improve the shrimp farming industry in Thailand.



Figure 1 Main producer countries of *Penaeus monodon* (FAO Fishery Statistics, 2006)

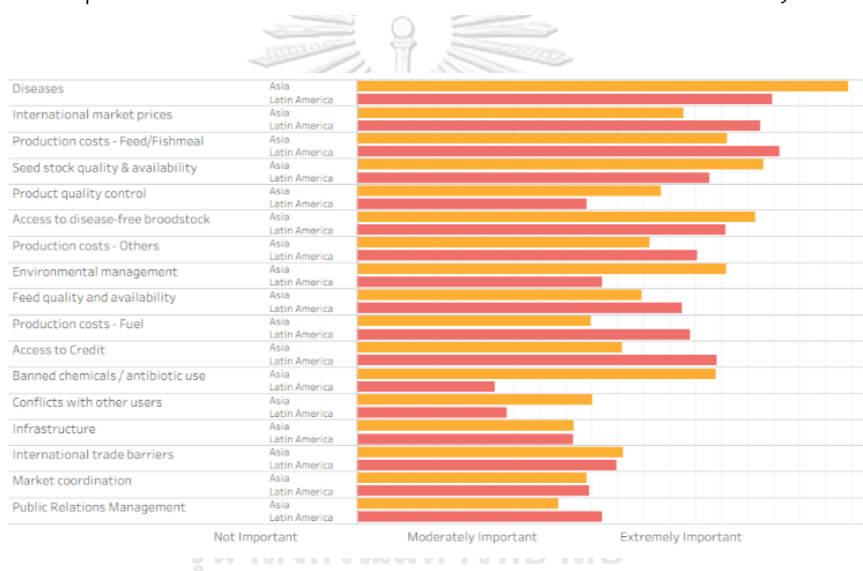


Figure 2 Top Issues & Challenges in Shrimp Aquaculture of Asia and America. (Sources: FAO (2017) and GOAL (2017) for 2016-2019)



Figure 3 The production of Shrimp Aquaculture in Asia: 2011 – 2018. (FAO Fishery Statistics, 2018)

1.2 White spot syndrome virus (WSSV)

White spot syndrome virus (WSSV) is the causative agent of white spot syndrome (WSD) as shown in Figure 4. WSSV is one of the major viral pathogens in shrimp farming industry in Asia (since 1992) and Latin America (since 1999). WSSV is an extremely virulent pathogen and having a potential to infect wide host range among decapod crustaceans such as marine shrimps, freshwater prawns, crabs, lobsters and crayfish (Chou et al., 1995; Durand et al., 1997; Lo et al., 1996). In *P. monodon*, WSSV and YHV caused high mortality (Mohan et al., 1998; Wongteerasupaya et al., 2003).

WSSV was first discovered in Taiwan in 1992. The morphology of WSSV is a rod-shaped enveloped virus, ranging in length from 210-420 nm and in diameter from 70-167 nm (Durand et al., 1997; Tsai et al., 2006). Attachment of the virus to host cells is the most critical step in WSSV infection which involves in the interaction between viral envelope proteins and host factor (Verma et al., 2017; Wu et al., 2005). It contains a very large genome of 305-kb double-stranded circular DNA (van Hulten et al., 2001). The WSSV virion has at least 58 structural proteins. Among them, 35 different proteins have been found in the envelope of the WSSV virion including VP28 and VP26 which are the most abundant proteins (Tang et al., 2007). During WSSV infection, gene expression occurs in three phases including immediate-early, early and late. The 16 ORFs have been identified as immediate-early genes transcribed 1-2 hours post-infection which encode transcription factors such as kinase and ubiquitin E3 ligase. Moreover, genes involved in nucleic acid metabolism such as DNA polymerase, are transcribed 2-6 hours post-infection, corresponding to early genes. At last, several WSSV late genes have been expressed 12 hours post-infection mainly structural proteins (Wang et al., 2004).

WSSV is widely spread to shrimp farms around the world, including Thailand. Infection of penaeid shrimp by WSSV can result in 100% cumulative mortality within 2 – 10 days. To solve this problem, shrimp immune system has been investigated. One of the effective mechanisms involved in shrimp antiviral immunity is RNA interference (Escobedo-Bonilla, 2013)



Figure 4 WSSV infection in black tiger shrimp (*P. monodon*) (Ramos-Carreño et al., 2014)

1.3 Shrimp immunity

The innate immune system of penaeid shrimp is greatly motivated by economical requirements because their culture is limited by the development of infectious disease. The innate defense mechanisms in shrimp are based on both cellular and humoral components of the circulatory system which interplay for detecting and eliminating foreign and potentially harmful microorganisms and parasites (Bachère et al., 2004). The cellular responses are phagocytosis, encapsulation and nodule formation while the humoral involve in the production of soluble components. The humoral responses include the antimicrobial peptides (AMPs), anticoagulant protein, proteinase inhibitor, pattern recognition receptor (PRR), and signal transduction pathway which important part of shrimp immune defense

system as a first line of defense against pathogens (Figure 5) (Jiravanichpaisal et al., 2006; Tassanakajon et al., 2013)

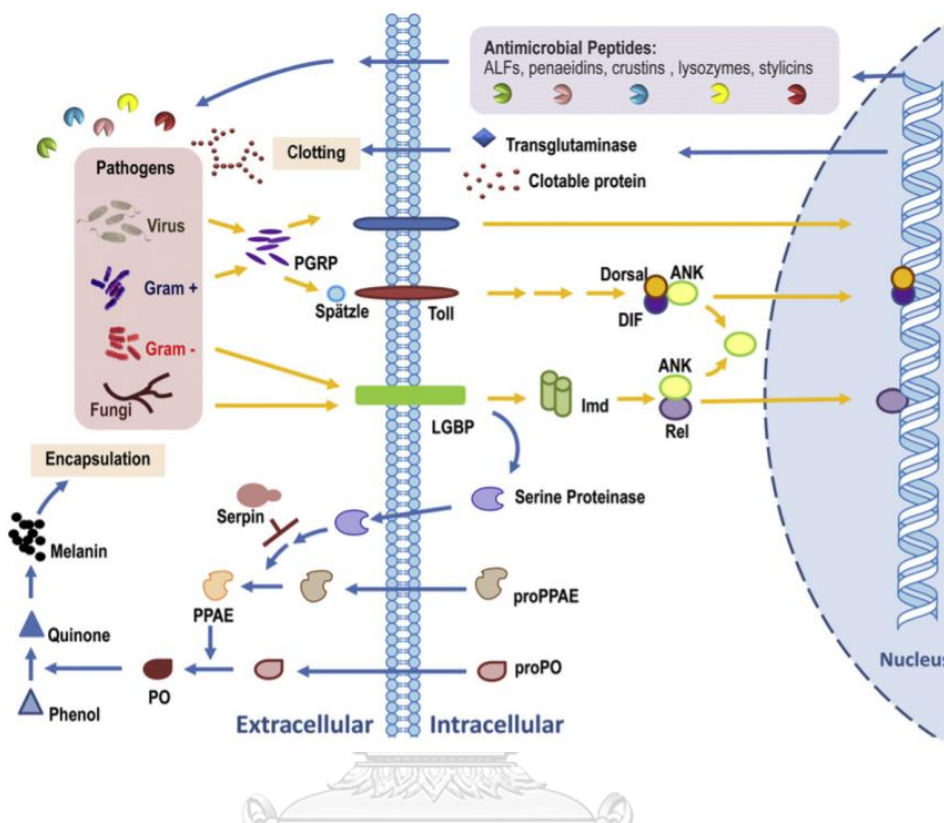


Figure 5 A schematic model of the shrimp immune system (Tassanakajon et al., 2013)

AMPs are gene-encoded peptides which typically small size biomolecules less than 150-200 amino acid residues and have amphipathic structure with cationic or anionic properties (Hancock and Diamond, 2000). AMPs have been discovered in plants, vertebrates, and invertebrates (Tossi and Sandri, 2002). The AMPs play role in shrimp immune defense system by killing/controlling the microorganisms and modulating other immune response which suggesting AMPs as major humoral immune effectors (Hancock and Scott, 2000). A number of families of gene-encoded AMPs have been reported including penaeidins (PEN), antilipopolysaccharide factors

(ALFs), crustins, stylicins and lysozymes (Rolland et al., 2010; Tassanakajon et al., 2013).

After WSSV infection, cell-surface receptors or pattern recognition proteins (PRPs) detect the extracellular signal molecules from the pathogen-associated molecular patterns (PAMPs) or the viral protein antigens. Then, the humoral responses are stimulated resulting in the activation of NF- κ B signaling pathways. The major signaling pathways in innate immune response are Toll and Imd (immune deficiency) pathways which regulate the expression of several AMPs (Naitza and Ligoxygakis, 2004; Tanji and Ip, 2005). Some AMPs and other immune-related genes, such as ALFs and PENS, possess direct antiviral activities, including anti-WSSV activity (Liu et al., 2006; Tharntada et al., 2009b; Woramongkolchai et al., 2011).

Toll and Imd pathways are composed of a different series of PRPs and transcription factor (Figure 6). Toll pathway plays a key role in the response to bacteria, fungi and some viruses. A series of signaling proteins compose of Myeloid differentiation factor 88 (MyD88), Tube, Pelle, and tumor necrosis factor receptor (TNFR)-associated factor 6 (TRAF6), Dorsal and Cactus (Huang et al., 2010; Li et al., 2012). The other pathway is the Imd pathway, this pathway is preferentially triggered by Gram-negative bacteria and some Gram-positive Bacilli. The bacteria and some RNA viruses are recognized by the membrane-bound PRP (Jearaphunt et al., 2015; Wang and Wang, 2013). The important signaling proteins in Imd pathway including Relish, transforming growth factor β -activated kinase 1 (TAK1)/TGF- β activated kinase 1/MAP3K7 binding protein 2 (TAB2) complex and IKK complex (Wang et al., 2013).

In the early stage of WSSV infection, the Toll/IMD-NF- κ B signaling pathways are activated and induce the expression of AMPs and other immune proteins to eliminate the infection (Janeway, 1989; Li and Xiang, 2013). At the same time, the expression of some viral genes can be initiated through NF- κ B activation which may

further activate the expression of other viral genes resulting in the WSSV infection cycle. Then, the activated Toll/IMD-NF- κ B signaling pathway, which can induce AMPs and other immune genes that are harmful to viruses, will be shut down to protective mechanism of the host immune system (Wang et al., 2014)

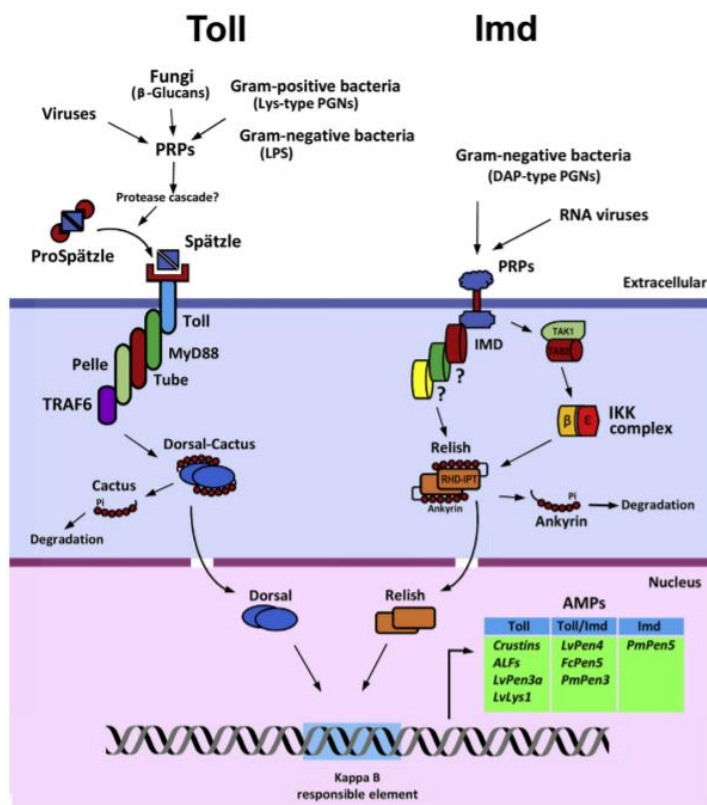


Figure 6 Penaeid shrimp Toll and Imd signaling pathways (Tassanakajon et al., 2018)

Apoptosis is a kind of programmed cell death. This is an important cellular defense mechanism that inhibits viral multiplication and eliminates infected cells in multicellular organisms (Everett and McFadden, 1999; Koyama et al., 2000). According to the apoptotic model (Figure 7), when WSSV infection occurs, the cellular sensors detect the presence of the virus and trigger the expression of the host gene including *PmCasp* (the effector caspase). Together with the mitochondrial stresses and the proapoptotic protein TSL, this causes the apoptosis program to be initiated as shown

in Figure 7A. Apoptosis occurs at the early stage of viral infection. The production of progeny virions will be severely hampered resulting in the limitation of virus spread in the host cell. On the other hand, WSSV has evolved various strategies such as production of anti-apoptosis proteins which binds to and inhibits *PmCasp* to inhibit apoptosis during virus infection as shown in Figure 7B. Thereby until sufficient progeny viruses have been produced, cell viability is prolonged and WSSV can complete its replication cycle (Everett and McFadden, 1999; Hay and Kannourakis, 2002). However, there are some few cases that virus induce apoptosis at the late stage of viral infection in order to facilitate release of progeny virus (Best, 2008; Best and Bloom, 2004).

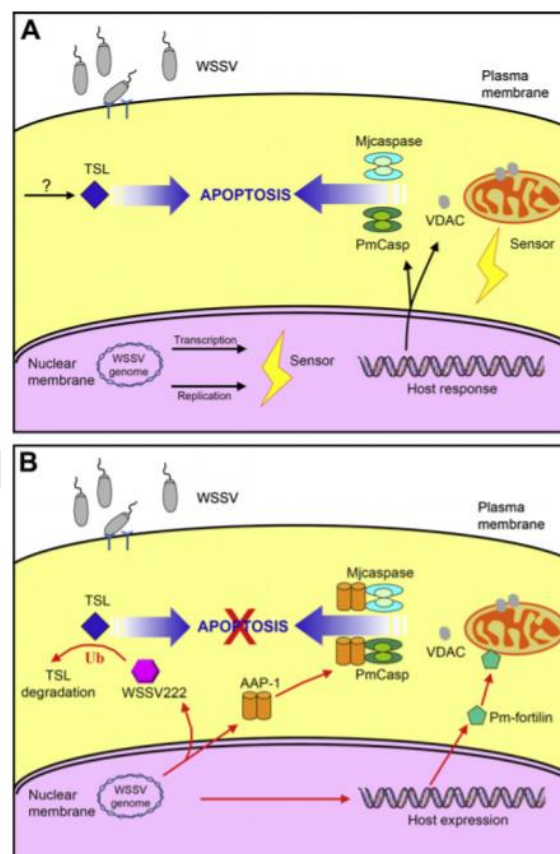


Figure 7 A model of the apoptotic interactions between a shrimp host cell and WSSV (Leu et al., 2013)

1.4 RNA interference

The RNA interference or RNAi pathway is one of the effective mechanisms involved in shrimp antiviral immunity as a key regulator in invertebrate antiviral immunity (Bartel, 2004). They play essential roles in various biological processes, such as development, differentiation and immune response by regulating the target gene expression at the post-transcriptional level (Ding and Voinnet, 2007; Hammond et al., 2001; McManus and Sharp, 2002). They are 3 types of small RNAs that are involved in the RNAi pathway including small interfering RNAs (siRNAs), microRNAs (miRNAs), and p-element induced wimpy testis (PIWI)-interacting RNAs (piRNAs), which correspond to 3 distinct RNA silencing pathways (Ding, 2010; Guo et al., 2018; Skalsky and Cullen, 2010). The siRNAs, miRNAs and piRNAs can guide target mRNA slicing when they are bound to a catalytically active Ago protein and have near-perfect sequences that are complementary to their respective target RNAs (Mussabekova et al., 2017). The siRNA works with Ago proteins in order to destroy cellular or viral ssRNAs in a specific sequence. For miRNA, it mostly functions as translation repressors of mRNA targets with mismatching of target mRNAs outside the seed region and regulate important biological processes (Skalsky and Cullen, 2010). While piRNA protects genomes against transposon mobilization and expression (Iwasaki et al., 2015). The three small RNA pathways including siRNA, miRNA, and piRNA pathways are well defined in *D. melanogaster* (Ding, 2010). It indicates two Dicers and five Agos which required for these pathways. Dicer1 and Dicer2 initiate miRNA and siRNA pathways, respectively, and the piRNA pathway is independent of Dicer. The dsRNA activates the siRNA pathway that involves Dicer2 and Ago2 and plays a major role in antiviral immunity. For miRNA pathway, Dicer1 and Ago1 are implicated and modulates the expression of cellular genes. Three Ago family proteins including PIWI, Aubergine (Aub), and Ago-3 participate in the piRNA pathway which regulates mobile genetic elements in germline cells (Fung et al., 2018).

The important function of RNAi has been studied. Administration of dsRNA or siRNA of viral genes can inhibit virus replication *in vivo* (Kim et al., 2007). While the dsRNA which targeting structural gene, suppresses virus replication in *P. monodon* (Attasart et al., 2011). Moreover, the role of miRNA-regulated DCP1-DCP2 complex which regulate the suppression of RNAi during RNA virus infection was studied. Shrimp miRNA miR-87 inhibited WSSV infection by targeting the host DCP2 gene while viral miRNA WSSV-miR-N46 suppressed the expression of DCP1 to affect virus infection (Sun and Zhang, 2019). Many studies have revealed that RNAi is an important antiviral defense mechanism in shrimp. The application of RNAi in viral-responsive shrimp for functional genomics and to control viral diseases was studied. In the WSSV challenge experiment, *P. monodon* were fed with feed coated bacteria containing VP28-dsRNA, the oral delivery of the WSSV-dsRNA reduced percentages in cumulative mortality and delayed average time to death compared to non-treated group indicating that RNAi has enormous potential in inhibiting the replication of the virus and improve the survival of shrimp. (Sarathi et al., 2008; Thammasonnet al.2015).

1.4.1 miRNA biogenesis and function

MicroRNAs (miRNAs) are a class of small noncoding RNAs with specific size of about 22 nt which function as regulators of gene expression by targeting mRNA for cleavage or translational repression. For miRNA biogenesis, the miRNA gene is transcribed by RNA polymerase II into primary miRNA (pri-miRNAs) (Lee et al., 2004). The pri-miRNAs are cleaved by the RNase III enzyme Drosha. Then, the nucleotide-long stem-loop structures named precursor miRNAs (pre-miRNAs) are exported to the cytoplasm by Exportin-5 (Bohnsack et al., 2004). Next, the loop structure of pre-miRNA is transferred into short dsRNA by the RNase III enzyme Dicer. The mature miRNA named guide stand while the other stand named passenger stand (Hammond et al., 2000). Each miRNA will be unwound and incorporated into argonaute protein

(Ago) of RNA induced silencing complex (RISC), which can further target specific mRNA by complementary binding of seed sequence (2-8 nt from 5' end) to target gene resulting in translational repression or degradation of mRNA transcript which depends on the percentage of complementary between miRNA and target. (Ha and Kim, 2014; Treiber et al., 2012; Waterhouse et al., 2001). In case of complementary of miRNA-mRNA, target mRNA is cleaved and degraded. On the other hand, in case of imperfect complementary of miRNA-mRNA, the translation of target mRNA is repressed (Bushati and Cohen, 2007; Hutvagner and Zamore, 2002) (Figure 8).

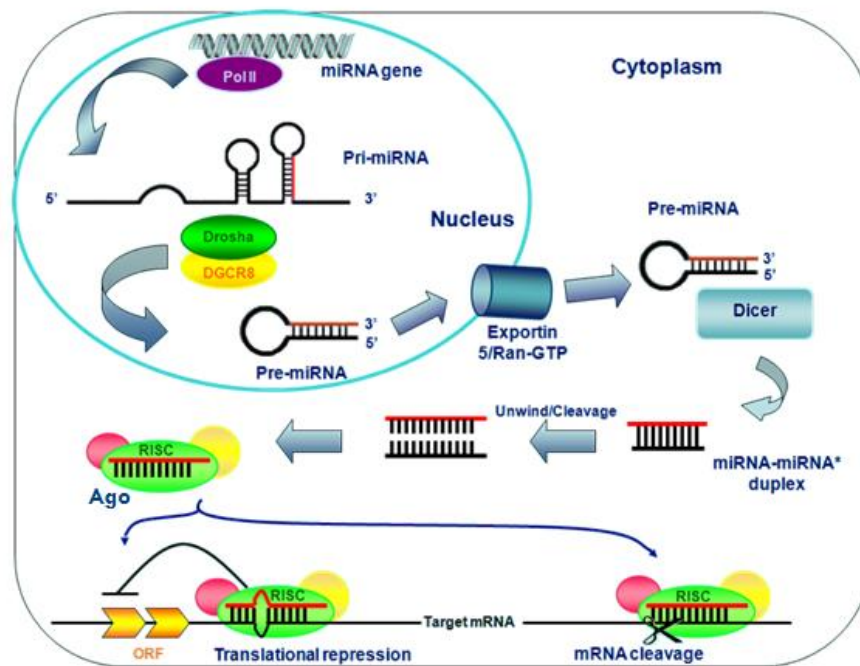


Figure 8 The model of miRNA biogenesis and function (Veronika, 2014)

The increasing evidence has indicated that miRNAs play various roles in the biological processes including cellular differentiation, proliferation, apoptosis (Dostie et al., 2003; Xu et al., 2003), etc. The miRNA in shrimp been studied in 2011. It reveals the 35 miRNAs in hemocyte of *Marsupenaeus japonicus*. Among them, 15 miRNAs homolog to arthropod. Moreover, 22 miRNAs showed differential expression

after WSSV infection (Ruan et al., 2011). Several miRNAs in *M. japonicus* were investigated including miR-7 which targets the 3'UTR of mRNA from wsv477 viral gene involves in virus-host interaction (Huang and Zhang, 2012), miR-965 which targets the viral wsv240 gene resulting in the inhibition of viral infection (Shu et al., 2016) and involving in phenoloxidase enzyme, apoptosis and phagocytosis (Zhu et al., 2016), miR-71 which regulates the autophagy and WSSV infection (He et al., 2017), miR-12 which promotes phagocytosis, apoptosis and antiviral immunity through downregulation of PTEN and BI-1 expression (Shu and Zhang, 2017) and miR-100 which inhibits the progression of WSSV infection by regulation of the superoxide dismutase activity, haemocyte phagocytosis and phenoloxidase activity (Wang and Zhu, 2018). The WSSV-responsive miRNAs in *P. monodon* hemocyte were identified using next-generation sequencing. According to the stem-loop real time RT-PCR, miR-315 and miR-750 were highly differentially expressed (Kaewkascholkul et al., 2016). The miR-315 was functional characterization in WSSV-infected *P. monodon* which attenuates proPO activation via PPAE3 gene suppression and facilitating the WSSV propagation in WSSV-infected shrimp (Jaree et al., 2018).

Previously, the functional characterization of miR-750 was studied in several research. The miR-750 was involved in cell developmental of *Heliothis virescens* nervous system (Chilana et al., 2013), olfactory transduction and regulation of actin cytoskeleton in *Apis mellifera* (Shi et al., 2015). In *M. japonicus*, miR-750 was upregulated in lymphoid organ at 6 and 24 h after WSSV infection (Huang et al., 2012), while miR-750 was downregulated in hemocyte at 24 and 48 h after *Vibrio alginolyticus* infection (Huang et al., 2012; Zhu et al., 2016). It infers that miR-750 play important roles in the *P. monodon* antiviral immunity after pathogen infection.

1.4.2 miRNA target identification

The miRNA target can be investigated in several techniques such as Biotin tagged miRNA, immunoprecipitation, 2D gel electrophoresis (2-DE) and computational prediction program (Thomson et al., 2011). This research focuses on two techniques such as 2-DE and computational prediction program.

1.4.2.1 Computational prediction program

The computational program is used to predict the interaction between miRNAs and target genes. The binding site of seed sequences which are the nucleotide 2 to 8 from 5' end of the miRNA are the recognition sequences on the miRNA target gene. The computational program predicts using the algorithms including the complementarity between miRNAs and target sites, mismatch at seed sequence and the thermal stability of miRNA-mRNA duplex. Several bioinformatic tools have been developed such as Targetscan, miRanda, PicTar and miRInspector (Alexiou et al., 2009). Our previous research, we used CU-Mir software developed by Dr. Kulwadee somboonviwat from King Mongkut's Institute of Technology Ladkrabang to predict miR-750 target gene.

1.4.2.2 2D gel electrophoresis

2D gel electrophoresis (2-DE) is still the most widely used method in quantitative and qualitative proteomic studies and is the technique that can resolve up to 10,000 protein species from large sets of complex protein mixtures (May et al., 2011). It is a combination of the two consecutive techniques including isoelectric focusing and sodium dodecyl sulfate polyacrylamide gel electrophoresis (SDS-PAGE). Traditionally proteins are first separated based on their isoelectric point (pI) value with an IPG strip which consists of an acrylamide gel that contains wide pores and pH gradient, by isoelectric focusing (IEF) with the aid of mobile ampholytes with different (pI) values. After IEF, the IPG strip is placed on top of a SDS-PAGE separate protein by

size (Görg et al., 2004). The limited sample availability is an issue in 2-DE analysis, especially concerning poor protein extraction. However, 2-DE technique has the limitation on resolving low abundant and hydrophobic proteins as well as those with molecular size out of the range of 5–150 kDa or with extreme pH range (< 3.5 and > 10) (May et al., 2011). The result is a gel with proteins spread out on its surface. These proteins can then be detected by a variety of means, but the most commonly used stains are silver and Coomassie Brilliant Blue staining. In quantitative proteomics, the software packages such as Delta2D, ImageMaster, Melanie, PDQuest and Progenesis are widely utilized for gel analysis and the interesting protein spots are marked for further MS analysis (Scherp et al., 2011)

The differentially expressed proteins were investigated using the 2-DE technique to identify the possible miRNA target. Previously, the target of miR-187 in human prostate cancer cells was identified which down-regulated upon miR-187 overexpression. The aldehyde dehydrogenase 1A3 (*ALDH1A3*) was characterized as miR-187 target (Casanova-Salas et al., 2015). Moreover, the targets of miR-663a under ER stress were identified using the 2-DE technique. The 77 differential expressed proteins were analyzed with computational program including Targetscan, miRanda, PicTar and miRInspector, it indicated that *PLOD3* was miR-663a target gene (Amodio et al., 2016). In shrimp, the 2-DE technique was also used to study the differentially expressed proteins in pathogen challenged shrimp (Chaikeeratisak et al., 2012; Somboonwiwat et al., 2012; Wang et al., 2007). However, the identification of miRNA target in shrimp using 2-DE technique has not been reported.

1.5 Purpose of the thesis

The miR-750 have been identified as the highly differentially in WSSV-infected *P. monodon* (Kaewkascholkul et al., 2016), suggesting its important role in shrimp antiviral immunity, However, the WSSV-responsive miR-750 function in *P. monodon* has not been studied. We applied the 2-DE technique and computational analysis to identify the miR-750 target genes. The involvement of Ago protein in miR-750 biogenesis was investigated. Moreover, the expression profiles of the predicted miR-750 target genes in response to WSSV infection in *P. monodon* stomach were analyzed by quantitative real-time PCR (qRT-PCR). The expression of shrimp immune responsive genes and the WSSV copy number were determined in WSSV-infected shrimp challenged with miR-750 mimic and miR-750 AMO in order to investigate the role of miR-750 in shrimp antiviral response.

CHAPTER II

MATERIALS AND METHODS

2.1 Materials

2.1.1 Equipments

-20°C Freezer (Whirlpool)

-80°C Freezer (Thermo Electron Corporation)

15 mL centrifuge tubes (Corning)

24-well cell culture cluster, flat bottom with lid (Corning)

50 mL centrifuge tubes (Corning)

96-Well Microplates White Opaque (Corning)

Autoclave model # MLS-3750 (SANYO E&E Europe (UK Branch) (UK Co.)

Automatic micropipette P10, P20, P100, P200 and P1000 (Gilson Medical Electrical)

C1000™ Thermal Cycler (Bio-Rad)

Centrifuge 5804R (Eppendorf)

Centrifuge Avanti™ J-301 (Beckman Coulter)

T-25 CytoOne® Flask, TC-Treated (SPL life science)

Gel Documentation System (GeneCam FLEX1, Syngene)

Incubator 30°C (Heraeus)

Incubator 37°C (Mettler)

Innova 4080 incubator shaker (New Brunswick Scientific)

Image scanner III (GE Healthcare life sciences)

Immobiline® Drystrip pH 4-7, 13 cm (GE Healthcare life sciences)

Laminar Airflow Biological Safety Cabinets ClassII Model NU-440-400E (NuAire, Inc., USA)

Microcentrifuge tube 0.6 ml and 1.5 ml (Axygen®Scientific, USA)

Minicentrifuge (Costar, USA)

MS 3 vortex mixer (IKA)

NanoDrop 2000 UV-Vis Spectrophotometer (Thermo scientific)

Orbital shaker SO3 (Stuart Scientific, Great Britain)

PCR Mastercycler (Eppendorf AG, Germany)

PCR thin wall microcentrifuge tubes 0.2 ml (Axygen®Scientific, USA)

pH-meter (Mettler Toledo)

Pipette tips 10, 100 and 1000 µl (Axygen®Scientific, USA)

Power supply, Power PAC3000 (Bio-Rad Laboratories, USA)

Refrigerated incubator shaker (New Brunswick Scientific, USA)

SpectraMax M5 Multi-Mode Microplate Reader (Molecular Devices)

Touch mixer Model#232 (Fisher Scientific)

Trans-Blot®SD (Bio-Rad Laboratories)

Transmission electron microscope (Hitachi - Science & Technology – H7650)

Tri-sodium citrate (Sigma)

Water bath (Mettler)

Whatman® 3 MM Chromatography paper (Whatman International Ltd., England)

2.1.2 Chemicals and Reagents

100 mM dATP, dCTP, dGTP and dTTP (Promega)

Absolute alcohol

Acrylamide, C₃H₅NO (Merck)

Agar powder, Bacteriological (Hi-media)

Agarose, low EEO, Molecular Biology Grade (Research Organics)

Amersham™ Hybond™ Blotting Membranes (GE Healthcare life sciences)

Ammonium persulfate, (NH₄)₂S₂O₈ (Bio-Rad)

Boric acid, BH_3O_3 (Merck)

Bromophenol blue (Merck)

CHAPS (OmniPur)

Chloroform, CHCl_3 (Merck)

Coomassie brilliant blue G250 (Fluka)

Diethyl pyrocarbonate (DEPC), $\text{C}_6\text{H}_{10}\text{O}_5$ (Sigma)

Dithiothreitol, DTT (Life technologies)

DMEM (Gibco)

Ethylene diamine tetraacetic acid disodium salt, EDTA (Ajax)

GeneRuler™ 100bp Plus DNA ladder (Thermo scientific)

GeneRuler™ 1kb DNA ladder (Thermo scientific)

Glycerol, $\text{C}_3\text{H}_8\text{O}_3$ (Ajax)

Glycine, USP Grade, $\text{NH}_2\text{CH}_2\text{COOH}$ (Research organics)

HEPES (1M) (Gibco)

IAA (TCI)

IPG buffer pH 4-7 (GE Healthcare life sciences)

Isopropanol, $\text{C}_3\text{H}_7\text{OH}$ (Merck)

Isopropyl- β -D-thiogalactoside (IPTG), $\text{C}_9\text{H}_{18}\text{O}_5\text{S}$ (USBiological)

N, N, N', N'-tetramethylethylenediamine (TEMED) (BDH)

PMSF (OmniPur)

Sodium acetate, CH_3COONa (Carlo Erba)

Sodium chloride, NaCl (Ajax)

Sodium citrate, $\text{Na}_3\text{C}_6\text{H}_5\text{O}_7$ (Carlo Erba)

Sodium dodecyl sulfate, $\text{C}_{12}\text{H}_{25}\text{O}_4\text{SNa}$ (Vivantis)

Sodium hydroxide, NaOH (Merck)

Sodium pyruvate (100 mM) (Gibco)

TEMED ((Thermo scientific)

TriReagent® (Molecular Research Center)

Tris-(hydroxyl methyl)-aminomethane, $\text{NH}_2\text{C}(\text{CH}_2\text{OH})_3$ (Vivantis)

Tryptone type I (HIMEDIA)

Tween™-20 (Fluka)

Urea (Affy Metrix USB)

Yeast extract powder (HIMEDIA)

2.1.3 Kits

2-D Clean-Up kit (GE Healthcare life sciences)

2-D Quant kit (GE Healthcare life sciences)

Dual-luciferase reporter assay system (Promega)

Effectene transfection reagent (Qiagen)

FavorPrep GEL/PCR Purification Kit (Favorgen)

FavorPrep Plasmid DNA Extraction Mini Kit (Favorgen)

Immobiline® Drystrip pH 4-7, 13 cm (GE Healthcare life sciences)

Tissue genomic DNA extraction (Favorgen)

Reverse transcriptase cDNA synthesis kit (Thermo scientific)

2.1.4 Enzymes

0.25% trypsin-EDTA (Gibco)

*Bam*HI (New England Biolabs)

*Hind*III (New England Biolabs)

Luna Universal qPCR Master Mix (New England BioLabs)

Poly-A-polymerase (New England Biolabs)

RiboLock RNase Inhibitor (Thermo scientific)

RNase-free DNaseI (Thermo scientific)

T4 DNA ligase (Thermo scientific)

Taq DNA polymerase (GeneDirex)

SacI-HF (New England Biolabs)

XbaI (New England Biolabs)

XhoI (New England Biolabs)

2.1.5 Antibiotics

Ampicillin (BioBasic)

Penicilin / Strep (Gibco)

2.1.6 Bacterial, yeast and virus strains

Escherichia coli strain XL1-Blue

Escherichia coli strain HT115

White spot syndrome virus (WSSV)

2.1.7 Software

Bio-Rad CFX Manager (Bio-Rad)

GraphPad Prism 6

ImageMaster 2D Platinum 6.0 (GE Healthcare)

SnapGene Viewer

2.2 General technique for molecular cloning

2.2.1 Competent cell preparation

E. coli XL1-blue or HT115 were grown in LB broth at 37 °C and shaking at 250 rpm overnight as a starter culture. The culture was inoculated into LB media (1:100) and grown at 37 °C and shaking at 250 rpm until optical density measured at a wavelength of 600 nm (OD_{600}) reached 0.4. The culture was chilled on ice for 10 min and centrifuge at 6,000 rpm at 4 °C for 5 min. The supernatant was discarded. The cell was washed with 0.5 volumes of ice-cold 10 mM $CaCl_2$. After centrifugation for discard the supernatant, the cell was resuspended in 0.025 volumes of ice-cold 0.1M $CaCl_2$ with 15% glycerol and mixed gently by pipetting. Finally, aliquots of 100 μ l of cell suspension were kept at -80 °C.

2.2.2 Transformation by heat shock method

The competent cell was thawed on ice. The 100 ng/ μ l of plasmid or 5 μ l of ligation mixture was mixed with the competent cell and incubated on ice for 30 min. Heat-shock by placing the mixture in 42 °C water bath for exactly 45 sec. Then, the cell was placed on ice for 1 min. After that, for cells recovery, the cell was grown in 1.5 ml nuclease-free microcentrifuge tube containing 1 ml of LB broth and incubated at 37 °C, 250 rpm for 1 hr. The cell culture was spread on the LB agar plate containing 100 μ g/ml of ampicillin and incubated at 37 °C for 14-16 hr.

2.2.3 Colony PCR technique

Each single colony on the plate was picked by the sterile tip and suspended in 10 μ l of nuclease-free water. For the PCR reaction, the reaction performed by *Taq* DNA polymerase (GeneDirex) which contain 1 μ l of suspended culture as a template, 1.25 μ l of 10x reaction buffer, 0.25 μ l of 10 mM dNTPs, 0.25 μ l of 10 μ M specific forward and reverse primer, and 0.3 U of *Taq* DNA polymerase. The total reaction volume 12.5 μ l was performed using thermal cycling conditions: 1 cycle of initial denaturation at 94 °C for 1 min followed by 34 cycles of 94 °C for 30 sec, 58 °C for 30 sec, 72 °C for 30 sec and final extension at 72 °C for 5 min. Then, the PCR products were analyzed by agarose gel electrophoresis. The cell suspension of positive clone was inoculated into LB broth containing 100 μ g/ml of ampicillin and cultured at 37 °C, 250 rpm for 14-16 hr.

2.2.4 Recombinant plasmid extraction

The cells culture harboring recombinant plasmid were grown in 5 ml LB broth containing appropriate antibiotics at 37°C, 250 rpm for overnight. Centrifuge at 10,000 x g for 1 min at room temperature for harvested cell. The plasmid was extracted using FavorPrep Plasmid DNA Extraction Mini Kit (Favorgen).

2.3 Identification of miR-750 target gene

2.3.1 Target gene prediction using computational program

In order to predict the miR-750 target gene, the CU-Mir software developed by Dr. Kulwadee somboonviwat from King Mongkut's Institute of Technology Ladkrabang was used. Sequences of miR-750 and the expressed sequence tag (EST) from *P. monodon* EST database in fasta format were used as input in the CU-Mir software to analysis the miR-750 target gene(s). This software finds the seed sequence (2-8 nucleotides from the 5'-end) of miRNA with 0 mismatch or 1 mismatch to mRNA. The cut-off of percent complementary was set at 65% which calculated from number of nucleotides that complementary to the target gene per total length of miRNA. The CU-Mir software interface was shown in Figure 9.

Then, the predicted mRNAs were searched homology against NCBI database using BLASTX algorithm to identify the target gene. Moreover, the predicted mRNAs were classified according to their Gene Ontology annotation of biological processes and molecular functions using Blast2GO software. The shrimp immune-related genes were selected for further analysis. Furthermore, the miRNA binding site on the target gene, which was characterized using ORF Finder (<https://www.ncbi.nlm.nih.gov/orffinder/>) and Expasy (<https://web.expasy.org/translate/>), could be on 5'-untranslated region (5'-UTR), open reading frame (ORF) or 3'-untranslated region (3'-UTR). Moreover, The RNAhybrid (<http://bibiserv.techfak.unibielefeld.de/rnahybrid/>) web tool was used to analyze the miRNA target position and miRNA/mRNA duplex spontaneously structure. The FASTA file of miRNA sequence and target gene sequences were used as input in this web tool. The structures with minimum free energy (MFE) less than -20 kcal/mol indicated spontaneous occurrence secondary structure.

The image shows the CU-Mir software interface. At the top, there is a green header with the text 'CU-Mir' and 'MicroRNA Target Identification' on the left, and 'About' on the right. Below the header, there are three main sections:

- MicroRNA SEQUENCES:** A section with the heading 'MicroRNA Sequence in FASTA format' and a text area containing the instruction 'Paste here your MicroRNA sequences in FASTA format'.
- EST SEQUENCES:** A section with the heading 'EST Sequence in FASTA format' and a text area containing the instruction 'Paste here your EST sequences in FASTA format'.
- OPTIONS:** A section containing four input fields: 'Seed Start Position' (with a value of 2), 'Seed End Position' (with a value of 8), '% Cutoff' (with a value of 2), and 'Number of mismatches' (with a dropdown menu showing 3). Below these fields are 'Reset' and 'Submit' buttons.

 At the bottom center, there is a small copyright notice: '© 2012 by kulwadee.co'.

Figure 9 miRNA target identification CU-Mir software

2.3.2 Identification of the full-length gene by RACE technique

Rapid amplification of cDNA ends (RACE) was performed using SMART™ RACE cDNA Amplification Kit (Clontech). The specific primers were designed to obtain the 5'- and 3'-ends of cDNAs (Table 1). The primer pairs of universal primer (UPM) and UbcQ1-5'-R1 or UbcQ1-3'-F1 were used for the first round of 5'- and 3'-RACE PCR. The PCR condition was as follows: denaturation at 94 °C for 2 min; 5 cycles of 94 °C for 30 s, 72 °C for 3 min and 5 cycles of 94 °C for 30 s, 68 °C for 30 s, 72 °C for 3 min followed by 25 cycles of 94 °C for 30 s, 65 °C for 30 s, 68 °C for 3 min and 68 °C for 10 min. And the second round of 5'- and 3'-RACE PCR used primer pairs of nested universal primer (NUP) and UbcQ1-5'-R2 or UbcQ1-3'-F2 for amplification. The PCR profile consisted of 94 °C for 2 min, following by 25 cycles of 94 °C for 30 s, 60 °C for 30 s, 68 °C for 3 min and 10 min at 68 °C. All RACE PCR products were cloned into pGEM® T-Easy vector (Promega) and sequenced by Bioneer service.

Table 1 Primers used for the RACE technique.

Primer	Sequence (5'-3')	Application
UbcQ1-5'-R1	CAACATCCAGTGGGACACTTCCTTAACC	5' RACE
UbcQ1-5'-R2	GAATGACTGTTGTGCCCTCGCCAAACTG	Nest PCR of 5' RACE
UbcQ1-3'-F1	GTGCGAGAAGGGTTTCTGTACAAG	3' RACE
UbcQ1-3'-F2	TTGGATAAGGCCTGAGGGGGTAGATCTG	Nest PCR of 3' RACE
UPM (long)	CTAATACGACTCACTATAGGGCAAGCAGT GGTATCAACGCAGAGT	5' & 3' RACE
UPM (shot)	CTAATACGACTCACTATAGGGC	5' & 3' RACE
NUP	AAGCAGTGGTAACAACGCAGAGT	Nest PCR of 5' & 3' RACE

2.3.3 2D gel electrophoresis

2.3.3.1 Protein preparation and two-dimensional electrophoresis

(2-DE)

To prepare the sample for proteomic analysis, 10 g *P. monodon* were divided into 4 groups including 1.) miR-750 mimic injection 2.) miR-750 scramble mimic injection 3.) miR-750 inhibitor and 4.) miR-750 scramble inhibitor injection. The miR-750 mimic, miR-750 inhibitor and its control which randomly scrambled generating miR-750 scramble mimic and miR-750 scramble inhibitor were purchased from Shanghai GenePharma Co., Ltd., the sequences were shown in Table 2. In order to get the appropriate dosage of miRNA-mimic for the experiment, the miR-750 mimic at difference amount (0, 2 and 4 nmole) was injected into the shrimp followed by the detection of miR-750 expression using quantitative stem-loop real-time PCR (stem-loop qRT-PCR). It was revealed that the more miR-750 mimic injected into shrimp, the more miR-750 expression was detected. Therefore, 4 nmole/shrimp of miRNA mimics were used in this experiment. Three shrimps of each group were injected with 4 nmole of each miRNA mimic or miRNA inhibitor and the scramble control.

After 24 hours post injection, the stomach was collected. The frozen stomach of individual shrimp was ground to fine powder and then thoroughly homogenized in the lysis buffer (8 M urea, 2 M thiourea, 50 mM DTT, 0.2% (v/v) Triton X-100 and 1 mM PMSF). After centrifugation at 12,000 x g at 4 °C for 20 min to collect the supernatant, the total protein of each individual samples were precipitated with three volume of ice-cold acetone: methanol (3:1 (v/v)) overnight at -20 °C. Then, the pellet was collected by centrifugation at 12,000 x g at 4 °C for 20 min and resuspended in rehydration buffer (8 M urea, 2 M thiourea, 4% (w/v) CHAPS and 1 mM PMSF) (Chaikeratisak et al., 2012). To obtain high purity protein, the sample was cleaned using 2-D Clean-Up kit (GE healthcare life sciences). The total protein samples from 3 individual shrimp were pooled in each group. The amount of total protein was quantified using a 2-D Quant kit (GE healthcare life sciences) according to the manufacturer's instruction.

For each sample, 250 µl rehydration buffer containing 1 mg protein supplemented with 1% (w/v) bromophenol blue, 50 mM dithiothreitol (DTT) and 0.5% (v/v) IPG buffer pH 4-7 (PlusOne) was loaded onto immobilized pH gradient (IPG) strip pH 4-7, 13 cm (GE Healthcare life sciences). Each IPG strip was rehydrated overnight at room temperature. First dimension isoelectric focusing electrophoresis (IEF) was subsequently performed using Ettan IPGphor 3 IEF system (GE healthcare life sciences). The condition was as follows: 2 h at 300 V, 2 h at 500 V, 2 h at 1,000 V, 2 h at 4,000 V and finally at 8,000 V to reach 80,000 Vh. Prior to the second dimension, the IEF strips were incubated in reducing solution (6 M urea, 30% glycerol, 2% (w/v) SDS, 50 mM Tris-HCl pH 8.8, 1% bromophenol blue, 1% (w/v) DTT) for 15 min and then incubated in alkylating solution (6 M urea, 30% glycerol, 2% (w/v) SDS, 50 mM Tris-HCl pH 8.8, 1% bromophenol blue, 2.5% (w/v) 2-iodoacetamide (IAA)) for 15 min at room temperature. For the second-dimension separation, the IPG strips

were stacked by 0.5% agarose containing 0.02% bromophenol blue and run in 12.5% SDS-PAGE at constant 20 mA/gel until tracking dye reached the gel bottom. After that, the gels were fixed in a solution containing 40% v/v ethanol and 10% v/v phosphoric acid for 30 min for further stained with Colloidal Coomassie Brilliant Blue G250.

Table 2 miRNA mimic sequences

Primer	Sequence sense (5'-3')	Sequence antisense (5'-3')
miR-750 mimics	CCAGAUCUAACUCUCCAGC	UGGAAGAGUUAGAUCUGGUU
miR-750 inhibitor	GCUGGAAGAGUUAGAUCUGG	
miR-750 scramble mimics	GCAAUCACCCGCUUCAUCU	AUUGAAGCGGGUGAUUGCUU
miR-750 scramble inhibitor	GGACGGGAUGUGACGUUAAU	

2.3.3.2 Gel image analysis

The gels were scanned with Imagescanner III (GE Healthcare life sciences). Then, the ImageMaster 2D Platinum 6.0 software (GE Healthcare life sciences) was used to perform image analysis including detecting protein spot, matching spot, quantifying spot and measuring difference spot intensity of each condition. The individual spot intensity was normalized to the total intensity volume of all spots presented in each gel and subjected to comparative analysis the differences intensity volume of each individual protein spot between the control and challenged group. Only the spots with reproducible differential changes were considered to be differentially expressed proteins.

2.3.3.3 Protein identification

The excised protein spots which were believed differentially expressed were analyzed by LC/ESI-MS/MS (Research instrument center, Khon Kaen University). Peptide ions of interested protein spot obtained from mass spectrometer were identified by MS/MS ion search using MASCOT (http://www.matrixscience.com/cgi/search_form.pl?FORMVER=2&SEARCH=MIS) and *P. monodon* EST database using Galaxy software (<https://usegalaxy.org/>). The screens of MASCOT and Galaxy software were shown in Figure 10 and 11, respectively.

The screenshot shows the MASCOT MS/MS Ions Search form. At the top, there is the Matrix Science logo and a search bar. Below the logo is a navigation menu with links: Home, Mascot database search, Products, Technical support, Training, News, Blog, Newsletter, Contact. The main heading is 'MASCOT MS/MS Ions Search'. The form contains several sections: 'Your name' and 'Email' input fields; 'Search title' input field; 'Database(s)' dropdown menu showing 'contaminants (AA)'; 'Amino acid (AA)' list with options like cRAP, NCBIprot, SwissProt, etc.; 'Enzyme' dropdown menu set to 'Trypsin'; 'Taxonomy' dropdown menu set to 'All entries'; 'Allow up to' dropdown menu set to '1 missed cleavages'; 'Quantitation' dropdown menu set to 'None'; 'Fixed modifications' dropdown menu set to '--- none selected ---'; 'Variable modifications' dropdown menu set to '--- none selected ---'; 'Peptide tol.' input field set to '1.2 Da'; 'MS/MS tol.' input field set to '0.0 Da'; 'Peptide charge' dropdown menu set to '2+'; 'Monoisotopic' radio button set to 'Average'; 'Data file' 'Choose File' button; 'Data format' dropdown menu set to 'Mascot generic'; 'Instrument' dropdown menu set to 'Default'; 'Decoy' checkbox; 'Precursor' input field; 'Error tolerant' checkbox; 'Report top' dropdown menu set to 'AUTO hits'; 'Start Search' button; and 'Reset Form' button.

Figure 10 MASCOT MS/MS Ions Search form Matrix Science. (http://www.matrixscience.com/cgi/search_form.pl?FORMVER=2&SEARCH=MIS)

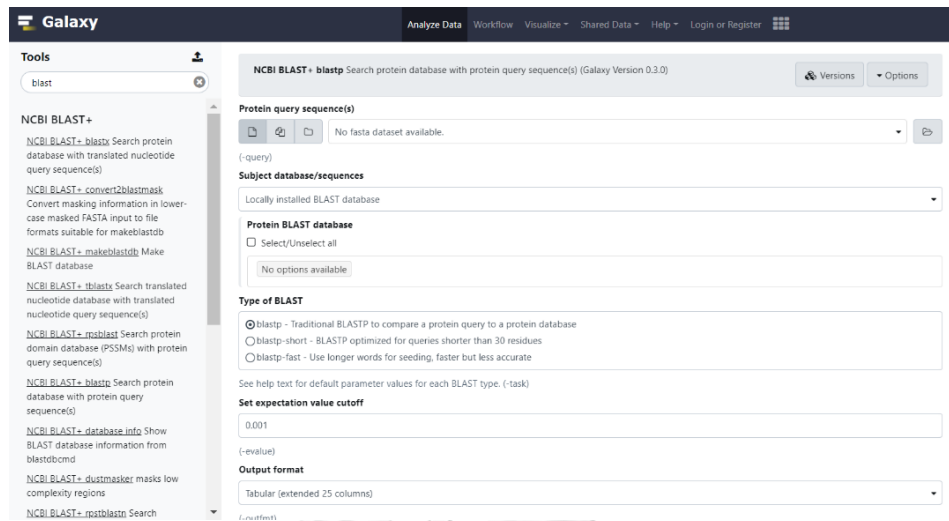


Figure 11 Galaxy software. (<https://usegalaxy.org/>).

2.4 Determination of miRNA and target gene expression

2.4.1 Sample preparation

2.4.1.1 Shrimp culture and virus infection

The healthy black tiger shrimp (*P. monodon*) size 3-5 g and 10-15 g were used in this research. They were raised in tanks filled with seawater at 15 ppt salinity. One ml of WSSV stock was ten-fold serial dilution with 0.85% NaCl. The WSSV solution 50 μ l and 100 μ l with the dosage that causes 100% shrimp death within three days were injected into the third abdominal segment of shrimp 3-5 g and 10-15 g, respectively. The stomach was individually collected at 0, 6, 24 and 48 h post-WSSV infection (hpi) by grinding to fine powder using liquid nitrogen and used as starting material for total RNA extraction.

2.4.1.2 RNA extraction and cDNA synthesis

The stomach fine powder was extracted individually with 500 μ l of TriReagent (Molecular Research Center) and vortexed for 15 sec. Then, 100 μ l of chloroform was

added. The sample was vortexed for 30 sec and centrifuged at 12,000 x g at 4 °C for 15 min. The total RNA in the upper aqueous was precipitated with 2 volume of cold isopropanol. After precipitation at -20 °C for 30 min, the sample was centrifuged at 12,000 x g at 4 °C for 20 min. Then, the pellet of total RNA was washed with 1 ml of 75% EtOH in DEPC-treated water and centrifuged at 12,000 x g at 4 °C for 15 min. The supernatant was completely removed by micropipette. The RNA pellet was air-dried for 5-10 min and resuspend with the appropriate amount of DEPC-treated water. Furthermore, RNA was treated with RNase-free DNaseI (Thermo scientific). The reaction contains 1 µg of total RNA in 1x RNase-free DNaseI reaction buffer and 1 unit of RNase-free DNaseI. The reaction was incubated at 37 °C for 30 min. Then, the solution was purified again using TriReagent (Molecular Research Center) as described above.

2.4.1.3 Quantification and qualification of RNA sample

Total RNA was quantified using a NanoDrop 2000 UV-Vis Spectrophotometer (Thermo scientific). RNA has its absorption maximum at 260 nm. An A₂₆₀ reading of 1.0 is equivalent to 40 µg/ml of RNA and the OD at 260 nm was used to determine the RNA concentration in the solution. The RNA quality was monitored by the ratio A₂₆₀/A₂₈₀ value and by 1.2% agarose gel electrophoresis. Approximately ratio 1.8-2.0 indicates RNA purity.

2.4.1.4 First-strand cDNA synthesis

First stand cDNA synthesis was performed using RevertAid First Strand cDNA Synthesis Kit (Thermo Scientific). In the reverse transcription reaction, 1 µg of total RNA was used as template RNA. The reaction was performed by mixing total RNA with 1 µl of 100 µM Oligo (dT)₁₈ primer, 4 µl of 5X reaction buffer, 1 µl of RiboLock RNase inhibitor (20U/µl), 2 µl of 10 mM dNTP mix and 1 µl of RevertAid M-MuLV

reverse transcriptase (200U/ μ l). Then, the total reaction volume 20 μ l was incubated at 42 °C for 60 min and terminated the reaction at 70 °C for 15 min. The first strand cDNA was stored at -20 °C until used.

Moreover, in order to synthesis specific cDNA for miR-750 and U6, 1 μ g of the total RNA was mixed with 1 μ l of 10 μ M Stem-loop specific miR-750 RT primer or 1 μ l of 10 μ M U6 RT primer, respectively. The sequence was shown in Table 3. Then, 2 μ l of 5X reaction buffer, 0.5 μ l of RiboLock RNase inhibitor (20U/ μ l), 1 μ l of 10 mM dNTP mix and 0.5 μ l of RevertAid M-MuLV reverse transcriptase (200U/ μ l) were added. The total reaction volume 10 μ l was performed as described above.

2.4.2 Quantitative real-time PCR (qRT-PCR) and data analysis

To analyze the transcription expression profiles of miR-750 and the interested genes, qRT-PCR was used. The expression of target gene was normalized to the endogenous reference elongation factor 1- α (EF1- α) while miR-750 expression was normalized to U6 as an internal control. The primer sets are listed in Table 3. The reaction was carried out using 5-fold dilution of cDNA template, 5 μ l of Luna Universal qPCR Master Mix (New England BioLabs) and 2.5 μ l of each 10 μ M primer at a final volume 10 μ l and performed by CFX96 Touch Real-Time PCR detection system (BioRad) with the following conditions: 98 °C for 2 min, followed by 40 cycles of 95 °C for 5 s and 60 °C for 30 s.

Table 3 The list of primers for analyzation of miR-750 and target genes expression

Gene	Primer	Sequence (5'-3')
<i>miR-750</i>	miR-750_F	CGCCTGCCAGATCTAACTCTTCC
	Stem-loop specific	GTCGTATCCAGTGCAGGGTCCCAGGTATTTCGCACTGG
	miR-750_RT	ATACGACGCTGGA
	Universal primer	CCAGTGCAGGGTCCGAGGTA
<i>U6</i>	U6_F	CTCGCTTCGGCAGCACA
	U6_RT_R	AACGCTTCACGAATTTGCGT
<i>UbcQ1</i>	Pm_UbcQ1_F	ATGGCGAGCTCTGGAAACTGCAATTCCATATGA
	Pm_UbcQ1_R	AGCCGCTCGAGAAAAATACAGATCTACCCCCTCAG
<i>VPS53</i>	Pm_VPS53_F	ATGGCGAGCTCCTCTTTGCTGGAGGAGAGAGT
	Pm_VPS53_R	CTCGAGTGCATGAGACAGCTGAGAT
<i>Act1</i>	Pm_Act1_F	ACTGGGACGACATGGAGAAG
	Pm_Act1_R	GTACGACCAGATGCGTACAG
<i>Scp</i>	Pm_Scp_F	CATTGCCAACCAGTTCAAGG
	Pm_Scp_R	GAGCGTACAGGTCCTGGTAG
<i>Tpm</i>	Pm_Tpm_F	CAAAGATCGTCGAGCTTGAG
	Pm_Tpm_R	ACCTCCTTCTGGAGCTTCTG
<i>Ctr</i>	Pm_Ctr_F	GCGTTGTCTGCATTGATGG
	Pm_Ctr_R	CCGGTCTTCTGTTCGATCC
<i>Hc</i>	Pm_HC_F	CCTTCTCCCTAAGGGTAATG
	Pm_HC_R	CTTGGATGTGACCGAAGTTG
<i>EF-1α</i>	EF-F	GGTGCTGGACAAGCTGAAGGC
	EF-R	CGTTCCGGTGATCATGTTCTTGATG

The data was analyzed using Bio-Rad CFX Manager. The obtained C_T cycles were used to calculate the relative expression ratio of the genes from different samples. The Amplification efficiency (E) was calculated from the following formula:

$$E = (\% \text{ Efficiency} * 0.01) + 1$$

Then, the relative expression was calculated by normalizing to the expression level at 0 hpi. U6 and elongation factor 1- α (EF1- α) were used as references for miR-750 and target genes, respectively. The Pfaffl mathematical model to calculating the relative expression ratios was used as the following equation:

$$\text{Relative expression ratios} = \frac{(E_{\text{target}})^{\Delta C_{T,\text{target}} (\text{control-sample})}}{(E_{\text{ref}})^{\Delta C_{T,\text{ref}} (\text{control-sample})}}$$

E_{target} is the real-time PCR efficiency of the miR-750 or interested target genes

E_{ref} is the real-time PCR efficiency of the internal control U6 of EF1- α

$\Delta C_{T,\text{target}}$ is CT value of control – sample of miR-750 or target genes at each time point

$\Delta C_{T,\text{ref}}$ is CT value of control – sample of internal control U6 or EF1- α at each time point

All the data were calculated and expressed as mean \pm standard deviation.

The statistical analysis was analyzed by One-way ANOVA using SPSS software, the level of significance was defined as P -value < 0.05.

2.5 Confirmation of interaction between miR-750 and its target gene

2.5.1 Construction of the luciferase reporter plasmid

2.5.1.1 PCR amplification of miR-750 and target genes

To evaluate the interaction between miR-750 and each target gene, the miR-750 target gene fragment containing miR-750 binding site was cloned into MCS of

pmiRGLO vector which carried the sequence of firefly and *Renilla* luciferase as reporter genes (Figure 12). The PCR reaction was performed on Thermal Cycler (Bio-Rad) to amplify miR-750 and target genes with its primer as shown in Table 4. The reaction contained 5 μ l of 10X reaction buffer, 1 μ l of 10 mM dNTPs, 1 μ l of 10 μ M forward primer, 10 μ M reverse primer, 0.25 μ l *Taq* DNA polymerase (5 U/ μ l) and 1 μ l of cDNA template. The total reaction volume 50 μ l was prepared on a 0.2 ml PCR tube. The PCR condition was 94 $^{\circ}$ C for 1 min followed by 34 cycles of 94 $^{\circ}$ C for 30 sec, 58 $^{\circ}$ C for 30 sec and 72 $^{\circ}$ C for 30 sec. The final extension was 72 $^{\circ}$ C for 5 min followed by 10 $^{\circ}$ C for 10 min. The PCR product was purified by FavorPrep GEL/PCR Purification Kit (Favorgen).

Table 4 The list of primers for cloning miR-750 and target genes into pmiRGLO vector

Primer	Sequence (5'-3')
Pm_UbcQ1_SacI_F	ATGGCGAGCTCTGGAAACTGCAATTCATATGA
Pm_UbcQ1_XhoI_R	AGCCGCTCGAGAAAAATACAGATCTACCCCCTCAG
Pm_Hc_SacI_F	TACGAGCTCCCTTCTCCCTAAGGGTAATG
Pm_Hc_XbaI_R	GGCTCTAGACTTGGATGTGACCGAAGTTG
Pm_Tpm_SacI_F	TACGAGCTCCCGAGACTGGTGAATCAAAG
Pm_Tpm_XbaI_R	CTAGTCTAGACCTTCTGGAGCTTCTGCA
Pm_Ctr_SacI_F	TACGAGCTCCAGCGGTATCTCCAACG
Pm_Ctr_XbaI_R	CTAGTCTAGAGGTTTGACGCCGGTCTT
Pm_Act1_SacI_F	TACGAGCTCTGGGACGACATGGAGAAG
Pm_Act1_XbaI_R	CTGCTCTAGACAATACCAGTGGTACGACCA
Pm_Scp_SacI_F	TACGAGCTCCATTGCCAACCAGTTCAAGG
Pm_Scp_XbaI_R	TAGTCTAGAAGCGTACAGGTCCTGGTAGC

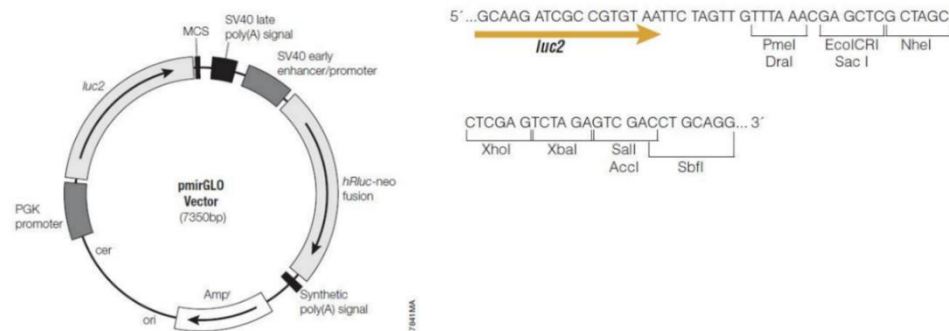


Figure 12 The pmirGLO Dual-Luciferase miRNA Target Expression Vector

2.5.1.1 Double digestion

The pmirGLO vector and purified PCR product of miR-750 target genes were double digested with their specific restriction enzyme. The reactions were performed with 20 units of each restriction enzyme at 37 °C, over-night. After that, the reactions were purified using FavorPrep GEL/PCR Purification Kit (Favorgen) for the further step.

2.5.1.2 Ligation of miR-750 target genes into pmirGLO vector

After purified the digestion reaction, the digested miR-750 target genes were ligated into pmirGLO vector using T4 DNA ligase (Thermo scientific). The amount of insert was calculated following by the formula:

$$\text{Insert (ng)} = \frac{(\text{Vector (ng)} \times \text{insert length (bp)})}{(\text{Vector length (bp)})} \times (\text{Insert: Vector ratio})$$

The reaction was performed as ratio 7:1 of insert and vector in final volume 10 µl including 50 ng vector, appropriated amount of PCR product (insert), 10X reaction buffer, and T4 DNA ligase (Thermo scientific). The reaction was incubated at 22 °C for 4 h.

2.5.1.3 Recombinant plasmid transformation

The ligation mixture was transformed into *E. coli* XL1-Blue competent cell by heat-shock as described in section 2.2.2. The recombinant cell was spread on LB agar plate containing 100 µg/ml of ampicillin. The plated was incubated at 37 °C for 16 h. After that, the colony PCR was performed as described in section 2.2.3. The positive clones were selected for recombinant plasmid extraction. The sequence correctness of recombinant plasmids was confirmed by sequencing.

2.5.2 HEK293-T cell culture

HEK293-T cells were cultured in Dulbecco's modified Eagle's medium (DMEM; Gibco) supplemented with 10% heat-activated fetal bovine serum (FBS), 10 mM HEPES, 1mM sodium pyruvate, 100 U/ml penicillin, and 100 mg/ml streptomycin (all from Gibco) named DMEM complete medium. Cell lines were grown in a humidified atmosphere at 37° C with 5% CO₂. Every 3-4 day, the cell lines were sub-cultured by washing with 2 ml of 1X PBS and trypsinization with 1 ml of 0.25% trypsin-EDTA at 37° C with 5% CO₂ for 2 min. After adding the DMEM complete medium, the cell lines were centrifuged at 1,000 x g for 3 min. Then, the supernatant was removed and the 1 ml of DMEM complete medium was added for resuspend the cell pellet. For subculture, 400 µl of cell suspension was subjected into new T-25 flask containing 5 ml DMEM complete medium for the next passage. Furthermore, 20 µl of cell suspension was a 5-fold dilution with DMEM complete medium and performed 2-fold dilution with 0.4% trypan blue for counting the cell viability and quantity using hemocytometer. The cell which 95% viability is suitable for cell transfection.

2.5.3 Transfection of miR-750 and pmiR-target gene vector

HEK293-T cells were seed on 24-well plate with 8×10^4 cell/350 µl DMEM medium/well and incubated at 37° C with 5% CO₂ for 24 h. HEK293-T cells plated on a 24-well plate were co-transfected with pmiR-target and miRNA mimic. The

transfection reactions were divided into 3 groups including 1) control group; HEK293-T cells were transfected with 200 ng of pmiR-GLO vector containing the target gene named pmiR-miR-750 target cassette, 2) miR-750 mimic group; HEK293-T cells were co-transfected with 10 pmol of miR-750 mimic and 200 ng of pmiR-miR-750 target cassette, and 3) miR-750 scramble group; HEK293-T cells were co-transfected with 10 pmole of miR-750 scramble and 200 ng of pmiR-miR-750 target cassette using effectene transfection reagent (QIAGEN). All the miRNAs were synthesized by Shanghai GenePharma Co., Ltd (Shanghai, China). The procedure of the reactions was performed as show in the Table 5

Table 5 The transfection components of miRNA mimic and pmiR-miR-750 target cassette into HEK293-T cells

Components	Control (μ l)	Add miR-750 mimic (μ l)	Add miR-750 mimic scramble (μ l)
EC buffer	55	55	55
200 ng/ μ l pmiR-miR-750 target cassette	1	1	1
Nuclease-free water	4	3	3
10 pmole/ μ l miR-750 mimic	-	1	-
10 pmole/ μ l miR-750 mimic scramble	-	-	1
Spin down			
Enhancer	1.6	1.6	1.6
Vortex for 1 sec. Spin down and incubate at room temperature for 5 min			
Effectene transfection reagent (QIAGEN)	5	5	5

Table 5 The transfection components of miRNA mimic and pmiR-miR-750 target cassette into HEK293-T cells (continued).

Components	Control (μl)	Add miR-750 mimic (μl)	Add miR-750 mimic scramble (μl)
Vortex for 1 sec. Spin down and incubate at room temperature for 10 min			
DMEM complete medium	350	350	350
Total volume	416.6	416.6	416.6

2.5.4 Luciferase activity

After 48 h of transfection, luciferase activities of firefly and Renilla luciferases were measured by the Dual-Luciferase® reporter assay system (Promega) following the manufacturer's instruction. Briefly, the DMEM complete medium was removed from 24-well plate. Then, HEK293-T cells were wash using 100 μl of 1x Phosphate buffered saline (PBS) and were lysed with 100 μl of 1X Passive Lysis buffer (PLB; Promega). After shaking the 24-well plate for 15 min at room temperature, the lysates were transferred into 1.5 ml tube. Then, PLB lysate was subjected in 96-Well Microplates White Opaque (Corning) with 20 μl/well. Luciferase Assay Substrate in Luciferase Assay Buffer II (LAR II; Promega) were dispensed 50 μl/well. The firefly luciferase activity was measured using SpectraMax M5 Multi-mode Microplate Reader (Molecular Devices) with 1000 ms luminescence integration. The internal control Renilla luciferase activity was measured after adding 50 μl of Stop & Glo Reagent (Promega).

In order to calculate the Luciferase activity, the firefly luciferase activity value (FL) was divided with Renilla luciferase activity value (RL) by the formula:

$$\% \text{ Luciferase activity} = \frac{(FL/RL)_{\text{sample}}}{(FL/RL)_{\text{control}}} \times 100\%$$

2.6 Study of miR-750 biogenesis using RNAi assay

2.6.1 Construction of dsRNA expression vector

In order to express the dsRNA for knockdown *P. monodon* Argonaute gene including *PmAgo1*, *PmAgo2*, *PmAgo3*, and *PmAgo4*, the recombinant plasmid expressing hairpin dsRNA precursor were constructed in pET-17b vector (Figure 13). The DNA fragment size 300-500 bp of *PmAgo1*, *PmAgo2*, *PmAgo3*, and *PmAgo4* were amplified using a specific primer as shown on Table 6. The reaction contained 5 μ l of 10X reaction buffer, 1 μ l of 10 mM dNTPs, 1 μ l of each 10 μ M forward primer and 10 μ M reverse primer, 0.25 μ l *Taq* DNA polymerase (5 U/ μ l) and 10 ng of plasmid pGEM_Ago1, pGEM_Ago2, pGEM_Ago3 or pGEM_Ago4. The reaction was performed using thermal cycling conditions: 1 cycle of initial denaturation at 94 $^{\circ}$ C for 1 min followed by 35 cycles of 94 $^{\circ}$ C for 30 sec, 58 $^{\circ}$ C for 30 sec, 72 $^{\circ}$ C for 30 sec and a final extension at 72 $^{\circ}$ C for 5 min. For cloning the sense stand of *PmAgo* gene into pET-17b vector harboring GFP fragment, the PCR product of sense-*PmAgo* gene and pET-17b_GFP vector were digested with *Xba*I and *Hind*III restriction enzyme. Then, sense-*PmAgo* genes were ligated into pET-17b_GFP in the section before the GFP fragment. The sequence correctness of recombinant plasmids pET-17b_PmAgo_GFP were confirmed by sequencing. These plasmids were used as a template for antisense-*PmAgo* amplification. After that, the PCR product of antisense-*PmAgo* genes and pET-17b_PmAgo_GFP were double digested with *Xho*I and *Bam*HI restriction enzyme. The antisense-*PmAgo* genes were ligated into pET-17b_PmAgo_GFP in the section after the GFP fragment. Therefore, the recombinant plasmids pET-17b harboring the cassette for producing the dsRNA of corresponding gene including sense-*PmAgo*, GFP and antisense-*PmAgo* were named pET17b-dsPmAgo. The diagram was shown in Figure 13. After sequences infallibility were verified, the recombinant plasmids pET17b-dsPmAgo were transformed into *E. coli* HT115 by the heat shock method as described in section 2.2.2. for expressing dsRNA.

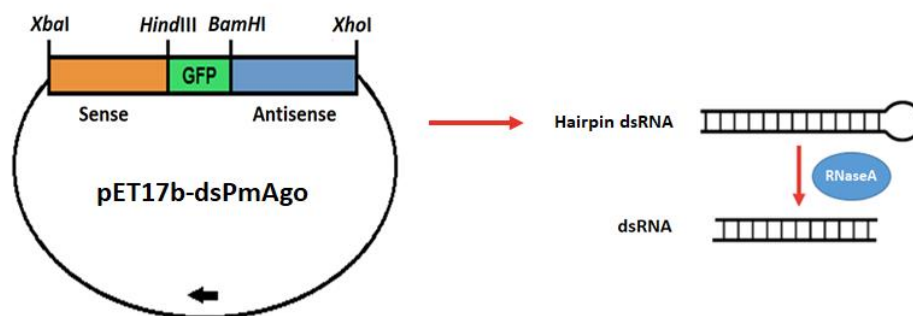


Figure 13 Diagram of pET17b-dsPmAgo constructs and double-stranded RNA product after RNase A digestion

Table 6 The list of primers for cloning *PmAgo* genes into pET-17b vector

Name	Sequence (5'-3')
PmAgo1_F_ds_XbaI	CAGTCTAGAAGGCCAGGCAGTAATAGAG
PmAgo1_R_ds_HindIII	CGGAAGCTTAGGTGCAGATCTAGCTGTTG
PmAgo1_F_ds_XhoI	ACGCTCGAGAGGCCAGGCAGTAATAG
PmAgo1_R_ds_BamHI	CGCGGATCCAGGTGCAGATCTAGCTGTTG
PmAgo2_F_ds_XbaI	TCGTCTAGAGATGGATTCGCTTCGCCTAC
PmAgo2_R_ds_HindIII	CCCAAGCTTCTGCCCTTTCACTATCTTGC
PmAgo2_F_ds_XhoI	ACGCTCGAGGATGGATTCGCTTCGCCTAC
PmAgo2_R_ds_BamHI	GACGGATCCCTGCCCTTTCACTATCTTGC
PmAgo3_F_ds_XbaI	GGCTCTAGAACTTCAGCTCAGGGAATC
PmAgo3_R_ds_HindIII	CGGAAGCTTGGGCAAATAGATTGTCCTG
PmAgo3_F_ds_XhoI	CCGCTCGAGACTTCAGCTCAGGGAATCAG
PmAgo3_R_ds_BamHI	GCGGGATCCGGGCAAATAGATTGTCCTGG
PmAgo4_F_ds_XbaI	GGCTCTAGATGCACCGCTAGACATCAAAC
PmAgo4_R_ds_HindIII	CCCAAGCTTCGTGCGACGACACAATAC
PmAgo4_F_ds_XhoI	CCGCTCGAGTGCACCGCTAGACATCAAAC
PmAgo4_R_ds_BamHI	CGTGGATCCCCTGCGACGACACAATAC

2.6.2 dsRNA production in *E. coli* HT115

A single colony of *E. coli* HT115 containing recombinant plasmid pET17b-dsPmAgo was grown in 5 ml LB media containing 100 µg/ml of Ampicillin and 12.5 µg/ml of Tetracycline at 37°C, 250 rpm for overnight. The bacterial starter was inoculated 1% in 100 ml of 2XYT medium containing 100 µg/ml of ampicillin and 12.5 µg/ml of tetracycline. The culture was incubated at 37°C, 250 rpm until the OD₆₀₀ reached 0.4. Then, the expression of hair-pin dsRNAs were induced with 0.4 mM IPTG for 4 h. After OD₆₀₀ of the culture reached 1 per ml, the bacterial cells were harvest by centrifugation at 6,000 x g for 5 min (Ongvarrasopone et al., 2007)

For the dsRNA purification, ten OD-ml of cell pellet was resuspended in 500 µl of 75% EtOH in DEPC and vortexed cell until the cell homogeneously. After incubated the cells at room temperature for 5 min, the cells pellet was collected by centrifuging at 16,000 x g at 4 °C for 10 min. The EtOH was completely removed and air dried for 15 min. Next, 200 µl of 150 mM NaCl in DEPC was added and incubated at room temperature for 1 h. The supernatant was collected by centrifuging at 16,000 x g at 4 °C for 10 min.

After that, 1 µl of 10 mg/ml RNaseA and 0.5 volume of 7.5 M LiCl₂ containing 50 mM EDTA in DEPC were added and incubated at 37 °C for 30 min in order to remove the RNA of bacterial host and single-stranded RNA of the GFP loop. To access the highest purity of dsRNA, 500 µl of TRIZOL reagent was used and following the protocol of RNA extraction as described above in section 2.4.2.1

2.6.2 Knockdown dsRNA-Ago

To suppress *PmAgo* genes, 10 g shrimp was challenged with specific dsRNA. The difference dosages of dsRNA including 10 µg/g shrimp, 15 µg/g shrimp and 20 µg/g shrimp were used in order to verify the appropriate amount for dsRNA suppression. For suppressing of *PmAgo3*, 15 µg/ g shrimp of dsRNA-*PmAgo3* was used.

After 24 and 48 post injection, the shrimp stomach were collected following with total RNA extraction. The RT-PCR technique was used to validate *PmAgo3* gene suppression. The primers for RT-PCR amplification were shown in Table 7

Table 7 The list of *PmAgo* genes primers for RT-PCR

Name	Sequence (5'-3')	Length (bp)
Pm_Ago1_F	GGTAGAAATCCGCGTGTG	18
Pm_Ago1_R	CGGTGAATGTGCTCTTCAG	19
Pm_Ago2_F	ACTCCACCTCCAGGAAATG	19
Pm_Ago2_R	ACCACGCCTACATCTCTG	18
Pm_Ago3_F	GGTGAAGGATTTCCCACT	19
Pm_Ago3_R	CACTGGGGAGTGAGTTGCTT	20
Pm_Ago4_F	TGCCAGCCTACAGTTAGATGTG	22
Pm_Ago4_R	TTTCTAGAGCTCCTTGCCATGTA	22

2.7 Study of miR-750 function against WSSV-infected shrimp

2.7.1 Overexpression of miR-750 in WSSV-infected shrimp

In this experiment, 5 g *P. monodon* were divided into 5 groups including 1) WSSV-infected shrimp, 2) miR-750 mimic in WSSV-infected shrimp, 3) miR-750 inhibitor in WSSV-infected shrimp, 4) miR-750 scramble mimic WSSV-infected shrimp, 5) miR-750 scramble inhibitor WSSV-infected shrimp. After shrimp were injected with 2 nmole of mimic miRNA for 2 h, then shrimp were infected with 50 μ l WSSV solution for each shrimp at 10^8 copies with the dosage that causes 100% shrimp death within three days by intramuscular injection. After 24 h WSSV injection, shrimp stomach was collected. The total RNA was extracted using TriZol reagent and cDNA synthesis was synthesized using RevertAid First Strand cDNA Synthesis Kit (Thermo

Scientific). Moreover, qRT-PCR was performed to determine miR-750 and target gene expression with specific primer as described in section 2.4.2.

2.7.2 Genomic extraction

In order to quantify the WSSV copy number in WSSV-infected shrimp, the genomic extraction of gill was performed using FavorPrep Tissue Genomic DNA Extraction Mini Kit. Package instruction was modified by elution with 30 μ l of pre-heated elution buffer. The individual extracted sample was kept at 4 °C until use. Total DNA was estimated using a NanoDrop 2000 UV-Vis Spectrophotometer (Thermo scientific). The quality of total DNA was examined using 1.2% agarose gel electrophoresis with 100 ng DNA sample.

2.7.3 Determination of WSSV copy number

To determine the WSSV copy number, qRT-PCR was performed. DNA samples 15 ng were analyzed, consisting of 5 μ l of Luna Universal qPCR Master Mix (New England BioLabs), 2.5 μ l of each 10 μ M VP28-140Fw (AGGTGTGGAACAACACATCAAG) and 10 μ M VP28-140Rv primer (TGCCAACTTCATCCTCATCA) for total volume of 10 μ l. Amplification of sample reactions was done at 98 °C for 2 min, followed by 40 cycles of 95 °C for 5 s and 60 °C for 30 s. The plasmid containing the WSSV VP28 gene was used in purpose to generate the standard curve for WSSV copy number determination. (Jaree et al., 2018)

2.7.4 Determination of miR-750, target genes and WSSV immune related-gene expression

After shrimp were challenged with mimic miRNA and WSSV, the effect on the expression of 13 immune genes: *ALFPm3*, *ALFPm6*, *SWDPm2*, *Penaeidin5* (PEN5), *PmKunitz*, *PmCaspase*, *PmCasp*, *PmCactus*, *PmDorsal*, *PmMyD88*, *PmRelish*, *PmIKK β* and *PmIKK ϵ* was investigated using qRT-PCR with the primers as shown in Table 8.

Meanwhile, miR-750 and targets gene expression were also investigated as described in section 2.4.2.

Table 8 The list of primers for determination of immune genes

Gene	Primer	Sequence (5'-3')
<i>ALFPm3</i>	<i>ALFPm3_F</i>	CCCACAGTGCCAGGCTCAA
	<i>ALFPm3_R</i>	TGCTGGCTTCTCCTCTGATG
<i>ALFPm6</i>	<i>ALFPm6_F</i>	ATGCTACGGAATTCCTCCT
	<i>ALFPm6_R</i>	ATCCTTGCAACGCATAGACC
<i>SWDPm2</i>	<i>SWDPm2_F</i>	CGGCATCATCACCACGTGCGAG
	<i>SWDPm2_R</i>	TCAGTAACCTTTCCAGGGAGAC
Penaeidin5	<i>PmPEN5_F</i>	ATCCCGACCTATTAGTACTC
	<i>PmPEN5_R</i>	TTATCCTTTCAATGCAGAACAA
<i>PmKunitz</i>	<i>PmKunitz_F</i>	GAGTACCATGGGACATCATCATCAT CATCATCACCTACTCCGCCCACTGGGAGA
	<i>PmKunitz_R</i>	CAGATGGATCCTCATCGGCCGCAGAGAAACC
<i>PmCaspase</i>	<i>Pmcaspase_F</i>	CGTGGTTCATTAGTCGCTG
	<i>Pmcaspase_R</i>	AACCTTTCGCATCAGGGTTG
<i>PmCasp</i>	<i>PmcasP_F</i>	TAAACTTCACGGCTGAACGG
	<i>PmcasP_R</i>	TCAGCATGGATGGGAATCAC
<i>PmCactus</i>	<i>Pmcactus_F</i>	AAGACACCGAACGATGGAAG
	<i>Pmcactus_R</i>	TGGGGGACTCGTTCTTTATG
<i>PmDorsal</i>	<i>PmDorsal_F</i>	TCACTGTTGACCCACCTTAC
	<i>PmDorsal_R</i>	GGAAAGGGTCCACTCTAATC
<i>PmMyD88</i>	<i>PmMyD88_F</i>	GTGCACCAGAGTCATTGTAG
	<i>PmMyD88_R</i>	GGGAGTGGAGAACTTATC

Table 8 The list of primers for determination of immune genes (continued)

Gene	Primer	Sequence (5'-3')
<i>PmRelish</i>	PmRelish_F	TCTCCAGGTGAGCACTCAGTTG
	PmRelish_R	GCTGTAGCTGTTGCTGTTGTTGAG
<i>PmIKKβ</i>	PmIKK β _F	CTGAGGGCATGACGCGACCAC
	PmIKK β _R	GCCTGCTCATCATAGTAGTCGAG
<i>PmIKKϵ</i>	PmIKK ϵ _F	ACCGTCTCGAGAAAAGGGTCCTA
	PmIKK ϵ _R	CGGATCGTCCAGAATGTTGAAGAG



CHAPTER III

RESULTS

3.1 Identification of miR-750 target gene

The regulatory role of miRNA on gene expression at either the post-transcriptional or translational level depends on its ability to bind to the target mRNA. According to the stem-loop real time RT-PCR analysis, miR-750 expression was significantly decreased suggesting its important role or involvement in shrimp immunity against WSSV infection in *P. monodon* (Kaewkascholkul et al., 2016). Therefore, identification of miR-750 target genes might provide the important clue for miR-750 function. The technique used to investigate the target of miR-750 are computational analysis and 2-D gel electrophoresis.

3.1.1 Identification of miR-750 target gene by computational analysis

3.1.1.1 miRNA target prediction using computational program with the criteria of seed sequence perfect complementary

The in-house software named CU-Mir for miRNA target prediction was used to analyze sequences of miR-750 and EST *P. monodon* database with the criteria perfect complementary at the seed sequence (complementary sequence). This program identified 140 possible target mRNAs of miR-750. The predicted target genes were annotated by searching against NCBI database using BLASTX algorithm. Then, the Gene Ontology annotation of biological processes using Blast2GO software was performed in attempt to classify the predicted mRNAs. The top twenty results of GO distribution by level 2 was classified into 8 biological process groups as shown on Figure 14.

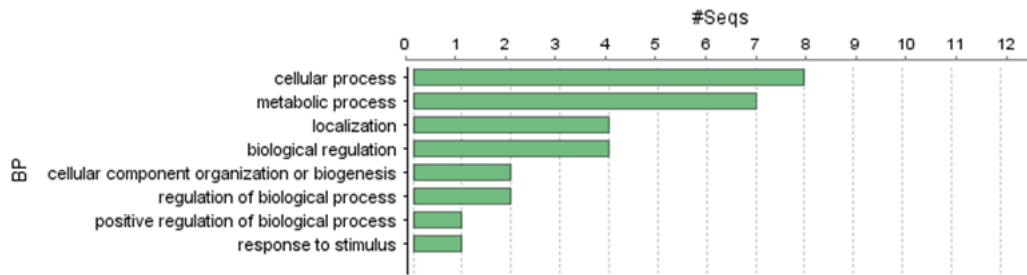


Figure 14 Biological process Go term distribution of miR-750 predicted target gene form CU-Mir with the perfect complementary at seed sequence criteria.

Of those, the interesting target genes which are related to shrimp immunity were chosen. They were Ubiquitin-conjugating enzyme E2 Q1 gene (*UbcQ1*) and Vacuolar protein sorting-associated protein 53 gene (*VPS53*) which are involved in proteolysis and autophagy, respectively. According to the prediction, the seed region (2-8 nt) of miR-750 located on the 3'-UTR and coding sequence of *UbcQ1* and *VPS53*, respectively (Figure 15).

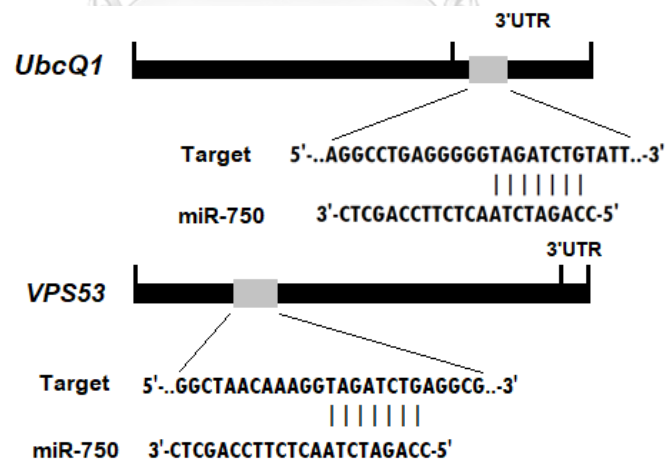


Figure 15 The prediction of *P. monodon* genes targeted by miR-750. The 3'-UTR of *UbcQ1* and ORF of *VPS53* could be targeted by miR-750.

Moreover, RNAhybrid software or BiBiserv (<http://bibiserv.techfak.unibielefeld.de/rnahybrid>) was used to confirm prediction results. The miRNA/target mRNA duplexes which occur spontaneously with low MFE (approximately < -15 kcal/mol) indicating the possibility of miRNA/mRNA interaction were chosen for further study. The secondary structure of miR-750 and predicted target genes are shown in Figure 16. The result show that the seed region of miR-750 was perfectly complementary to the target sequence of *UbcQ1* and *VPS53* with the MFE about -26.2 kcal/mol and -20.5 kcal/mol, respectively.

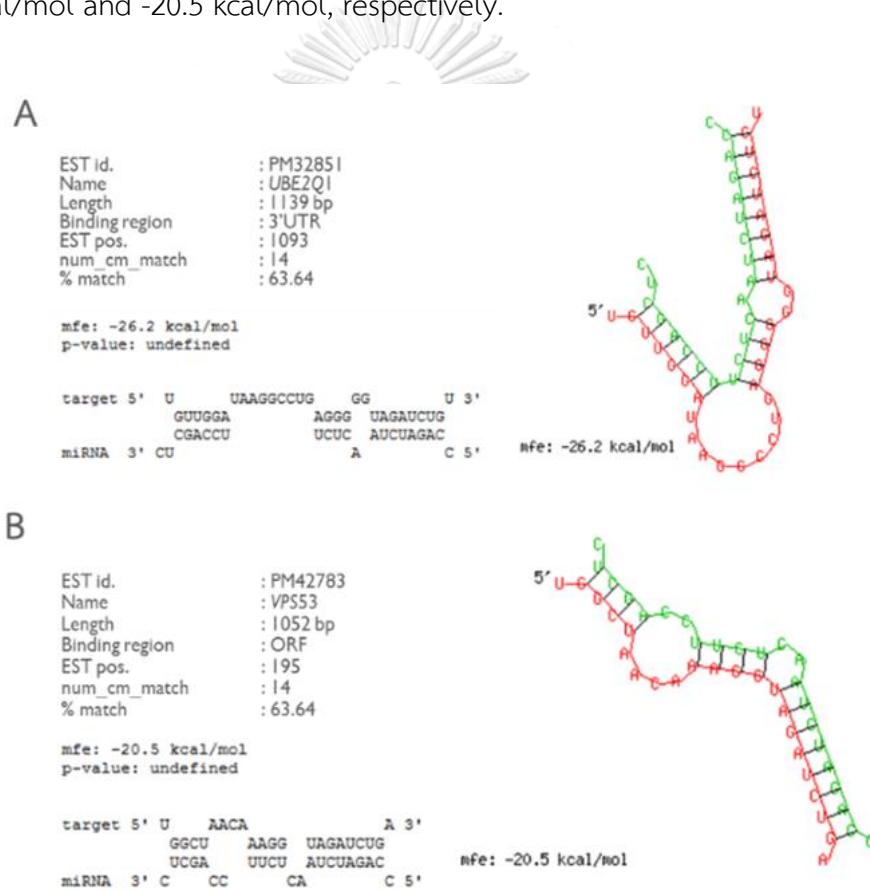


Figure 16 The miRNA/target mRNA duplexes between miR-750 and target genes (A) *UbcQ1* (B) *VPS53* using RNAhybrid software or BiBiserv.

3.1.1.2 Expression analysis of predicted miR-750 target genes

To investigate the correlation in expression of miR-750 and its target genes, *UbcQ1* and *VPS53*, in stomach of WSSV-infected shrimp, the quantitative real-time PCR (qRT-PCR) analysis was performed. The relative expression of miR-750 and target genes including *UbcQ1* and *VPS53* were determined in WSSV-infected *P. monodon* stomach at 0, 6, 24, and 48 hpi, using U6 and elongation factor-1 α (EF-1 α) as internal controls, respectively. The result indicated that the expression of miR-750 was up-regulated at 24 hpi and down-regulated at 6 and 48 hpi (Figure 17 A). Furthermore, *UbcQ1* was down-regulated at 24 hpi and up-regulated at 48 hpi while the expression of *VPS53* was down-regulated at 6, 24 and 48 hpi (Figure 17 B and C). According to the expression pattern of miR-750 and *UbcQ1*, they show the negative correlation at 24 and 48 hpi implying that *UbcQ1* might be the target gene of miR-750.

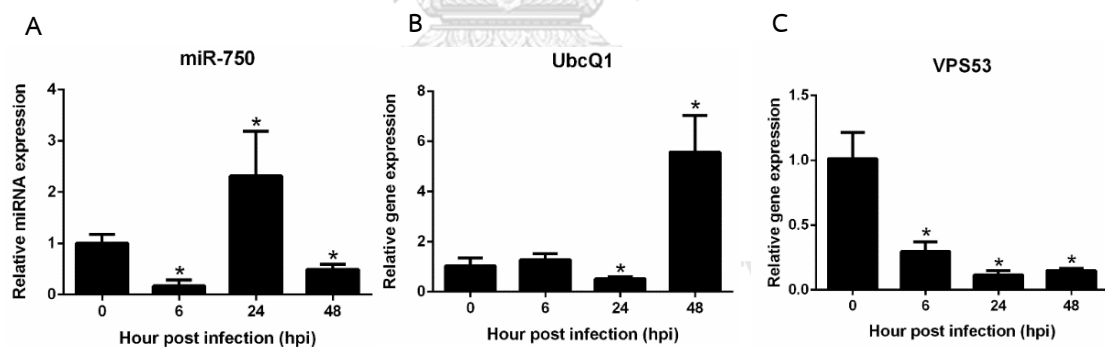


Figure 17 Expression analysis of the predicted miR-750 target gene. The expression analysis of miR-750 (A) and its target genes including *UbcQ1* (B) and *VPS53* (C) in 10 g WSSV-infected *P. monodon* stomach at different time point using the qRT-PCR technique. The * indicates the significant difference at $P < 0.05$.

3.1.1.3 Identification of the full-length *UbcQ1*

Moreover, the function of enzyme E2 was studied and found that it could reduce the mortality of shrimp infected with WSSV and inhibit replication of WSSV (Chen, et al., 2011) implying important role of *UbcQ1* in shrimp immunity against WSSV infection.

According to the sequence of *UbcQ1* (EST P32851) from EST *P. monodon* database, only the partial sequence of *UbcQ1* was obtained. It has 1,139 bp of ORF and 3'-UTR. This partial sequence contains 96 amino acid with 100% identity to Ubiquitin-conjugating enzyme E2 Q2 [*Daphnia magna*] accession number KZS01471.1. In order to obtain the full-length gene of *UbcQ1*, the RACE technique was performed. The result showed that the ORF of *UbcQ1* has 1137 bp encoding 378 amino acid and miR-750 binding position is on 3'-UTR. (Figure 18)

A

```

aagcagtggtatcaacgcagagtacatgggggcagtcgccatcttctcgtcggaagaa 61
K Q W Y Q R R V H G G S R H F L V G K E
ggagagagagacgactcgcgctgagctgtcatctctgctgtgtatcttctcgcagttctt 121
G E R D D S R - A V I S A V Y F L A V L
ccgcaattgattccatgccaggaataacggcgccattgaaattatcATGGCGTGTGTTGAC 181
P Q L I P C Q E - R R I E I I M A C L N
ACCCTCAGCAGGAAATACGGGTACTGGAGAACGGGTTCCAAAACAGACGAGCTGTTC 241
T L K Q E I R V L E N A F P K T D E L F
CAAGTGGTGGCGCCAGTGTGACGAACTGACCTGCCGATTTATTTCCAAAACGAACAG 301
Q V V A A S V D E L T C R F I S K T N K
AAATATGACATTACGCCAATATCACAGAGACGTACCCACACTCCCCTCCAGTCTGGTTT 361
K Y D I H A N I T E T Y P H S P P V W F
GCAGAGACTGAGGACACTAACGTTACTAATGCCATTGAACGGCTCAGCAACACCAACGGC 421
A E T E D T N V T N A I E R L S N T N G
AGAGATAATCATGTGTTACAGCAGGTGAAGCTCCTTCTGCGTGAATTGTGTGAGCAGTAT 481
R D N H V L Q Q V K L L L R E L C A A Y
GGGATGGAGGAACACCTGACCTAGAGGACAGACTAGACCTTGTCTGTACCTCAGTCT 541
G M E E P P D L E D R L D L V S V P Q V
ATTAATGGGAATGACAGTATTGACCATCATGAAGAATATGAAGATTCTGAGATGGAAGAG 601
I N G N D S I D H H E E Y E D S E M E E
GAGGAGGAAGACATGGAGGAGCATTCCACTTGGAGATGGAGGACAACCTCCCTCCCAT 661
E E E D M E E D I H L E M E D N S S S H
GCAGCCCAAAAGATGAAGGCTGACCCAGGTAATTTGGCCACGTTGGACCGGCTGAAG 721
A A Q K D E G I D P G N L A T L D R L K
GCCAACCAGCGGCAAGATTACCTTAGGGGATCCATTTCTGGTAGTGTGCAGGCCACAGAT 781
A N Q R Q D Y L R G S I S G S V Q A T D
CGCCTCATGAAGGAGCTCAGGGATATATACCGCTCAGATAGCTTCAAAAAGAGGATATAC 841
R L M K E L R D I Y R S D S F K K G V Y
AGTGTGGAGTTAGTAATGACAGTCTTTATGAATGGAATGTCAAACCTTCTGATAGTGGAC 901
S V E L V N D S L Y E W N V K L L I V D
TCTGATTCAACACTCCACAATGACCTGGTGTCTGCTCAAGGAGAGGAGGGAACAGACCAC 961
S D S P L H N D L V L L K E K E G T D H
ATACTATCAACTTCCATTTAAGGAGATGTACCCCTTTGAGCCTCCATTGTGGCGGTT 1021
I L F N F H F K E M Y P F E P P F V R V
GTTTCATCCGGTATTAGTGGGGGCTACGTGCTGGTGGTGGTGGCCATTTGTATGGAGCTT 1081
V H P V I S G G Y V L V G G A I C M E L
CTCACCAAGCAGGGATGGAGTTCAGCGTACACAATTGAGGCCGTTATCATGCAAAATAGCC 1141
L T K Q G W S S A Y T I E A V I M Q I A
GCAACATTGGTTAAGGGTAAAGCAAGAATCCAATTTGGGGCAAAATAAGCTGGCAAAGTT 1201
A T L V K G K A R I Q F G A N K A G K V
AGCGGGCAGTACAGTTTGGCGAGGCGCACACAGTCAATCAAGTCACTTGTACAGATTAT 1261
S G Q Y S L A R A Q Q S F K S L V Q I H
GAAAAGAAATGGCTGGTTACACACCACTAAGGAAGATGGTTAAggaagtgtcccactggat 1321
E K N G W F T P P K E D G - G S V P L D
gttgtcccaagcctctactctcatcctctctgtaccctcactctggctgtcaccgctgctt 1381
ctccaccgctccacactctccttggccccaccatttccactctctcatggtaactctcc 1441
ttcacatcaacatctaggagtggtttaagttttatctctaaactttgtagaacaacataa 1501
ttggcaaatgcagtagttagtctgtagtcaactgtatcttctctctctctctctctctct 1561
attcatgaatattaagaatcagggagttcagtttaatttttttttttttttttttttttttt 1621
taaaaacaaaaatacagtgctgacatatatgactagaagaaatgtaaatctttatcttca 1681
tttaattacttctggactaggatggctgttggacacaggagatgaactgtcagaaataa 1741
tcaatttatatgcttaccctctctttaaattttgttaaagtattctagctctttataactgag 1801
gaatgatgctttctggactacaatatgctatgccccagataagtctgtatattgtattggt 1861
ggaaatgtgatctgtttatcttctcttaacagaaatattgtcacttttgtgagagaag 1921
ggtttctgtacaagttttgttaaactagagagagctgtttttccactatgatttttgaa 1981
tgattttctgctagtagtcttttgagaggcttgagtgtaaggggtgttttacattctgctg 2041
taatttttagataatctctctctcttatttcagttttatgtgcattgattccatcaacaaa 2101
catactctcatcacatttgctctctttgtcatgtttttggaaactgcaattccatattgac 2161
aaaggtagctcatcattattaccctgtatagtagtgcagtttattcagttgttttcattta 2221
cattgcattgtgataatggataaattgactgagacagaaatgtagatattgtcaggggata 2281
caacagtggtggataaaggcctgagggggtagatctgtatttttgaaatttcagaagctctg 2341
atcaagcatgcaatgactgtaggagtaggagatagtagtatcatcatagctacaaattcctg 2401
ttctctattattgtagctgtagcaacttatttttttaattttttccccatgataaagc 2461
agcaatcctctggcctgtgctggaagttcatagctattgtagctctgtggtgagagaaatg 2521
tacctctcaggttggcctgtgtaatacaaaaataaagtttatacttatcacttggccaactcca 2581
gggatttttttggagaacaaatagtagttgcaaatatggtgggaggggaaatgttttag 2641
aatcccatcttctctctttaaattggcactgatattgctgttttggatgaaagaattgga 2701
aaatacttttaagaattatacttcagaaatggtaattgggttccatgattttgtttgg 2761
caacctgaaactaatcatgtcaagtaaaaggggtgaaatgcatcaatgatcatttgaatg 2821
taagattttttgtcagaaatgaaatgttctagcagcttagtcataattgaagattttac 2881
aaagatccagtaacttttagatgggtgtgttagagaagtgaagtgagataaacttaaggg 2941
cattagagttgcagctgcttttgggagctttcagttaatgccattcagtgagggaaatttg 3001
aaaatgaacatgaaagatgggaattcttccccgatcgcagctgcttattgtgtgtgact 3061
gattatctttttcacactctttaaagaggaatagaagtgcttaataataaagcaagcagatgt 3121
aaatatttgaatatttttttagaatgaaatgtttgaattcaaaagacaacatttact 3181
acctttctgtctttttttttgttttaaaatgtgtagtcaactgaaatttgattgggttc 3241
ctgcctctgtctgttttggaaaaaaataaagctgctcttttgcataaaaaaa 3301
aaaaaaaaaaaagtactctgctgtgataccactgcttaact 3342

```




Figure 18 Nucleotide and deduced amino acid sequences of *UbcQ1* from *P. monodon* identified by 5' - and 3' -RACE technique. Schematic diagram showing the full-length gene of *UbcQ1* and miR-750 binding position at 3'-UTR, the nucleotide and translated amino acid sequences of *UbcQ1* (A). The nucleotide sequences are shown in capital letter and amino acids are shown in one letter symbol under the corresponding codons. The position of miR-750 binding site is highlighted in light gray and the numbers on the right show coordinates of the nucleotides in each line (B).

3.1.1.4 Confirmation of interaction between miR-750 and *UbcQ1* by luciferase reporter system

To validate the interaction between miR-750 and *UbcQ1*, the recombinant plasmid containing miR-750 binding site, pmiRGLO-*UbcQ1*, was co-transfected with miR-750 mimic or scramble into HEK293T cells. Theoretically, if miRNA binds to the target region, the luciferase protein translation is inhibited and the activity of luciferase is decreased. After 48 h post transfection, the luciferase activity of transfected cells was measured. The result showed that in the presence of mimic miR-750, the luciferase activity is not reduced as expected when compared with the controls (Figure 19). The result indicated that miR-750 might not directly target *UbcQ1*.

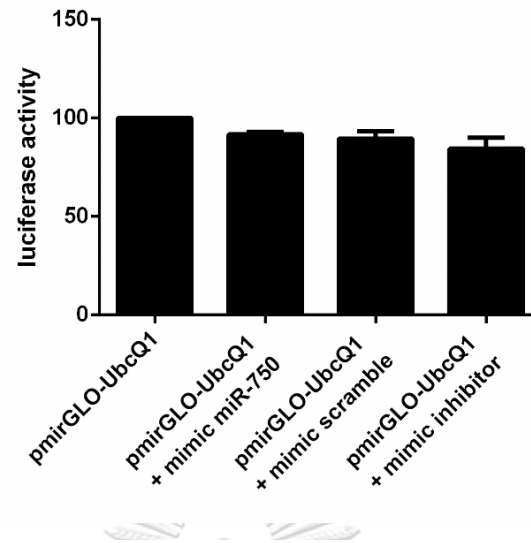


Figure 19 *In vitro* miRNA/target interaction analysis of miR-750 and *UbcQ1*. The pmirGLO-*UbcQ1* was co-transfected with miR-750 mimic, mimic scramble or mimic inhibitor into HEK293-T cells. The luciferase activity was measured at 48 h after transfection. The experiments were done in duplicate.

3.1.1.5 miRNA target prediction using computational program with the criteria that allow 1 seed sequence mismatch

According to the *UbcQ1* is not miR-750 target gene, the miR-750 target genes were predicted again with the criteria of 1 mismatch at seed sequence of miR-750 using CU-Mir software in purpose to increase the probability of miR-750 target gene prediction. The 241 target sequences were identified as the possible miR-750 target genes. After GO annotation was performed, the biological processes of the predicted target sequences were classified into 18 categories as shown in Figure 20. Among the identified target genes, 20 genes that are probably involved in shrimp immunity were listed in Table 9.

Table 9 Predicted target genes using CU-Mir software with 1 mismatch at seed sequence.

EST id.	EST pos.	Gene name
gi 0058870 gb PM58870.1	5	angiotensin converting enzyme [<i>Astacus leptodactylus</i>]
gi 0071814 gb PM71814.1	1366	cytoglobin [<i>Penaeus vannamei</i>]
gi 0041337 gb PM41337.1	205	E3 ubiquitin-protein ligase Nedd-4 [<i>Folsomia candida</i>]
gi 0041339 gb PM41339.1	343	E3 ubiquitin-protein ligase Nedd-4 isoform X2 [<i>Pogonomyrmex barbatus</i>]
gi 0019642 gb PM19642.1	302	E3 ubiquitin-protein ligase ubr3-like [<i>Centruroides sculpturatus</i>]
gi 0041351 gb PM41351.1	1414	ectopic P granules protein 5 homolog [<i>Aptenodytes forsteri</i>]
gi 0061369 gb PM61369.1	1096	effector caspase [<i>Penaeus monodon</i>]
gi 0061369 gb PM61369.1	1025	effector caspase [<i>Penaeus monodon</i>]
gi 0030130 gb PM30130.1	188	inositol-requiring enzyme-1 [<i>Penaeus vannamei</i>]
gi 0054521 gb PM54521.1	643	lectin D, partial [<i>Penaeus japonicus</i>]
gi 0014794 gb PM14794.1	307	MAP3K13 isoform 15, partial [<i>Pan troglodytes</i>]
gi 0080293 gb PM80293.1	2365	mdm2-binding protein-like [<i>Parasteatoda tepidariorum</i>]
gi 0045450 gb PM45450.1	176	mitogen-activated protein kinase kinase 4 [<i>Penaeus vannamei</i>]
gi 0053806 gb PM53806.1	94	retinoid X receptor [<i>Penaeus monodon</i>]
gi 0053806 gb PM53806.1	52	retinoid X receptor [<i>Penaeus monodon</i>]
gi 0048262 gb PM48262.1	184	reverse transcriptase, partial [<i>Penaeus monodon</i>]
gi 0024307 gb PM24307.1	378	Sorting nexin-5 [<i>Daphnia magna</i>]

Table 9 Predicted target genes using CU-Mir software with 1 mismatch at seed sequence (continued).

EST id.	EST pos.	Gene name
gi 0095651 gb PM95651.1	58	thrombospondin II, partial [<i>Penaeus monodon</i>]
gi 0031210 gb PM31210.1	99	ubiquitin-like modifier-activating enzyme atg7 isoform X2 [<i>Oryza sativa Japonica</i>]
gi 0053884 gb PM53884.1	207	WD and tetratricopeptide repeat protein 1 [<i>Pteropus alecto</i>]
gi 0065773 gb PM65773.1	31	actin [<i>Amphidinium carterae</i>]
gi 0060441 gb PM60441.1	3	sarcoplasmic calcium-binding protein [<i>Lingula anatina</i>]

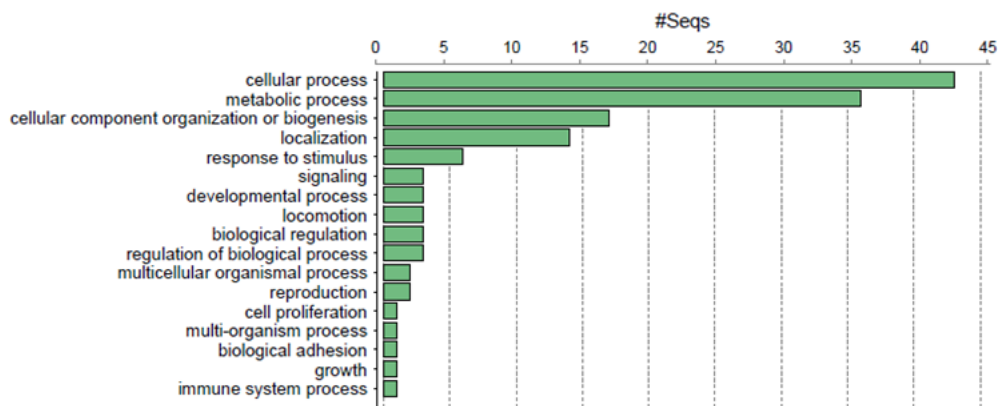


Figure 20 Biological process Go term distribution of miR-750 predicted target genes from CU-Mir with 1 mismatch criteria.

3.1.2 Identification of miR-750 target protein by 2-D gel electrophoresis

According to the miRNA function, it can target specific mRNA and regulates the target gene expression at a post-transcription level resulting in translational repression or degradation of mRNA transcript. However, there are some reported on upregulation of gene expression by miRNA under specific conditions. The 2-D gel electrophoresis (2-DE) technique was used to identify miR-750 target protein. In this study, miRNA mimics, miRNA scramble, miRNA AMO, and miRNA AMO scramble were injected into the shrimp and the 2-DE technique was performed to identify differentially expressed proteins.

3.1.2.1 Optimization of miRNA mimic dosage

To get appropriate dosages of miRNA mimic for injecting shrimp, miR-750 mimic at 1 nmole, 2 nmole, and 4 nmole was injected into 10 g shrimp, followed by the detection of miR-750 expression level in *P. monodon* stomach by stem-loop qRT-PCR. It was revealed that the miR-750 expression increased as the amount of miRNA mimic increased (Figure 21). The highest amount of miRNA mimic (4 nmole/shrimp) was selected for 2-DE experiment.

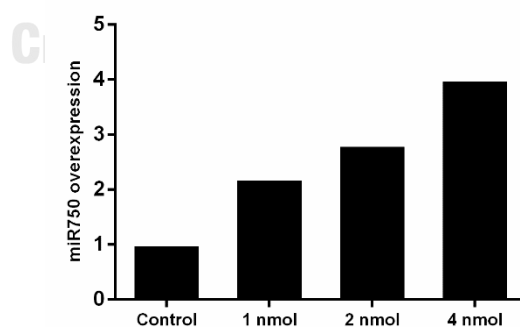


Figure 21 Determination of the dosage of miRNA mimic used to overexpress miR-750 in *P. monodon*. Shrimp was injected with 1 nmole, 2 nmole or 4 nmole miR-750 mimic. The expression of miR-750 in shrimp stomach was determined after 24 hour post miR-750 mimic injection using qRT-PCR.

3.1.2.2 Differentially expressed proteins in stomach of mimic miR-750-injected shrimp

In this experiment, miR-750 mimic was injected into shrimp to overexpress miR-750 in shrimp and the control group was shrimp injected with miR-750 mimic scramble. Suppression of miR-750 in shrimp was performed by injecting miR-750 AMO and the control group was shrimp injected with miR-750 AMO scramble. The stomach proteins extract (1 mg) of each pooled protein sample of 3 shrimps were separated by 2-DE. After staining with Coomassie Brilliant Blue G-250, the protein expression profile of each group was analyzed by ImageMaster 2D Platinum 6.0 software (Figure 22). The protein expression profiles were compared. The altered protein spot results were divided into 2 conditions; Condition I: down-regulated proteins which showed low protein expression levels in miR-750 mimic injected group and high protein expression levels in miR-750 inhibitor injected group when compared to the control, Condition II: up-regulated proteins which showed high protein expression levels in miR-750 mimic injected group and low protein expression levels in miR-750 inhibitor injected group. Based on these criteria, 5 down-regulated protein spots and 8 up-regulated protein spots were identified (Table 10). The spot intensity is shown in Table 11.

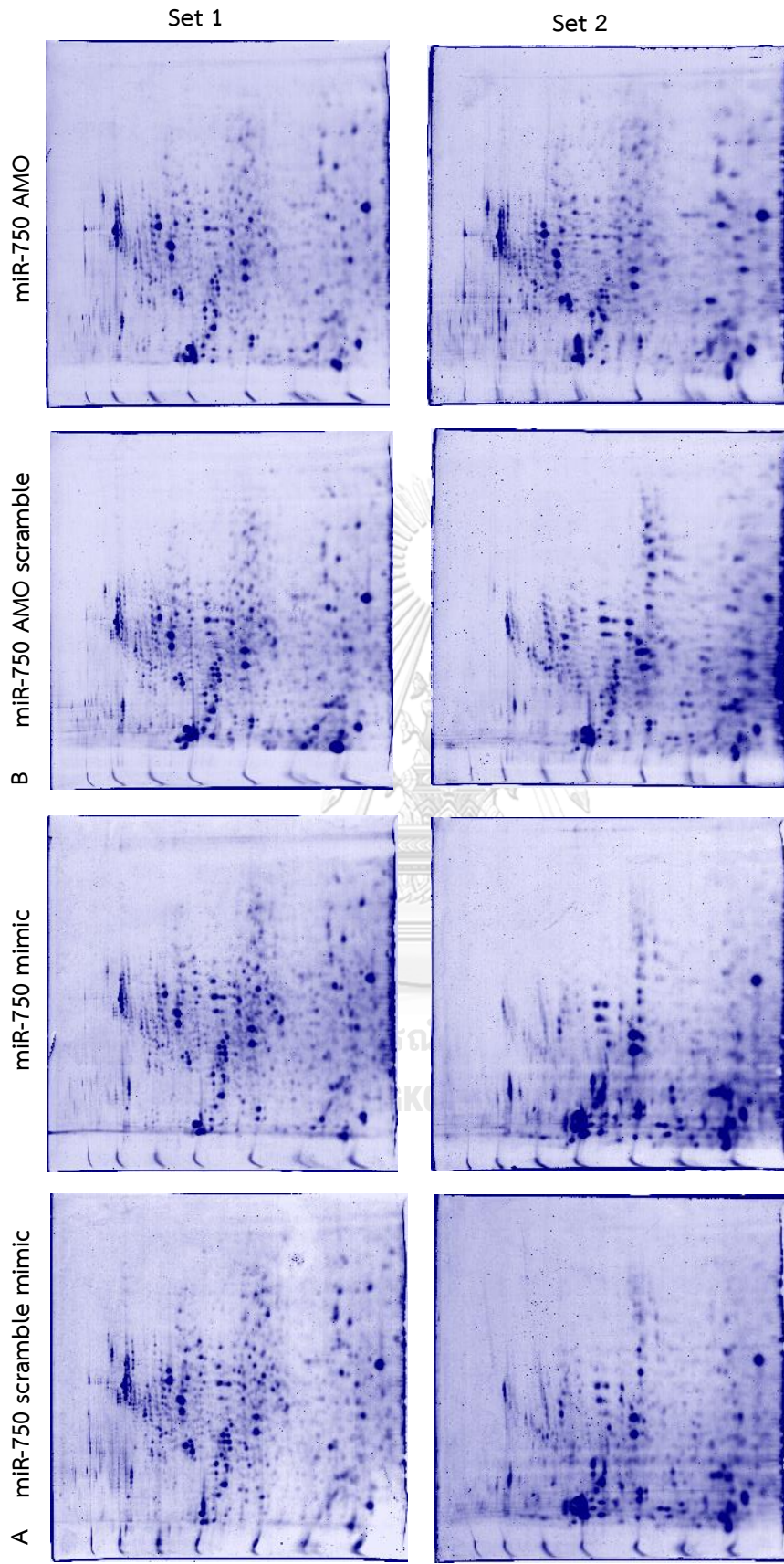


Figure 22 Effect of miR-750 on stomach protein expression profile of *P. monodon*.

In each group, shrimp was injected with 4 nmole miRNA mimic. For the miR-750 overexpressed group, shrimp were injected with miR-750 mimic and miR-750 scramble (control) (A). In the miR-750 suppressed group, shrimp were injected with miR-750 AMO and miR-750 AMO scramble (control) (B.). After 24-hour post miRNA mimic injection, shrimp stomach was collected and 2-DE was performed. Representative gels from each group are shown. The experiment was done in duplicate (set 1 and set 2).

Table 10 The differentially expressed protein spots from stomach of *P. monodon* challenged with miR-750 mimic, miR-750 scramble, miR-750 AMO and miR-750 AMO scramble.

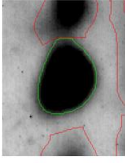
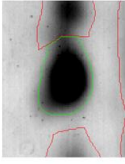
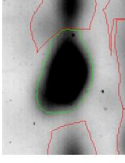
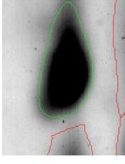
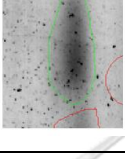
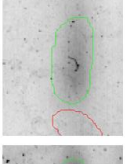
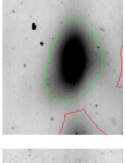
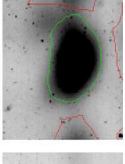
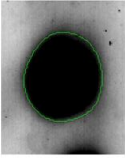
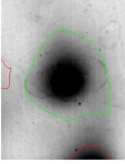
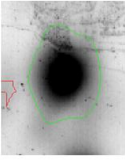
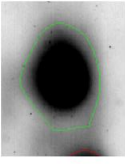
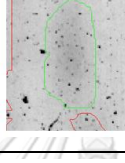
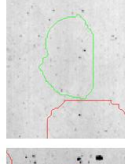
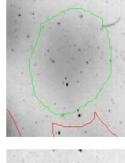
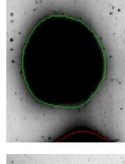
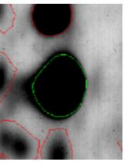
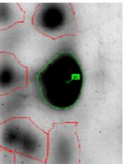
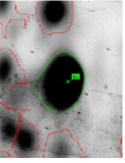
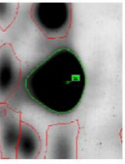
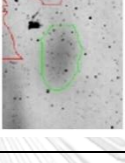
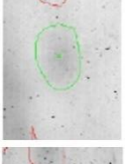
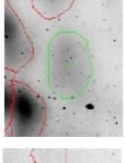
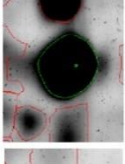
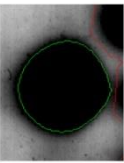
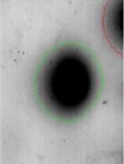
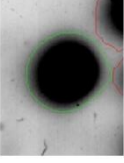
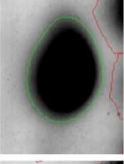




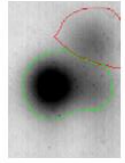
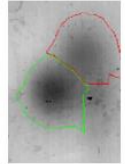
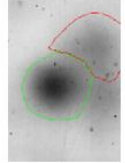
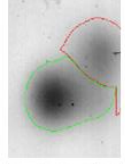
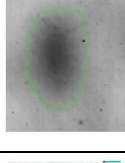
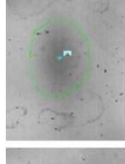
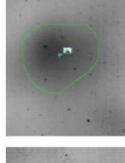
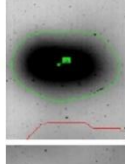
Condition	Spot Name	Protein spot in set 1				Protein spot in set 2			
		miR-750 scramble	miR-750 mimic	miR-750 AMO scramble	miR-750 AMO	miR-750 scramble	miR-750 mimic	miR-750 AMO scramble	miR-750 AMO
1: Down-regulated protein spots after miR-750 mimic injection	180								
	244								
	246								
	281								
	348								

Table 10 The differentially expressed protein spots from stomach of *P. monodon* challenged with miR-750 mimic, miR-750 scramble, miR-750 AMO and miR-750 AMO scramble.

Condition	Spot Name	Picture in set 1				Picture in set 2			
		miR-750 scramble	miR-750 mimic	miR-750 AMO scramble	miR-750 AMO	miR-750 scramble	miR-750 mimic	miR-750 AMO scramble	miR-750 AMO
2: Up-regulated protein spots after miR-750 mimic injection	357								
	360								
	382								
	443								
	444								
	458								

Table 10 The differentially expressed protein spots from stomach of *P. monodon* challenged with miR-750 mimic, miR-750 AMO, miR-750 scramble and miR-750 AMO scramble.

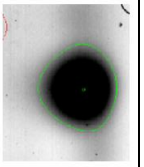
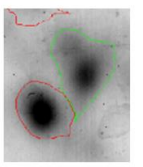
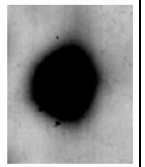

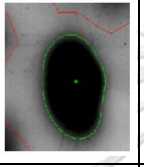

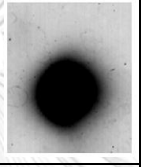

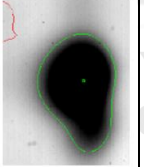
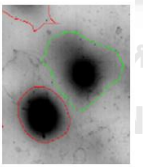
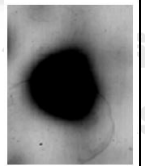

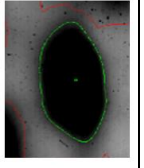

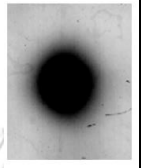

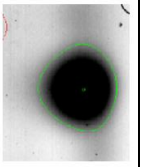
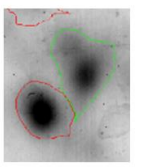
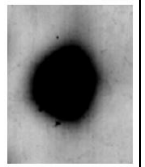

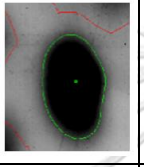

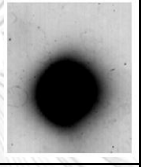

Condition	Spot Name	Picture in set 1				Picture in set 2			
		miR-750 scramble	miR-750 mimic	miR-750 AMO scramble	miR-750 AMO	miR-750 scramble	miR-750 mimic	miR-750 AMO scramble	miR-750 AMO
	578								
	589								
3: Constant expressed protein spots	586								

Table 11 The %intensity of differentially expressed protein spots.

Spot ID	Observed MW (kDa)/pI	Spot intensity (%)					
		miR-750 Scramble (Ctrl)	miR-750 mimic	Ratio miR-750 /Ctrl	miR-750 AMO Scramble (Ctrl)	miR-750 AMO	Ratio miR-750 AMO/Ctrl
Condition I: Down-regulated protein spots after miR-750 mimic injection							
180	76 / 5.05	0.44 ± 0.03	0.39 ± 0.00	0.90 ± 0.07	0.43 ± 0.03	0.48 ± 0.05	1.12 ± 0.02
244	63 / 5.48	0.41 ± 0.19	0.21 ± 0.14	0.49 ± 0.12	0.31 ± 0.07	0.49 ± 0.02	1.62 ± 0.44
246	62 / 5.38	0.63 ± 0.49	0.37 ± 0.23	0.64 ± 0.13	0.35 ± 0.12	0.73 ± 0.12	2.27 ± 1.14
348	18 / 4.70	0.33 ± 0.14	0.19 ± 0.07	0.56 ± 0.02	0.22 ± 0.04	0.54 ± 0.21	2.40 ± 0.47
281	55 / 4.75	0.74	0.31	0.41	0.40	0.44	1.11
Condition II: Up-regulated protein spots after miR-750 mimic injection							
357	42 / 5.36	0.32 ± 0.06	0.46 ± 0.01	1.47 ± 0.26	0.58 ± 0.39	0.19 ± 0.04	0.46 ± 0.37
360	42 / 5.21	0.28 ± 0.13	0.39 ± 0.09	1.51 ± 0.38	0.31 ± 0.16	0.20 ± 0.01	0.73 ± 0.35
382	39 / 5.35	0.37 ± 0.02	0.57 ± 0.19	1.54 ± 0.46	0.33 ± 0.11	0.23 ± 0.03	0.75 ± 0.32
443	32 / 4.88	0.65 ± 0.24	0.90 ± 0.42	1.36 ± 0.15	0.53 ± 0.06	0.43 ± 0.05	0.80 ± 0.00
444	32 / 5.03	0.53 ± 0.26	0.95 ± 0.63	1.70 ± 0.35	0.54 ± 0.11	0.41 ± 0.07	0.75 ± 0.02
468	31 / 4.24	0.43 ± 0.26	0.71 ± 0.48	1.62 ± 0.14	0.42 ± 0.00	0.34 ± 0.02	0.79 ± 0.05
578	14 / 4.15	0.50 ± 0.11	0.75 ± 0.39	1.45 ± 0.47	0.57 ± 0.12	0.41 ± 0.01	0.74 ± 0.16
589	27 / 5.34	0.17	0.25	1.51	0.22	0.18	0.84
Constant expressed protein spot							
586	14 / 5.54	0.38 ± 0.23	0.38 ± 0.22	1.07 ± 0.06	0.43 ± 0.21	0.36 ± 0.21	0.83 ± 0.07

3.1.2.3 Protein spot identification

A total of 13 up- and down-regulated protein spots were excised and subjected to MS analysis. Firstly, the derived peptide sequences were search against NCBInt using the MASCOT. The results showed that spot ID 180 and 444 were Hemocyanin. While spot ID 244, 246, 357, 360, 382, 458, 578 and 589 were Actin1. Moreover, the spot ID 348 was Sarcoplasmic calcium-binding protein. From the MASCOT report, it should be noticed that one identified protein was found as up- and down-regulated proteins after miR-750 mimic injection. Actin1 was found in down-regulated protein after miR-750 mimic injection including spot ID 244 and 246 and was found in up-regulated protein after miR-750 mimic injection including spot ID 357, 360, 382, 458, 578 and 589. While the Hemocyanin was found in down-

regulated protein after miR-750 mimic injection (spot ID 180) and was found in up-regulated protein after miR-750 mimic injection (spot ID 444).

Due to the lack of *P. monodon* genome sequence, some protein spots including spot ID 281 and 443 could not be identified by MASCOT. To investigate the unknown protein, the derived peptide sequences were search against nucleotide translated protein of EST *P. monodon* database using Galaxy software. The Galaxy report revealed that spot ID 281 and 443 were Tropomyosin and Chymotrypsin, respectively. The detailed information of the identified proteins, including the spot numbers, the accession number, predicted MW/pI and sequence coverage, was listed in Table 12.

This result indicating that 13 protein spots, which differentially expressed in the effect of miR-750 overexpression or silencing, were identified into 5 proteins including Actin1, Chymotrypsin, Hemocyanin, Sarcoplasmic calcium-binding protein and Tropomyosin. The mRNA/miRNA-750 interaction was then analyzed by RNAhybrid software.

Note that, only 2 candidate miR-750 target including Actin1 and Sarcoplasmic calcium-binding protein were also predicted by computational analysis prediction results with criteria 1 mismatch at seed sequence as shown in Table 9. It was implied that these 2 genes have the higher chance to be miR-750 target genes.

Table 12 The selected differentially expressed protein spots from stomach of mimic miR-750-challenged *P. monodon* resolved by 2-DE and identified by LC-nano ESI-MS/MS.

Spot	Observed		Predicted		Mascot report				Galaxy report		
	pI	MW	pI	MW	Protein ID	Nucleotide ID	Protein Hit	%coverage	Pm_EST ID	Protein Hit	%coverage
180	5.05	76	5.30	78	AEF77775.1	JF357966.1	Hemocyanin	12.00	PM89203	Hemocyanin gamma subunit 1	13.62
244	5.48	63	5.23	42	AAC78681.1	AF100986.1	Actin 1	37.76	PM92039	Muscle actin	36.66
246	5.38	62	5.23	42	AAC78681.1	AF100986.1	Actin 1	27.39	PM92039	Muscle actin	27.75
281	4.75	55	-	-					PM92564	Tropomyosin	46.96
348	4.70	18	4.76	22	BAL72725.1	AB703461.1	Sarcoplasmic calcium-binding protein	15.03	PM92039	Muscle actin	18.48
357	5.36	42	5.23	42	AAC78681.1	AF100986.1	Actin 1	28.99	PM91069	Actin	28.28
360	5.21	42	5.23	42	AAC78681.1	AF100986.1	Actin 1	28.99	PM92039	Muscle actin	31.96
382	5.35	39	5.23	42	AAC78681.1	AF100986.1	Actin 1	22.34	PM92039	Muscle actin	26.10
443	4.88	32	-	-					PM93083	Chymotrypsin	13.01
444	5.03	32	5.10	51	AAL27460.1	AF431737.1	Hemocyanin, partial	11.36	PM89203	Hemocyanin gamma subunit 1	10.18
458	4.24	31	5.23	42	AAC78681.1	AF100986.1	Actin 1	16.22	PM92039	Muscle actin	17.89
578	4.15	14	5.23	42	AAC78681.1	AF100986.1	Actin 1	15.69	PM92039	Muscle actin	17.30
589	5.34	27	5.23	42	AAC78681.1	AF100986.1	Actin 1	26.06	PM91702	Actin 1	20.26

Condition I: Down-regulated protein spots after miR-750 mimic injection

Condition II: Up-regulated protein spots after miR-750 mimic injection

3.1.2.4 RNA hybrid prediction of candidate miR-750 target gene

The miRNA-target-mRNA hybrid structures of 5 candidate miR-750 target genes were analyzed using RNAhybrid software of BiBiserv and minimum free energy (MFE) of obtained structures were calculated. The low MFE indicated spontaneous occurrence secondary structure resulting in possibility miR-750 target gene. The full-length of Actin1 (*Act1*), Hemocyanin (*Hc*), Sarcoplasmic calcium-binding protein (*Scp*), the partial of Chymotrypsin (*Ctr*) and Tropomyosin (*Tpm*), were used as the input data. The results and detailed information of the predicted miRNA-target-mRNA duplex structure, including the gene name, spot ID, nucleotide position of miR-750 binding site, number of mismatches at seed sequence, energy and RNA hybrid structure were shown in Table 13.

The result showed that the *Hc* has 2 miR-750 binding sites located on the nucleotide position 1016 and 1094 with the energy -20.8 and -19.7 kcal/mol, respectively. And the energy of *Act1*, *Ctr*, *Hc*, *Scp* and *Tpm* less than -15 kcal/mol indicating that these 5 genes might possibility to miR-750 target gene.

Table 13 Prediction of miRNA-target-mRNA duplex structure using RNAhybrid software.

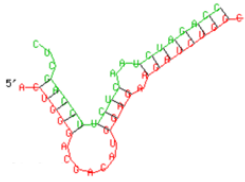
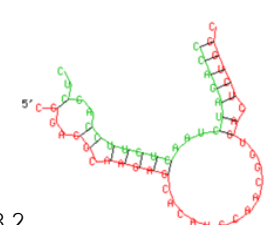
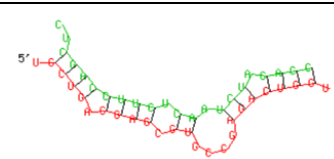
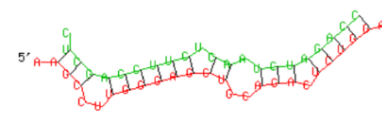
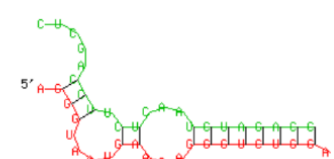

Gene name	Spot ID	Gene location of target sequence	Mismatch	RNA hybrid structure and energy (kcal/mol)
Actin1 (<i>Act1</i>)	244, 246, 357, 360, 382, 458, 578, 589	ORF	0	 <p>MFE = -24.6</p>

Table 13 Prediction of miRNA-target-mRNA duplex structure using RNAhybrid software. (continued)

Gene name	Spot ID	Gene location of target sequence	Mismatch	RNA hybrid structure and energy (kcal/mol)
Chymotrypsin (<i>Ctr</i>)	443	ORF	1	 MFE = -18.2
Tropomyosin (<i>Tpm</i>)	281	OEF	1	 MFE = -24.1
Hemocyanin (<i>Hc</i>)	180, 444	ORF	1	 MFE = -24.8
		ORF	0	 MFE = -19.7
Sarcoplasmic calcium-binding protein (<i>Scp</i>)	348	ORF	0	 MFE = -17.9

3.1.2.5 Transcriptional analysis of selected differentially expressed genes

Besides expression at the post-translational level, the candidate miR-750 target gene expression at the transcriptional level was performed in WSSV-infected shrimp stomach using qRT-PCR to see if they were related. The expression profiles were shown in Figure 23. The results showed that *Act1*, *Ctr*, *Scp* and *Tpm* were down-regulated at 24 h after WSSV infection (hpi) which related to miR-750 expression that up-regulated at 24 hpi (Figure 17A). Moreover, at 48 hpi, the expression of *Scp* and *Tpm* were downregulated. Meanwhile, the expression of *Hc* was up-regulated at 24 hpi and down-regulated at 6 and 48 hpi.

When the transcriptional and translational expression of the target genes were compared, we showed that 4 genes including *Act1*, *Ctr*, *Scp* and *Tpm* were the target of miR-750 which were downregulated while miR-750 was upregulated.

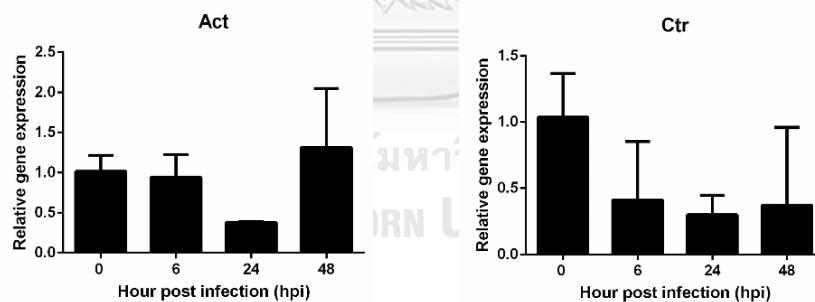


Figure 23 qRT-PCR analysis of candidate miR-750 target genes identified by 2-DE.

The expression level of candidate miR-750 target genes including Actin1 (*Act1*), Chymotrypsin (*Ctr*), Hemocyanin (*Hc*), Sarcoplasmic calcium-binding protein (*Scp*) and Tropomyosin (*Tpm*) was determined in stomach of 10 g WSSV-infected *P. monodon*. The significantly difference of relative gene expression is indicated by * which $P < 0.05$, ** which $P < 0.01$ and *** which $P < 0.001$.

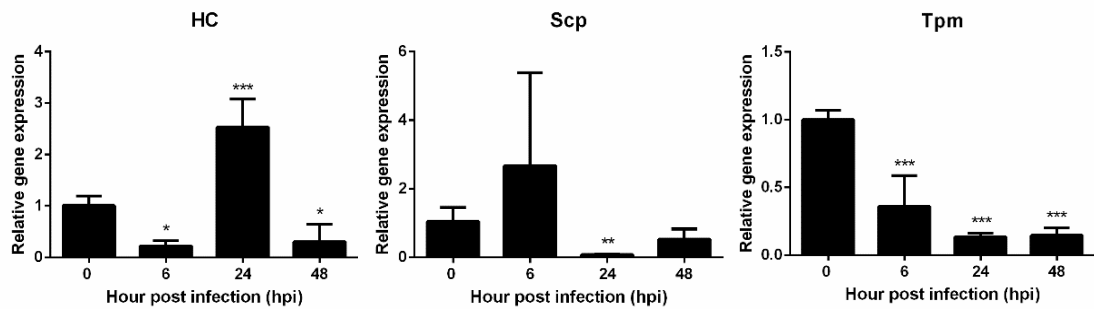


Figure 23 qRT-PCR analysis of candidate miR-750 target genes identified by 2-DE.

The expression level of candidate miR-750 target genes including Actin1 (*Act1*), Chymotrypsin (*Ctr*), Hemocyanin (*Hc*), Sarcoplasmic calcium-binding protein (*Scp*) and Tropomyosin (*Tpm*) was determined in stomach of 10 g WSSV-infected *P. monodon*. The significantly difference of relative gene expression is indicated by * which $P < 0.05$, ** which $P < 0.01$ and *** which $P < 0.001$ (continued).

3.1.2.6 Confirmation of interaction between miR-750 and 4 candidate miR-750 target genes by luciferase reporter system

3.1.2.6.1 Construction of the luciferase reporter plasmid

Each candidate gene was cloned into pmiRGLO vector at 3'-UTR of luciferase gene in order to verify the interaction between miR-750 and target gene. To construct the reporter vectors, the PCR technique was performed to amplify 4 miR-750 target genes. After PCR purification, the PCR products and pmiRGLO vector were double digested with *SacI* and *XbaI* at 37 °C for overnight. After that, the digested genes were ligated in to pmiRGLO vector. Next, the colony PCR was performed to identify the positive clone of each gene (Figure 24). The recombinant plasmid pmiR_target gene were double digested with *SacI* and *XbaI* in sight to verification of luciferase reporter pmiR_target gene construction (Figure 25). The sequencing results showed that, 4 candidate genes of miR-750 including *Act1*, *Ctr*, *Scp* and *Tpm* were successfully cloned into pmiRGLO vector

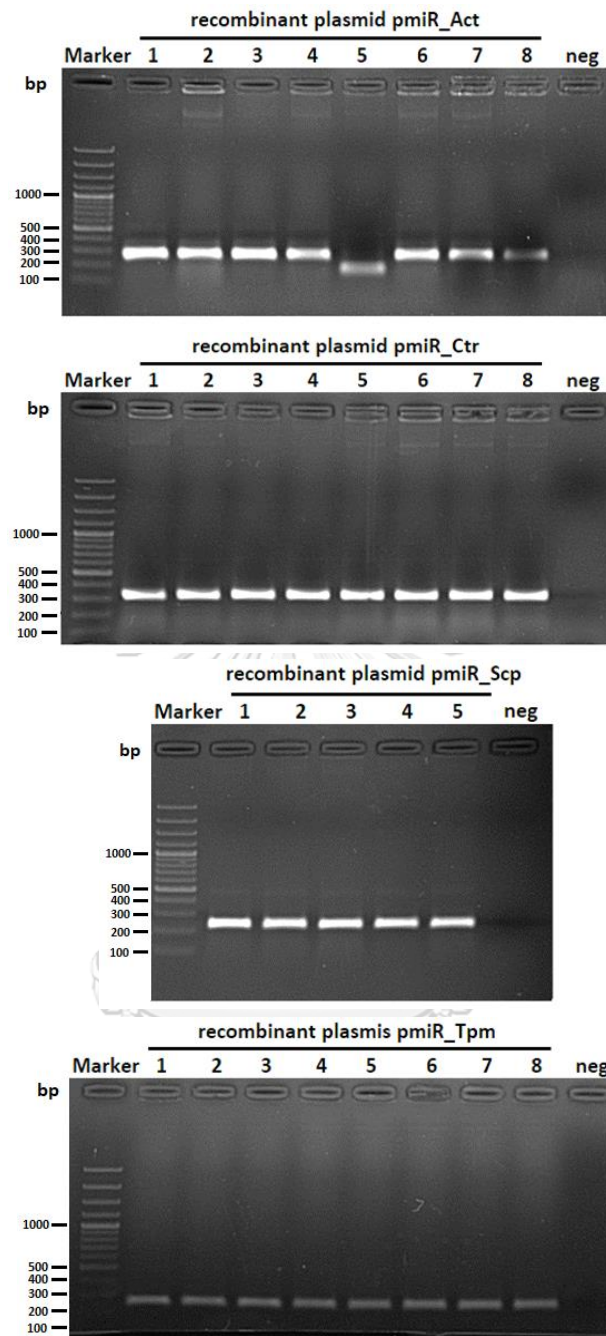


Figure 24 Colony PCR of recombinant plasmid pmiR_target genes. Marker is 100 bp DNA ladder (Thermo Scientific). Recombinant plasmids were picked, and colony PCR was performed using specific primer. The positive clone showed approximately 200-300 bp product size on 1.4% agarose gel electrophoresis. The Actin1 (*Act1*), Chymotrypsin (*Ctr*), Sarcoplasmic calcium-binding protein (*Scp*) and Tropomyosin (*Tpm*) in each lane represented clone number of each gene.

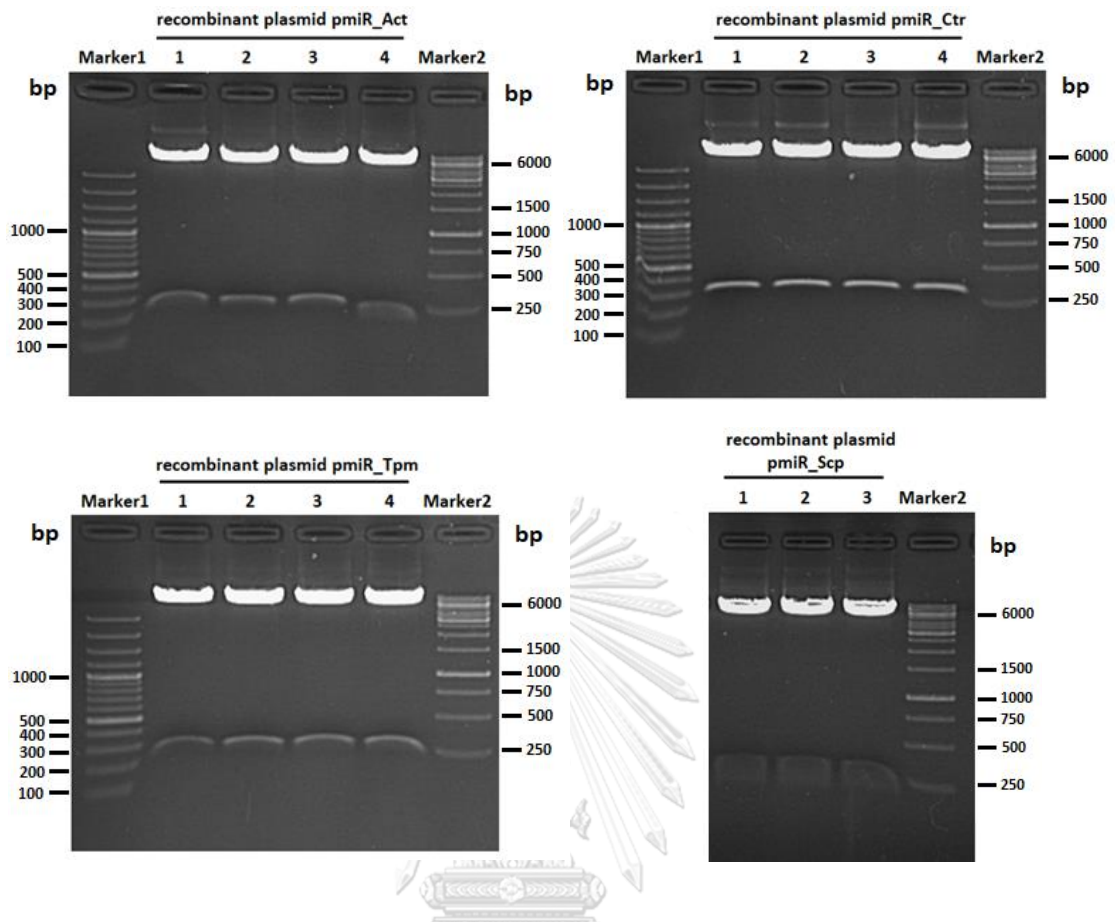


Figure 25 Verification of luciferase reporter pmiR_target genes constructs. The recombinant plasmids were digested with *SacI* and *XbaI* as run on 1.4% agarose gel electrophoresis. Marker1 is 100 bp DNA ladder (Thermo Scientific). Marker 2 is 1kb DNA ladder (Thermo Scientific). One positive clone of each genes were selected for

CHULALONGKORN UNIVERSITY

3.1.2.6.2 Luciferase activity

To validate the interaction between miR-750 and 4 candidate target genes, the reporter plasmid of each gene including pmiR_Act, pmiR_Ctr, pmiR_Scp and pmiR_Tpm was co-transfected with miR-750 mimic or scramble at 10 pmole into HEK293-T cells. After 48 h post transfection, the luciferase activity of transfected cells was measured (Figure 26). The results revealed that in the presence of miR-750 mimic, the luciferase activity of *Scp* was slightly reduced for about 20% when compared to the control pmiR_Scp and scramble group. While the luciferase

activities of the other target genes were not different. It was implied that miR-750 might directly target *Scp* but not target *Act1*, *Ctr* and *Tpm* genes.

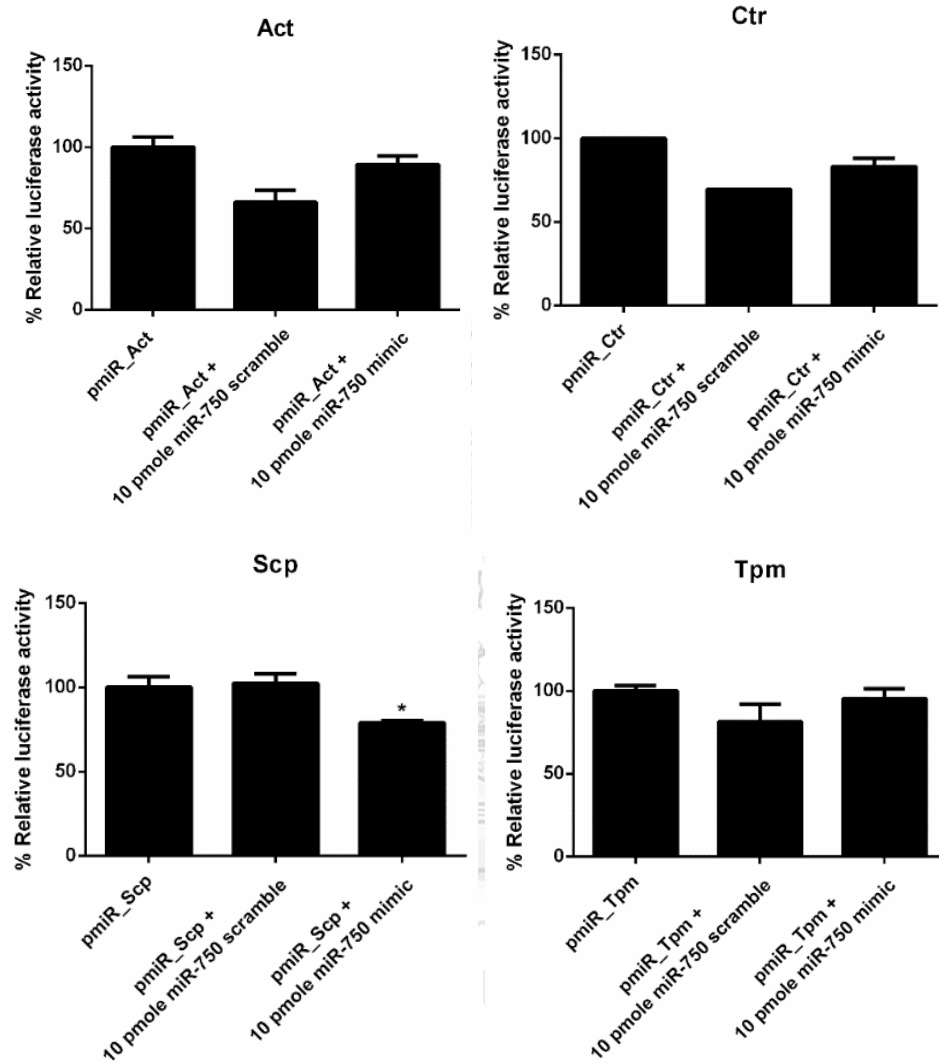


Figure 26 The interaction of miR-750 and target genes by luciferase reporter assay. Each reporter plasmid of pmiR_Act1, pmiR_Ctr, pmiR_Scp and pmiR_Tpm was co-transfected with miR-750 mimic or miR-750 scramble into HEK293-T cells. The luciferase activities were measured at 48 h after transfection. The experiments were done in duplicate. The * indicates significant difference of % relative luciferase activity ($P < 0.05$).

3.2 Study of miR-750 biogenesis

In miRNA biogenesis, the miRNA will be incorporated into RNA induced silencing complex (RISC) containing Argonaute protein (*Ago*). Then, this complex target specific mRNA of miRNA resulting in translational repression or degradation of mRNA transcript. *Ago* required for effective RNAi in *P. monodon* (Dechklar et al., 2008) but *Ago* that is involved in miRNA biogenesis is not known. To investigate miR-750 biogenesis, *Ago* genes, *Ago1-3*, were suppressed with each specific dsRNA-*Ago* and the expression of miR-750 target gene was determined.

3.2.1 Construction of dsRNA expression vector

In order to produce the dsRNA-*Ago* in *E. coli*. HT115, the dsRNA expression vector of *PmAgo* gene including *PmAgo1*, *PmAgo2*, *PmAgo3* and *PmAgo4* were constructed. The PCR technique was performed to amplify sense stand (section A) and antisense stand (section B) of dsRNA-*Ago*. The purified of PCR product was shown in Figure 27. The section A was double digested with *Xba*I and *Hind*III while the section B was digested with *Bam*HI and *Xho*I. Each section was cloned into pET-17b. The sequences were confirmed. After that, the recombinant plasmids pET-17b harboring the cassette for producing the hairpin dsRNA of corresponding gene including namely pET17b-dsPmAgo1-4 were cloned into *E. coli*.HT115 for dsRNA-*Ago* production.

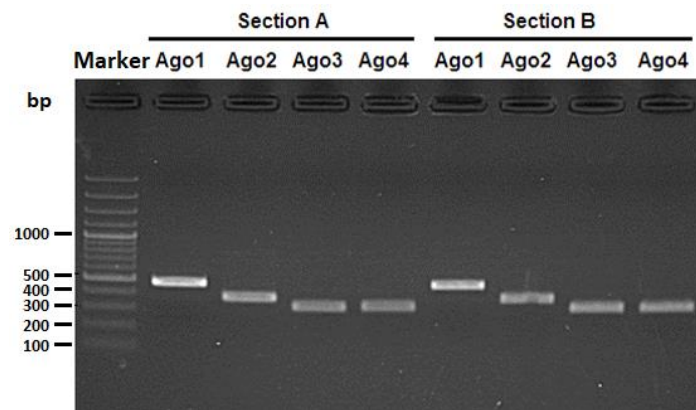


Figure 27 The purified PCR products of section A and section B of *PmAgo1-4* genes. Marker is 100 bp DNA ladder (Thermo Scientific). The purified PCR products approximately 300-500 bp were run on 1.4% agarose gel electrophoresis.

3.2.2 The dsRNA-*PmAgo* preparation

The *E. coli* HT115 which lacks ribonuclease III, an enzyme that normally degrades dsRNA was used for dsRNA-*PmAgo1-4* production. The *E. coli* HT115 containing pET17b-dsPmAgo was cultured and induced the expression of T7 RNA polymerase by 0.4 mM IPTG resulting in the dsRNA-*PmAgo* production. The dsRNA-*PmAgo* was purified as shown in Figure 28.

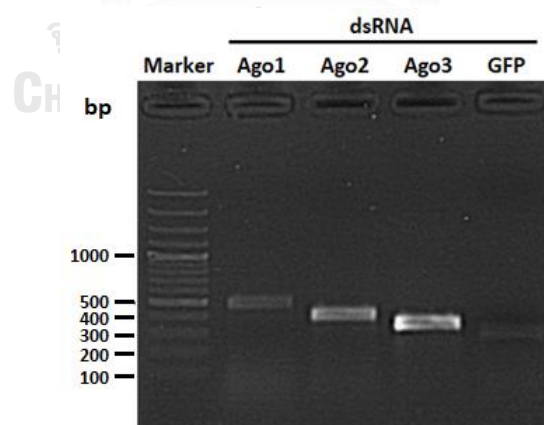


Figure 28 Double-stranded RNA of the *PmAgo1-4* genes produced by *in vivo* expression in bacteria. The *E. coli* HT115 harboring pET17b-dsPmAgo was induced with 0.4 mM IPTG to over-produced dsRNA-*PmAgo in vivo*. The dsRNA-*PmAgo1-4* were run on 1.4% agarose gel electrophoresis. Marker is 100 bp DNA ladder (Thermo Scientific).

3.2.3 Silencing of *PmAgo* genes using specific dsRNAs

To study the importance of *PmAgo* genes in miR-750 biogenesis, the *PmAgo* genes expression were suppressed by dsRNA mediated gene silencing approach. The 10 g *P. monodon* shrimp were injected with dsRNA. Then, shrimp stomach was collected, and total RNA extraction was performed using Trizol reagent. The injection of *dsRNA-PmAgo3 in vivo* at dosage of 15 µg/g shrimp could suppressed *PmAgo3* expression at 24- and 48-hpi (Figure 29) and could be used for further investigation of miR-750 biogenesis on miR-750 target gene expression. However, the suppression of *PmAgo1* and *PmAgo2* in stomach was not successfully.

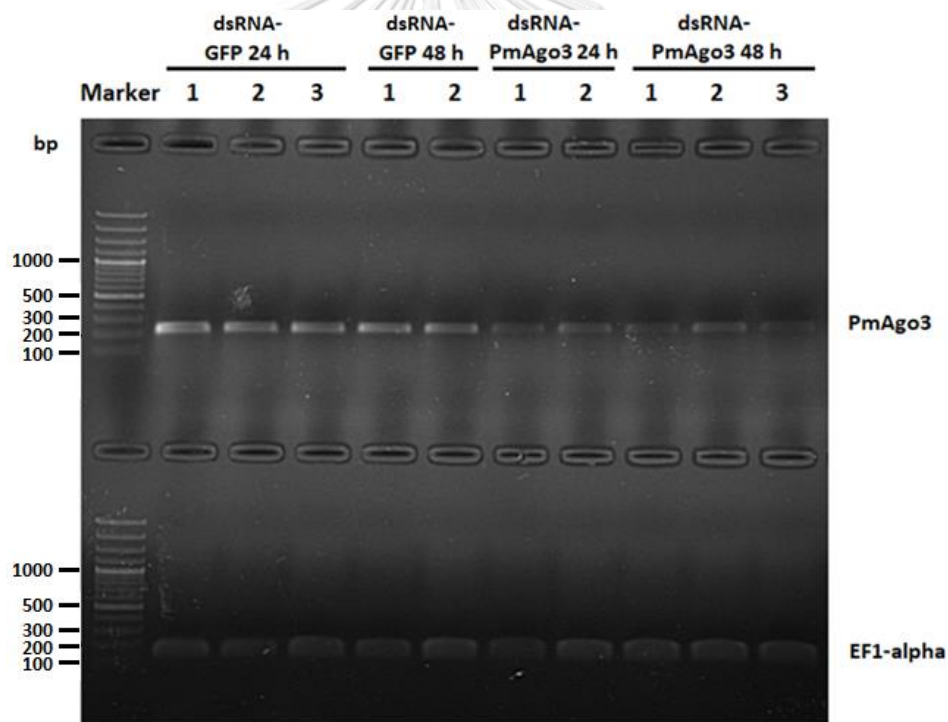
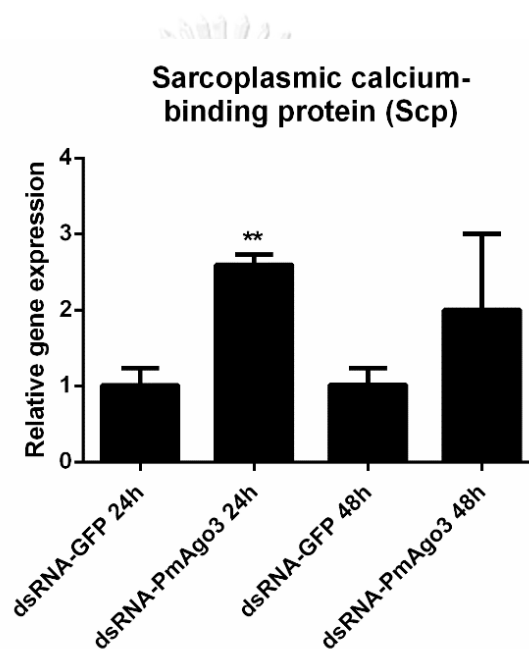


Figure 29 Knockdown of *PmAgo3* gene in *P. monodon* stomach at 24- and 48-h post dsRNA-*PmAgo3* infection. The amount of *PmAgo3* gene in the stomach of 10 g *P. monodon* was determined by semi-quantitation RT-PCR. The control group was injected with dsRNA-GFP. EF1-alpha was used as an internal control for equal loading. Marker is 100 bp DNA ladder (Thermo Scientific).

To investigate if *PmAgo3* gene interact to miR-750, the expression of miR-750 target gene, *Scp*, was determined in dsRNA-*PmAgo3* challenged shrimp by qRT-PCR (Figure 30). We hypothesized that the upregulation of miR-750 target gene should be observed in *PmAgo3* suppression if *PmAgo3* is involved in miR-750 biogenesis. The result showed that *Scp* was significantly up-regulated at 24 h after *PmAgo3* suppression (Figure 30). This result implies that *PmAgo3* involved in miR-750 biogenesis.



CHULALONGKORN UNIVERSITY

Figure 30 The relative gene expression of miR-750 target gene upon *PmAgo3* silencing in *P. monodon*. The normal shrimp was injected with the dsRNA-GFP or dsRNA-*PmAgo3* *in vivo*. The *Scp* gene expression was determined in stomach of 10 g dsRNA-*PmAgo3* challenged *P. monodon* at 24- and 48-h post injection (hpi). The experiments were done in triplicate. The significantly difference relative gene expression was indicated by ** which $P < 0.01$.

3.3 Study of miR-750 function against WSSV-infected shrimp

In order to reveal the role of miR-750 in WSSV infection in shrimp, the miR-750 was suppressed or overexpressed in WSSV-infected shrimp. Then, the evaluation of virus infection was performed by determination of WSSV copy number. Furthermore, the shrimp immune-related genes from several systems in shrimp innate immunity including *ALFPm3*, *ALFPm6*, *PEN5*, *SWDPm2*, *PmKunitz*, *PmCasp*, *PmCaspase3*, *PmDorsal*, *PmMyD88*, *PmCactus*, *PmRelish*, *PmlKK β* and *PmlKK ϵ* were analyzed for their expression by qRT-PCR.

3.3.1 miR-750 overexpression or silencing in WSSV-infected shrimp

P. monodon size of about 3 g were divided into 4 groups including 0.85% NaCl, WSSV infection, miR-750 overexpression in WSSV-infected shrimp, and miR-750 overexpression. The WSSV solution with the dosage that causes 100% shrimp death within three days (1×10^8 copies/shrimp) was injected into shrimp. For the miR-750 overexpression, shrimp was injected with 2 nmole miR-750 mimic. After stomach collection and total RNA extraction, miR-750 expression was determined at 24 and 48 hpi using qRT-PCR (Figure 31).

The results revealed that, the level miR-750 was highly up-regulated in WSSV-infected group at 48 hpi when compare to the control 0.85% NaCl. Moreover, the miR-750 overexpression in WSSV-infected shrimp, the miR-750 expression was much higher than WSSV infection alone.

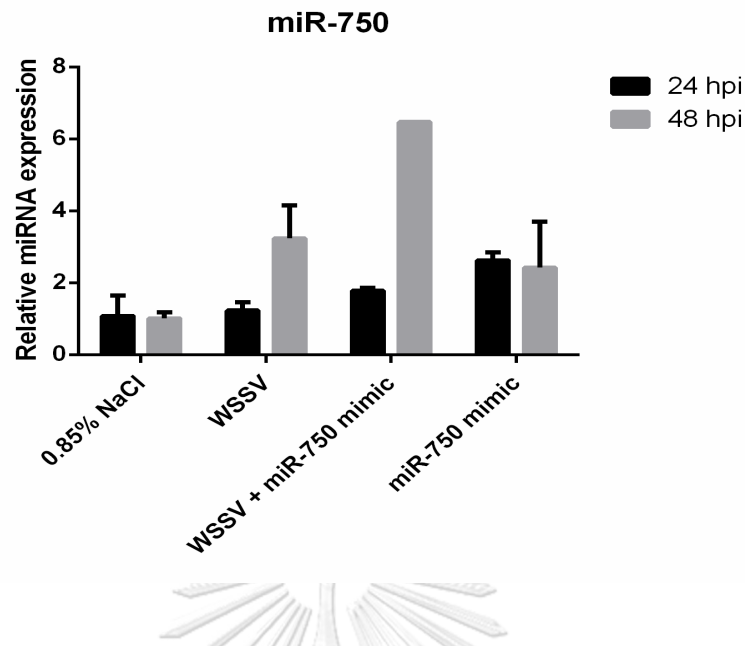


Figure 31 The relative miR-750 expression in WSSV challenge-shrimp stomach at 24 and 48 hpi. This experiment was divided into 4 groups. The 3 g shrimp was challenged with 0.85% NaCl, WSSV, WSSV and miR-750 mimic, and miR-750 mimic. The stomach was collected at 24 and 48 hpi and used for expression analysis. The relative expression of miR-750 in shrimp stomach was determined using stem-loop qRT-PCR and normalized by U6.

To investigate the role of miR-750 in WSSV-infected shrimp, WSSV-infected shrimp was challenged with miR-750 mimic, miR-750 SC, miR-750 AMO, and miR-750 AMO SC. After 48 hpi, shrimp stomach was collected, followed by total RNA extraction. The qRT-PCR technique was used to investigate shrimp immune-related genes expression, *Scp* gene expression, and miR-750 expression. Additionally, the genomic DNA was extracted from gill tissue and used for determining the WSSV copy number. The results showed that the expression of *Scp* showed the negative correlation to miR-750 expression which was down-regulated in miR-750 overexpression and up-regulated in miR-750 suppression. It indicated that *Scp* was highly possibility to be miR-750 target gene.

On the other hand, the expression of miR-750 was silenced by miR-750 AMO resulting in the reduction 50% of WSSV copy number compared to the controls (WSSV and WSSV + miR-750 AMO scramble). While miR-750 overexpression upon miR-750 mimic injection increases the WSSV copy number when compares to the controls (WSSV and WSSV + miR-750 SC). It was implied that miR-750 facilitated WSSV infection in shrimp (Figure 32).



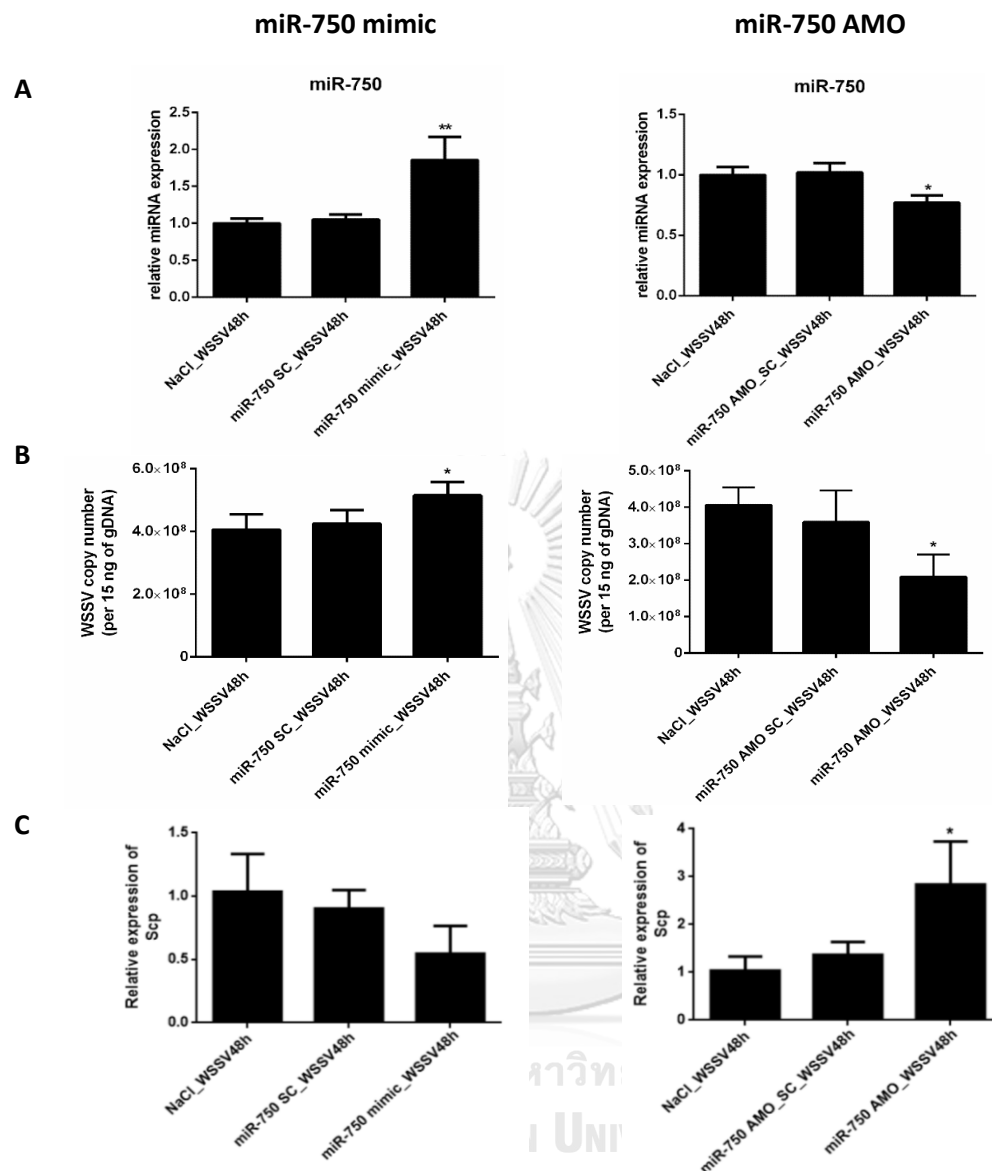


Figure 32 The influence of miR-750 overexpression or silencing on WSSV copy number. In this experiment, shrimp were divided into 5 groups, 3 shrimp of each experimental group were injected with miR-750 mimic and miR-750 AMO and the control groups were injected with 0.85% NaCl, miR-750 SC and miR-750 AMO SC. The stomach was collected at 48 hpi. The expression of miR-750 (A) and *Scp* (C) in shrimp stomach were analyzed by qRT-PCR. Their relative expression were normalized by U6 and EF1-alpha, respectively. The WSSV copy number in shrimp gills (B) was investigated. The experiments were done in triplicate. The * and ** indicate the significant difference at $P < 0.05$ and $P < 0.01$, respectively.

3.3.1 The effect of miR-750 overexpression and suppression on shrimp immune gene expression

After shrimp were challenged with miR-750 mimic and miR-750 AMO to miR-750 overexpress or silence miR-750 *in vivo*, the selected shrimp immune-related genes including *ALFPm3*, *ALFPm6*, *PEN5*, *SWDPm2*, *PmKunitz*, *PmCasp*, *PmCaspase*, *PmDorsal*, *PmMyD88*, *PmCactus*, *PmRelish*, *PmIKK β* and *PmIKK ϵ* were examined for mRNA expression level using qRT-PCR. The results indicated that *ALFPm3* and *ALFPm6* were dramatically down-regulated in miR-750 suppression by miR-750 AMO when compare to the control (WSSV-infected shrimp) but their expression levels were not significantly changed in miR-750 overexpression while the *SWDPm2* expression were upregulated in miR-750 silencing. Moreover, *PEN5* was down-regulated in miR-750 overexpression suggesting that miR-750 overexpression might have an effect on antimicrobial peptide expression. Interestingly, *PmCasp* and *PmCaspase* were downregulated in miR-750 overexpression while the *PmCaspase* showed the upregulation in the absent of miR-750, these results indicated that the presence of miR-750 also affected apoptosis-related gene. However, the expressions of the others were not altered (Figure 33).

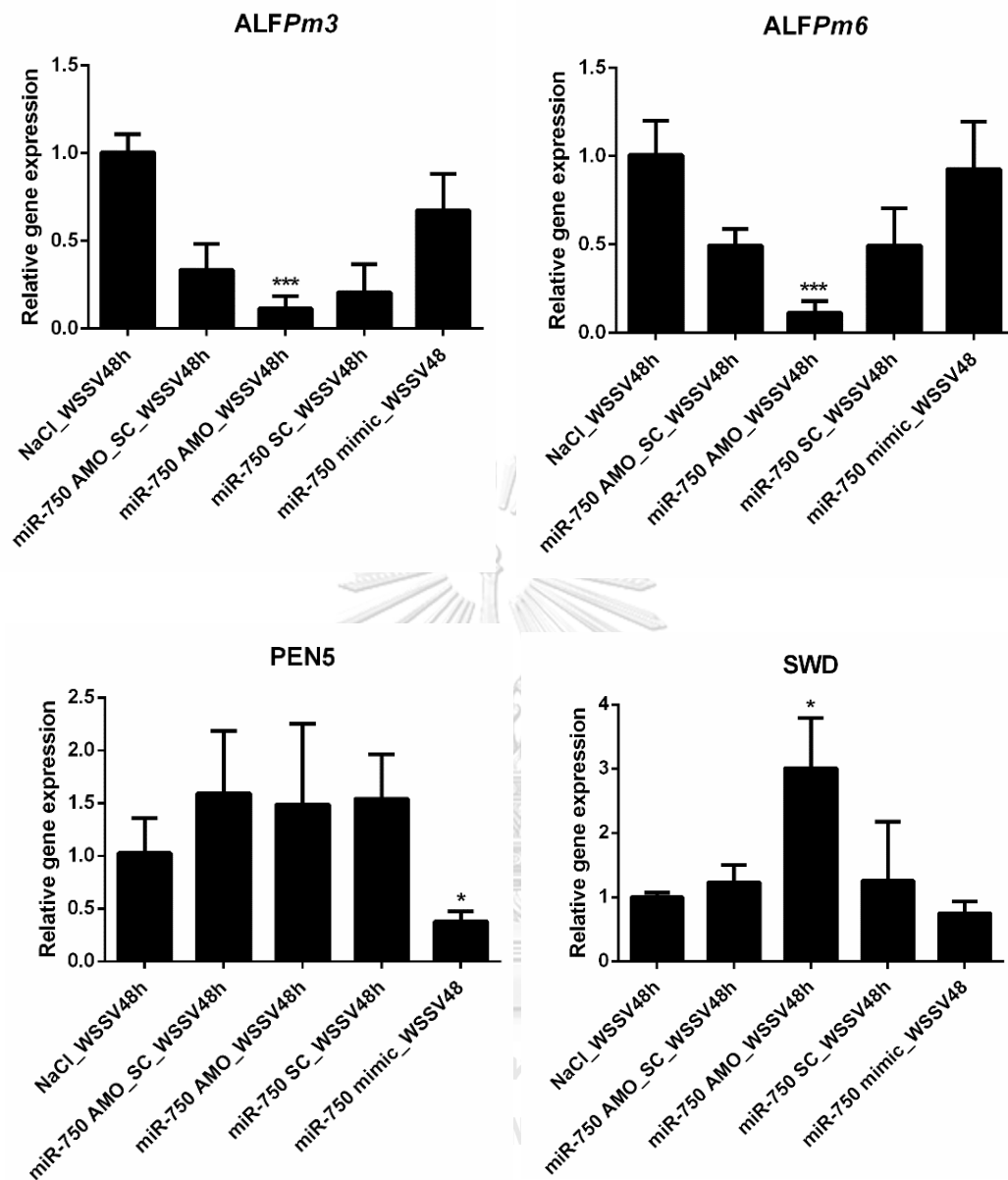


Figure 33 The effect of miR-750 overexpression and suppression in WSSV-infected shrimp on immune-related genes expression. Shrimp were divided into 5 groups, 3 shrimp of each experimental group were injected with miR-750 mimic, miR-750 AMO and the control groups were injected with 0.85% NaCl, miR-750 SC and miR-750 AMO SC. The stomach was collected at 48 hpi. The expression of immune-related genes in shrimp stomach were analyzed using qRT-PCR. The EF1-alpha was used as an internal control. The experiments were done in triplicate. The * and *** indicate the significantly difference at $P < 0.05$ and $P < 0.001$, respectively.

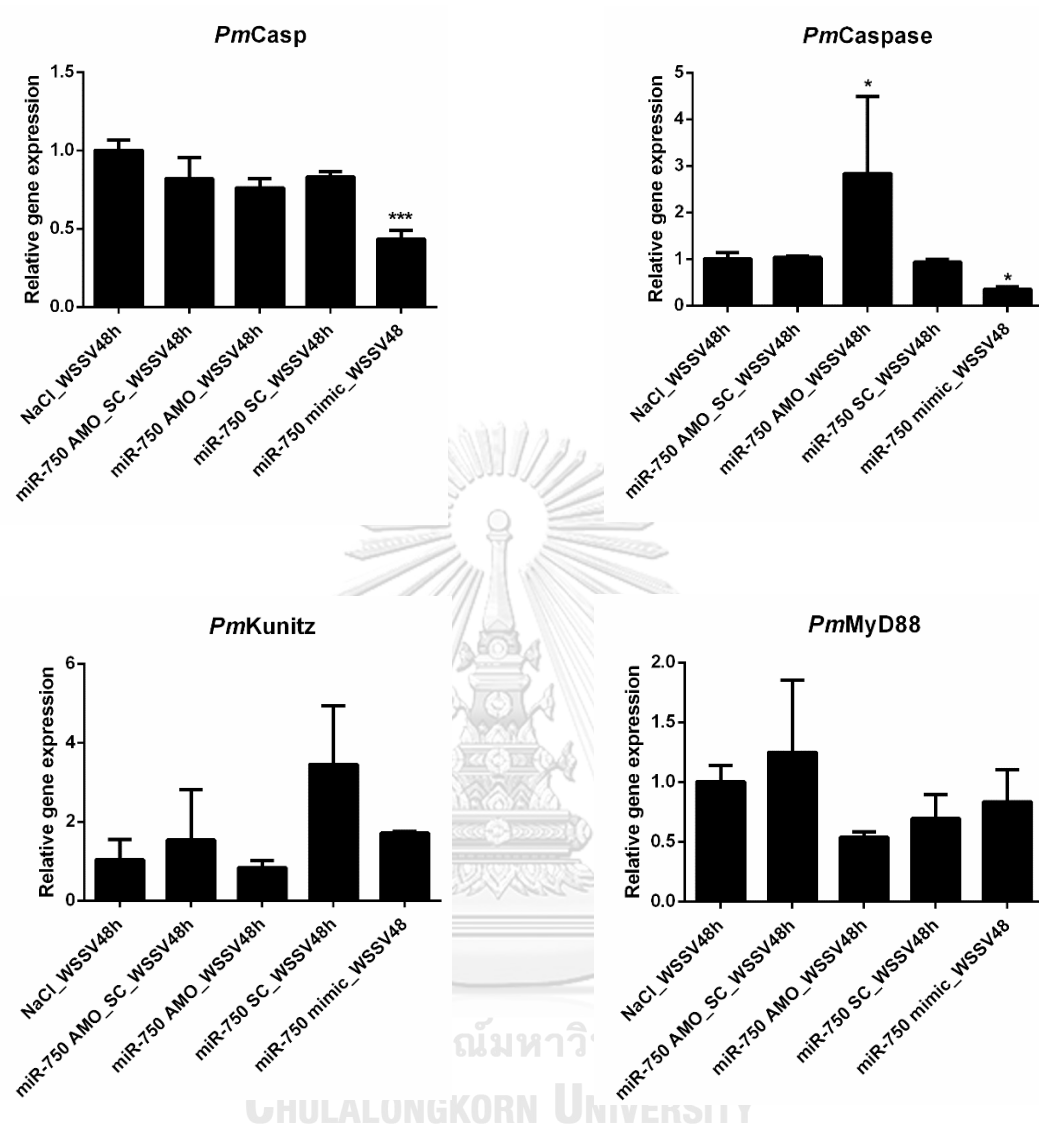


Figure 33 The effect of miR-750 overexpression and suppression in WSSV-infected shrimp on immune-related genes expression. Shrimp were divided into 5 groups, 3 shrimp of each experimental group were injected with miR-750 mimic, miR-750 AMO and the control groups were injected with 0.85% NaCl, miR-750 SC and miR-750 AMO SC. The stomach was collected at 48 hpi. The expression of immune-related genes in shrimp stomach were analyzed using qRT-PCR. The EF1-alpha was used as an internal control. The experiments were done in triplicate. The * and *** indicate the significantly difference at $P < 0.05$ and $P < 0.001$, respectively.

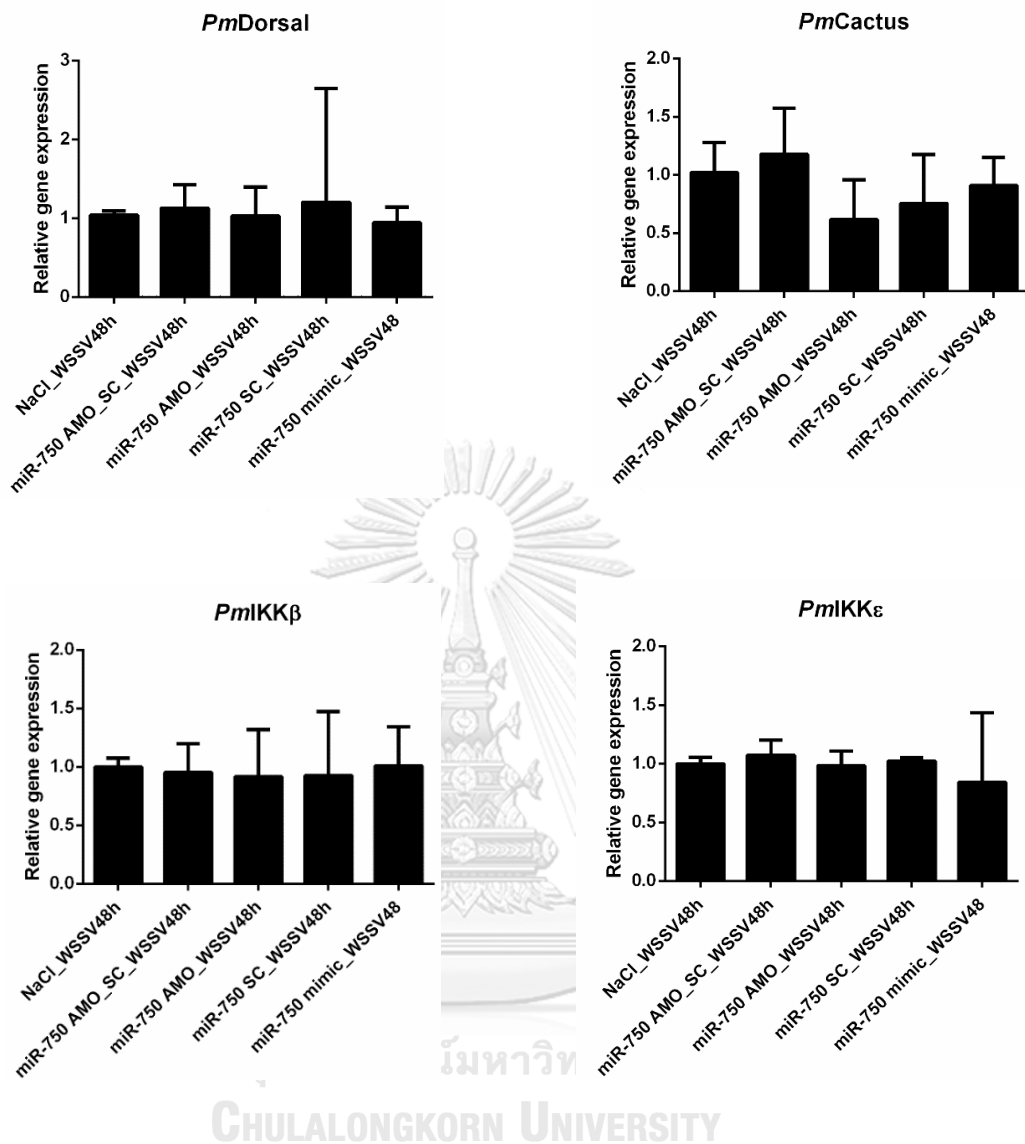


Figure 33 The effect of miR-750 overexpression and suppression in WSSV-infected shrimp on immune-related genes expression. Shrimp were divided into 5 groups, 3 shrimp of each experimental group were injected with miR-750 mimic, miR-750 AMO and the control groups were injected with 0.85% NaCl, miR-750 SC and miR-750 AMO SC. The stomach was collected at 48 hpi. The expression of immune-related genes in shrimp stomach were analyzed using qRT-PCR. The EF1-alpha was used as an internal control. The experiments were done in triplicate. The * and *** indicate the significantly difference at $P < 0.05$ and $P < 0.001$, respectively.

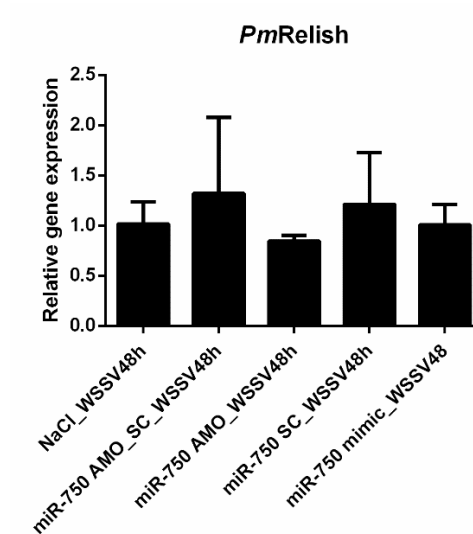


Figure 33 The effect of miR-750 overexpression and suppression in WSSV-infected shrimp on immune-related genes expression. Shrimp were divided into 5 groups, 3 shrimp of each experimental group were injected with miR-750 mimic, miR-750 AMO and the control groups were injected with 0.85% NaCl, miR-750 SC and miR-750 AMO SC. The stomach was collected at 48 hpi. The expression of immune-related genes in shrimp stomach were analyzed using qRT-PCR. The EF1-alpha was used as an internal control. The experiments were done in triplicate. The * and *** indicate the significantly difference at $P < 0.05$ and $P < 0.001$, respectively.

CHAPTER IV

DISCUSSION

MicroRNAs (miRNAs) serve as regulators in many cellular processes and are required in the virus-host interaction (Umbach and Cullen, 2009). The role of miRNAs in antiviral immunity has been studied in many researches. The host miRNAs and/or viral miRNAs are involved in virus infection processes in various ways. Virus regulates cellular response, in which the viral miRNAs has an influence on the virus infection (Jopling et al., 2006; Pfeffer et al., 2004) For instance, viral miRNAs regulate the expression of host miRNAs using host miRNA machinery in purpose to enhance viral replication (Hussain et al., 2008; Hussain et al., 2012; Singh et al., 2012; Singh et al., 2014; Zhou et al., 2014). In contrast, host miRNA regulate their own transcripts as well as viral mRNAs to control viral infection (Hussain and Asgari, 2010; Jayachandran et al., 2013; Zhao et al., 2014).

The first study on miRNA in penaeid shrimp was reported in 2011. Thirty-five miRNAs were identified in hemocyte of *Masupenaeus japonicus*. Among them, 22 miRNAs had differentially expression after WSSV infection (Ruan et al., 2011). In 2016, WSSV-responsive miRNAs from *P. monodon* hemocyte were identified using next-generation sequencing. According to the stem-loop real time RT-PCR, miR-315 and miR-750 were highly differentially expressed (Kaewkascholkul et al., 2016). This implied that they might play an important role in shrimp immunity against WSSV infection in *P. monodon* and the interested WSSV-responsive miR-750 was chosen for functional characterization in this study.

Previously, the functional characterization of miR-750 were studied in difference species. In *Heliothis virescens*, miR-750 was involved in cell developmental of nervous system (Chilana et al., 2013). Furthermore, miR-750 was

involved in olfactory transduction and regulation of actin cytoskeleton in *Apis mellifera* (Shi et al., 2015). Moreover, the upregulation of miR-750 after WSSV infection at 6 and 24 hpi was found in *M. japonicus* lymphoid organ (Huang et al., 2012) while miR-750 was downregulated in hemocyte at 24 and 48 h after *Vibrio alginolyticus* infection (Huang et al., 2012; Zhu et al., 2016). Even though the function and target genes of miR-750 were not clearly indicated the high upregulation of miR-750 was revealed to play important roles in the antiviral immunity of shrimp upon its expression after pathogen infection.

In order to characterize miR-750 function in the shrimp antiviral response against WSSV infection, two techniques including computational program analysis and 2-D gel electrophoresis (2-DE) were performed. The computational analysis of the miR-750 target genes using CU-Mir identified 140 possible target mRNAs. After filtered the results, the interesting shrimp immune related target genes were chosen for characterization including ubiquitin-conjugating enzyme E2 Q1 gene (*UbcQ1*) and vacuolar protein sorting-associated protein 53 gene (*VPS53*). *VPS53* gene is involved in autophagic process (Noda et al., 2012; Suwansa-Ard et al., 2016). In addition, *UbcQ1* is related to the ubiquitination reaction that targets a protein for degradation. According to the previous study, the protein expression profile of *P. monodon* ubiquitin conjugating enzyme E2 (*PmUbc*) in WSSV-challenged shrimp was up-regulated (Keezhedath et al., 2013). Moreover, the function of enzyme E2 have been studied in Chinese white shrimp indicating that the enzyme E2 reduced the shrimp mortality after WSSV infection and inhibited WSSV replication resulting in the important against WSSV infection (Chen et al., 2011).

According to the prediction results, miR-750 was found to target on 3'-UTR and ORF region of *UbcQ1* and *VPS53*, respectively. Most of miRNAs target on 3'-UTR of mRNA but 3'-UTR is not the only binding region of miRNA because it also targets

on 5'-UTR or ORF of mRNA (Akbari Moqadam et al., 2013; Forman and Collier, 2010; Moretti et al., 2010). The fallibility from miRNA-target prediction might occurrence. Therefore, miRNA-target interactions should be verified using *in vitro* miRNA reporter assay and *in vivo* silencing or enhancing of miRNA in shrimp (Huang et al., 2014; Shu et al., 2016; Yang et al., 2017). The luciferase reporter assay was used to validate the miR-750 and *UbcQ1* interaction. Because of this sensitivity, luciferase assays have been particularly useful for functional genomics in cell-base assays, such as RNAi screening, and benefit for miRNA-target interaction analysis (Yun and Dasgupta, 2014). The luciferase activity between miR-750 and *UbcQ1* was not reduced as expected when compare with the controls. The result indicated that miR-750 might not directly target *UbcQ1*.

The criteria of perfect complementary match at seed sequence used for the computational prediction limited our finding. Generally, the mismatch of seed sequence miRNA against mRNA may also happen because of perfect seed base-pairing is not an essential factor (Chi et al., 2012; Shin et al., 2010). In purpose of increasing the probability of miRNA target gene identification, 1 mismatch at seed sequence was allowed and used in CU-Mir software for miRNA target gene prediction, higher number of target genes (241 sequences) were identified and classified into 18 categories using GO annotation. Among them, 20 predicted genes were involved in shrimp immunity.

The other technique that can be used for miRNA target identification is 2-DE. Previously, this technique was used to identify the target of *Bombyx mori* nucleopolyhedrosis virus (BmNPV)-encoded miRNA miR-415 (BmNPV-miR-415). After BmNPV-miR-415 was transfected in BmN cells, the rapamycin isoform 2 (TOR2) was up-upregulated. However, the result confirmation showed that TOR2 is not directly a target gene of BmNPV-miR-415 (Cao et al., 2017). Moreover, this 2-DE technique was

also used to identify miR-187 which significantly downregulated in prostate cancer (PCa). The 2-DE result showed 7 down-regulated expression protein upon miR-187 overexpression. Among them, aldehyde dehydrogenase 1A3 (*ALDH1A3*) was characterized as miR-187 target (Casanova-Salas et al., 2015). This proteomic approach was applied to investigate the target of miRNA at protein level in the presence of enhancing miRNA due to the fact that miRNA can bind to the target gene resulting in translational repression or degradation of mRNA transcript (Bushati and Cohen, 2007; Hutvagner and Zamore, 2002; Martinez and Tuschl, 2004). We expected that the protein expression level of miRNA target should decrease after mimic miRNA injection and increase after mimic miRNA AMO injection. The spots identified based on this assumption were selected as possible of miRNA targets. Moreover, the protein spots which were up-regulated after mimic miRNA injection and down-regulated after mimic miRNA AMO injection were also selected because the effect of miRNA even if it might not be directly targeted (Patil et al., 2015). This is first report on miRNA target identification using 2-DE technique in shrimp.

We examined the protein expression profiling of stomach tissue in miR-750 mimic-challenged *P. monodon* at 24 h. The altered proteins which follow the assumption were selected and annotated. Five downregulated protein spots, and 8 upregulated protein spots after miR-750 mimic injection were identified by 2-DE. According to the MS results, 3 protein spots including spot ID 281, 348 and 443 were successfully annotated as Tropomyosin (*Tpm*), Sarcoplasmic calcium-binding protein (*Scp*) and Chymotrypsin (*Ctr*), respectively. However, some of the spots were identified as the same proteins. For instance, two spots ID 180 and 444 presented the same protein hit Hemocyanin (*Hc*) while the other 8 protein spots including spot ID 244, 246, 357, 360, 382, 458, 578 and 589 were Actin1 (*Act1*). This may have resulted from different isoforms or other post-translational modifications (Chai et al.,

2010; Chaikerasitak et al., 2012; Fan et al., 2013; Zhu et al., 2018a). Western blot analysis should be further performed to confirm protein expression level. However, these 5 proteins Actin1, Chymotrypsin, Hemocyanin, Sarcoplasmic calcium-binding protein and Tropomyosin were differentially expressed in the effect of miR-750 overexpression or silencing indicating that these proteins might involve in miR-750 and involve in shrimp immunity due to their function.

Four proteins including Actin1, Hemocyanin, Sarcoplasmic calcium-binding protein and Tropomyosin were found as differential expressed allergy-related proteins during WSSV infection (Hernandez-Perez et al., 2019). Interestingly, Tropomyosin functions in actin filaments regulation, muscle contraction and cell function (Gunning et al., 2005). The involvement of Actin1 in viral infection was reported in several researches. Actin1 interacts with viral proteins during their lifecycle like attachment, internalization and replication (Cudmore et al., 1997; Sodeik, 2000). Moreover, polymerization of Actin 2 is an important process in phagocytosis in multicellular organism in innate immune response (Kaplan, 1977). Furthermore, Actin might mediate the viral movement by interacting with VP26 after WSSV infection and fusion into the host cytoplasm (Xie and Yang, 2005). All these data suggested that the cytoskeletal system had a close relationship against WSSV infection, which might participate in transporting viral proteins (Zhu et al., 2018b). From our result, the expression of *Act1* and *Tpm* at transcriptional level was determined in WSSV-infected shrimp stomach using qRT-PCR. The expression profiles showed the downregulation of *Act1* and *Tpm* at 24 hpi whereas miR-750 expression was up-regulated at 24 hpi. However, the luciferase reporter assay revealed that miR-750 might not interact with *Act1* and *Tpm* indicating that *Act1* and *Tpm* might not miR-750 target gene but important to WSSV infection in shrimp.

For Hemocyanin, this protein involved in oxygen transport within the hemolymph and related in antiviral innate immunity which was upregulated after WSSV infection (Coates and Nairn, 2014). In the previous study, the one of the up-regulated protein spots in serum of WSSV-infected *L. vannamei* analysis by 2-DE was identified as hemocyanin (LvHcL48). The LvHcL48 significantly inhibited the transcription of the WSSV genes wsv069 and wsv421 coupled with a significant reduction in WSSV copy numbers (Zhan et al., 2019). From our result, the *Hc* gene expression was up-regulated in WSSV-infected shrimp stomach at 24 hpi which not correlation to miR-750 indicating that *Hc* gene might not miR-750 target gene but response to WSSV infection.

Chymotrypsin is a serine protease participated in a wide range of biological reactions such as degradative processes, blood clotting, humoral and cellular immunities (Krem and Di Cera, 2002). In the previous research, the chymotrypsin suppression reduced shrimp mortality and WSSV copy number in *F. chinensis*. Moreover, chymotrypsin was activated during apoptosis and was likely to participate in the process of virus propagation of WSSV infection (Grabarek et al., 2002; Xue et al., 2013). From our result, the protein level of chymotrypsin was up-regulated after miR-750 mimic injection. The interaction confirmation of miR-750 and *Ctr* gene using luciferase reporter assay indicated that *Ctr* gene might not directly target by miR-750. However, chymotrypsin involves in shrimp immunity and important to WSSV infection.

Sarcoplasmic calcium-binding protein is a protein that participates in calcium cell signaling pathways by binding to calcium ion which play important role in many cellular process and has a function in facilitating WSSV infection (Biradar et al., 2013). This protein is a cytosolic EF-hand-type calcium binding protein (Cox, 2013; Gao et al., 2006; Ikura, 1996) which has main function in maintenance the intracellular

calcium ion level as calcium ion buffering, regulation the amount of free (unbound) calcium ion in the cytosol of the cell, known as calcium homeostasis (Hermann and Cox, 1995). Our study showed that, *Scp* gene was down-regulated after WSSV infection and was regulated by miR-750 that are up-regulated in WSSV-infected *P. monodon*. The interaction between miR-750 and *Scp* was confirmation. This result indicated that *Scp* gene has a high possibility to be miR-750 target gene.

In WSSV infection, the viral proteins trigger calcium ion release from internal stores including endoplasmic reticulum (ER) or Golgi complex through receptor to the cytosol (Zhou et al., 2009). The low-level of sarcoplasmic calcium-binding protein, calcium ion buffering protein, might disrupt normal physiological function by interfering with the calcium homeostasis by increasing of free (unbound) calcium ion in cytosol (Rabah et al., 2005; Takashi, 1984). Moreover, viral proteins are capable of perturbing the intracellular calcium ion homeostasis by modulating calcium ion pumps and/or channels on the cell membrane and intracellular calcium storage such as ER resulting in the free cytosolic calcium ion rapidly increases by the entry into the cytosol. The viral proteins (e.g. the proteins encoded by WSSV ORFs 136 and 486 in GenBank Accession No. AF440570) contain an EF-hand calcium-binding motif take over the increasing of calcium ion in cytosol to their benefit in the replication cycle (Biradar et al., 2013; Wang et al., 2007). On the other hand, the calcium ion homeostasis also involves in apoptosis pathway. The release of calcium ion from ER through the inositol trisphosphate (IP₃) receptor resulted in transmission of calcium ion to surrounding mitochondria that are uptaken by the mitochondria. The accumulation of calcium ion in the mitochondria leads to the mitochondrial membrane permeabilization by stimulating the opening of the mitochondrial permeability transition pore (mPTP, Orrenius et al., 2003) resulting in the release of pro-apoptotic factors, in particular cytochrome c which trigger apoptosis pathway.

When WSSV infection occur, the ER calcium ion storage is perturbed as discuss above. The low level of calcium ion in the ER resulting in the down-regulated ER-mitochondria calcium ion signaling which reduce the calcium ion level in mitochondria and inhibit apoptosis pathway (Pinton et al., 2000). Our results suggesting that the miR-750 was up-regulated after WSSV infection *P. monodon* and inhibited the sarcoplasmic calcium-binding protein which perturb the calcium ion homeostasis and might suppress apoptotic pathway facilitating WSSV infection. The decrease of copy number after miR-750 mimic silencing and the increase in WSSV copy number after miR-750 mimic overexpression also confirmed this speculation.

To investigate the influence of miR-750 on shrimp response during WSSV infection, the expression levels of shrimp immune genes of antimicrobial peptide (ALFPm3, ALFPm6, PEN5 and SWDPm2), Toll pathway (*PmDorsal*, *PmMyD88* and *PmCactus*), IMD pathway (*PmRelish*, *PmIKK β* and *PmIKK ϵ*), serine proteinase inhibitors (*PmKunitz*) and apoptosis pathway (*PmCasp*, *PmCaspase3*) were determined in the miR-750 silenced or enhanced WSSV-infected shrimp stomach. ALFPm3 and ALFPm6 were down-regulated in miR-750 silencing during WSSV infection. Previously, ALFPm3 function in reduction the WSSV propagation and prolonging the survival of shrimp (Ponprateep et al., 2012; Tharntada et al., 2009a). However, the effect of miR-750 against ALFPm3 and ALFPm6 was not clear due to the unexpected decrease of ALFPm3 and ALFPm6 expression in miR-750 scramble and miR-750 AMO scramble challenged group indicating that miR-750 might not be involved in ALFPm3 and ALFPm6 regulation.

Previously, SWDPm2 gene was up-regulated at 6 h and down-regulated at 24 h after WSSV infection (Amparyup et al., 2008). The silencing of SWD significantly accelerated the death of the WSSV-infected (Yang et al., 2018). When considered with the upregulated expression of SWDPm2 and the decrease of WSSV copy

number in the miR-750-silenced shrimp, and the decrease of *SWDPm2* expression in late phase of WSSV infection, miR-750 might control the *SWDPm2* expression of WSSV infection.

PEN5 was down-regulated in the enhancing of miR-750 during WSSV infection. Previously report revealed that the suppression of PEN5 transcript levels by RNA interference mediated gene silencing led to an increase of WSSV infection in *P. monodon* (Woramongkolchai et al., 2011). When considered with the increase of WSSV copy number in enhancing of miR-750 mimic and decrease of PEN5 indicating that miR-750 might indirectly control PEN5 expression in order to facilitate WSSV infection.

Furthermore, miR-750 influences the expression of two different effector caspase genes (*PmCasp* and *PmCaspase*). Caspases are the important effector molecules that mediate the apoptotic process. In WSSV-infected shrimp, expression of *PmCasp* was increased at both RNA and protein levels in the gills, reaching maximal levels at 48 hpi, whereas the expression of *PmCaspase* was not significantly changed in pleopods (Leu et al., 2008; Wongprasert et al., 2007). Suppression of the *PjCaspase* gene of *M. japonicus* leads to the inhibition of apoptosis following WSSV infection and an increase in the WSSV copy number (Wang et al., 2008). The model of apoptotic interaction between WSSV and shrimp has been reported. When a WSSV infection occurs, cellular sensors detect the invading virus, and activate signaling pathways that lead to the expression of apoptosis protein including an effector caspase and initiate the apoptosis program. Then, WSSV induces the expression of a shrimp anti-apoptosis protein to inhibit mitochondria-triggered apoptosis because the virus needs to prevent apoptosis in order to replicate. After WSSV succeeds in replicating in sufficient numbers, the infected penaeid shrimp was death (Leu et al., 2013). According to our result, *PmCasp* and *PmCaspase* were significantly down-

regulated in miR-750 overexpression suggesting that miR-750 might cause inhibition of apoptosis in order to promote WSSV infection.

In conclusions, during WSSV infection, the *Scp* was targeted by miR-750 led to the perturbation of calcium ion homeostasis facilitating viral replication. This result also indicated that the perturbation of calcium ion homeostasis might reduce of AMPs (PEN5) production and inhibit apoptosis process in order to promote WSSV replication.



CHAPTER IV

CONCLUSIONS

1. Bioinformatic analysis suggested that the predicted target mRNA of miR-750 were *UbcQ1*, *Act1* and *Scp*.
2. Proteomic analysis has successfully identified the differential expressed proteins in the stomach of miR-750-mimic challenged *P. monodon*. The 5 down-regulated protein spots were annotated as *Act1*, *Hc*, *Scp* and *Tpm* while the 8 up-regulated protein spots were annotated as *Act1*, *Ctr* and *Hc*.
3. The relative gene expression analysis by qRT-PCR of candidate miR-750 target genes indicating that *Scp* was down-regulated in WSSV-infected *P. monodon* stomach indicating the negative correlation to miR-750 expression.
4. The miR-750/mRNA interaction was confirmed by dual luciferase reporter assay. The luciferase activity of *Scp* target sequence was reduced for 20% suggesting that *Scp* is the miR-750 target gene.
5. Suppression of *PmAgo3* gene increased the expression of the miR-750 target gene, *Scp*, suggesting that *PmAgo3* might involve in miR-750 biogenesis.
6. In miR-750 mimic challenged WSSV-infected shrimp, the expression of miR-750 and its target gene, *Scp*, was analyzed. The expression of *Scp* showed negative correlation to miR-750 expression which was decrease whereas miR-750 was increased as expected.
7. Overexpression of miR-750 led to the significant high level of WSSV copy number while silencing of miR-750 led to the significant low level of WSSV copy number in WSSV-infected shrimp.
8. The immune related gene including PEN5, *PmCasp*, and *PmCaspase* was down-regulated in miR-750 overexpression of WSSV-infected *P. monodon* stomach when compared with that of the control WSSV-infected group.

9. During WSSV infection, the *Scp*, that are involved in calcium ion homeostasis, was targeted by the up-regulated miR-750 led to the perturbation of calcium ion homeostasis making a cellular environment that benefits virus life cycles.



REFERENCES

- Akbari Moqadam, F., R. Pieters, and M.L. den Boer. 2013. The hunting of targets: challenge in miRNA research. *Leukemia*. 27:16-23.
- Alexiou, P., M. Maragkakis, G.L. Papadopoulos, M. Reczko, and A.G. Hatzigeorgiou. 2009. Lost in translation: an assessment and perspective for computational microRNA target identification. *Bioinformatics*. 25:3049-3055.
- Amodio, G., E. Sasso, C. D'Ambrosio, A. Scaloni, O. Moltedo, S. Franceschelli, N. Zambrano, and P. Remondelli. 2016. Identification of a microRNA (miR-663a) induced by ER stress and its target gene PLOD3 by a combined microRNome and proteome approach. *Cell biology and toxicology*:1-19.
- Amparyup, P., S. Donpuksa, and A. Tassanakajon. 2008. Shrimp single WAP domain (SWD)-containing protein exhibits proteinase inhibitory and antimicrobial activities. *Developmental & Comparative Immunology*. 32:1497-1509.
- Attasart, P., R. Kaewkhaw, C. Chimwai, U. Kongphom, and S. Panyim. 2011. Clearance of *Penaeus monodon* densovirus in naturally pre-infected shrimp by combined ns1 and vp dsRNAs. *Virus Research*. 159:79-82.
- Bachère, E., Y. Gueguen, M. Gonzalez, J. De Lorgeril, J. Garnier, and B. Romestand. 2004. Insights into the anti-microbial defense of marine invertebrates: the penaeid shrimps and the oyster *Crassostrea gigas*. *Immunological Reviews*. 198:149-168.
- Bartel, D.P. 2004. MicroRNAs: Genomics, biogenesis, mechanism, and function. *Cell*. 116:281-297.
- Best, S.M. 2008. Viral subversion of apoptotic enzymes: escape from death row. *Annual Review of Microbiology*. 62:171-192.
- Best, S.M., and M.E. Bloom. 2004. Caspase activation during virus infection: more than just the kiss of death? *Virology*. 320:191-194.
- Biradar, V., S. Narwade, M. Paingankar, and D. Deobagkar. 2013. White spot syndrome

- virus infection in *Penaeus monodon* is facilitated by housekeeping molecules. *Journal of Biosciences*. 38:917-924.
- Bohnsack, M.T., K. Czaplinski, and D. Gorlich. 2004. Exportin 5 is a RanGTP-dependent dsRNA-binding protein that mediates nuclear export of pre-miRNAs. *RNA*. 10:185-191.
- Bushati, N., and S.M. Cohen. 2007. MicroRNA functions. *Annual Review of Cell and Developmental Biology*. 23:175-205.
- Cao, X., Y. Huang, D. Xia, Z. Qiu, X. Shen, X. Guo, and Q. Zhao. 2017. BmNPV-miR-415 up-regulates the expression of TOR2 via Bmo-miR-5738. *Saudi Journal of Biological Sciences*. 24:1614-1619.
- Casanova-Salas, I., E. Masiá, A. Armiñán, A. Calatrava, C. Mancarella, J. Rubio-Briones, K. Scotlandi, M.J. Vicent, and J.A. López-Guerrero. 2015. MiR-187 targets the androgen-regulated gene ALDH1A3 in prostate cancer. *PloS One*. 10:e0125576.
- Chai, Y.-M., S.-S. Yu, X.-F. Zhao, Q. Zhu, and J.-X. Wang. 2010. Comparative proteomic profiles of the hepatopancreas in *Fenneropenaeus chinensis* response to white spot syndrome virus. *Fish & Shellfish Immunology*. 29:480-486.
- Chaikeeratisak, V., K. Somboonwiwat, H.C. Wang, C.F. Lo, and A. Tassanakajon. 2012. Proteomic analysis of differentially expressed proteins in the lymphoid organ of *Vibrio harveyi*-infected *Penaeus monodon*. *Molecular Biology Reports*. 39:6367-6377.
- Chen, A.J., S. Wang, X.F. Zhao, X.Q. Yu, and J.X. Wang. 2011. Enzyme E2 from Chinese white shrimp inhibits replication of white spot syndrome virus and ubiquitinates its RING domain proteins. *Journal of Virology*. 85:8069-8079.
- Chi, S.W., G.J. Hannon, and R.B. Darnell. 2012. An alternative mode of microRNA target recognition. *Nature Structural & Molecular Biology*. 19:321-327.
- Chilana, P., A. Sharma, V. Arora, J. Bhati, and A. Rai. 2013. Computational identification

- and characterization of putative miRNAs in *Heliothis virescens*. *Bioinformation*. 9:2-6.
- Chou, H.Y., C.Y. Huang, C.H. Wang, H.C. Chiang, and C.F. Lo. 1995. Pathogenicity of a baculovirus infection causing white spot syndrome in cultured penaeid shrimp in Taiwan. *Diseases of Aquatic Organisms*. 23:165-173.
- Coates, C.J., and J. Nairn. 2014. Diverse immune functions of hemocyanins. *Developmental & Comparative Immunology*. 45:43-55.
- Cox, J. A. (2013). Sarcoplasmic Calcium-Binding Protein Family: SCP, Calerythrin, Aequorin, and Calexcitin. *Encyclopedia of Metalloproteins*, 1875-1881.
- Cudmore, S., I. Reckmann, and M. Way. 1997. Viral manipulations of the actin cytoskeleton. *Trends in Microbiology*. 5:142-148.
- Dechklar, M., A. Udomkit, and S. Panyim. 2008. Characterization of Argonaute cDNA from *Penaeus monodon* and implication of its role in RNA interference. *Biochemical and Biophysical Research Communications*. 367:768-774.
- Dierberg, F.E., and W. Kiattisimkul. 1996. Issues, impacts, and implications of shrimp aquaculture in Thailand. *Environmental Management*. 20:649-666.
- Ding, S.W., and O. Voinnet. 2007. Antiviral immunity directed by small RNAs. *Cell*. 130:413-426.
- Ding, S.W. 2010. RNA-based antiviral immunity. *Nature Reviews Immunology*. 10:632-644.
- Dostie, J., Z. Mourelatos, M. Yang, A. Sharma, and G. Dreyfuss. 2003. Numerous microRNPs in neuronal cells containing novel microRNAs. *RNA*. 9:180-186.
- Durand, S., D.V. Lightner, R.M. Redman, and J.R. Bonami. 1997. Ultrastructure and morphogenesis of white spot syndrome baculovirus (WSSV). *Diseases of Aquatic Organisms*. 29:205-211.
- Everett, H., and G. McFadden. 1999. Apoptosis: an innate immune response to virus

- infection. *Trends in Microbiology*. 7:160-165.
- Fan, L., A. Wang, and Y. Wu. 2013. Comparative proteomic identification of the hemocyte response to cold stress in white shrimp, *Litopenaeus vannamei*. *Journal of Proteomics*. 80:196-206.
- Forman, J.J., and H.A. Collier. 2010. The code within the code: microRNAs target coding regions. *Cell Cycle*. 9:1533-1541.
- Fung, E., K. Hill, K. Hogendoorn, R.V. Glatz, K.R. Napier, M.I. Bellgard, and R.A. Barrero. 2018. De novo assembly of honey bee RNA viral genomes by tapping into the innate insect antiviral response pathway. *Journal of invertebrate pathology*. 152:38-47.
- Gao, Y., C.M. Gillen, and M.G. Wheatly. 2006. Molecular characterization of the sarcoplasmic calcium-binding protein (SCP) from crayfish *Procambarus clarkii*. *Comparative Biochemistry and Physiology Part B: Biochemistry and Molecular Biology*. 144:478-487.
- Görg, A., W. Weiss, and M.J. Dunn. 2004. Current two-dimensional electrophoresis technology for proteomics. *Proteomics*. 4:3665-3685.
- Grabarek, J., M. Dragan, B.W. Lee, G.L. Johnson, and Z. Darzynkiewicz. 2002. Activation of chymotrypsin-like serine protease(s) during apoptosis detected by affinity-labeling of the enzymatic center with fluoresceinated inhibitor. *International Journal of Oncology*. 20:225-233.
- Gronski, R. 2000. Shrimp culture in Thailand: environmental impacts and social responses. *New Solutions*. 10:367-376.
- Gunning, P.W., G. Schevzov, A.J. Kee, and E.C. Hardeman. 2005. Tropomyosin isoforms: diving rods for actin cytoskeleton function. *Trends in Cell Biology*. 15:333-341.
- Guo, Z., Y. Li, and S.W. Ding. 2018. Small RNA-based antimicrobial immunity. *Nature reviews Immunology*. 19:31-44.

- Ha, M., and V.N. Kim. 2014. Regulation of microRNA biogenesis. *Nature Reviews Molecular Cell Biology*. 15:509-524.
- Hammond, S.M., E. Bernstein, D. Beach, and G.J. Hannon. 2000. An RNA-directed nuclease mediates post-transcriptional gene silencing in *Drosophila* cells. *Nature*. 404:293-296.
- Hammond, S.M., A.A. Caudy, and G.J. Hannon. 2001. Post-transcriptional gene silencing by double-stranded RNA. *Nature Reviews Genetics*. 2:110-119.
- Hancock, R.E., and G. Diamond. 2000. The role of cationic antimicrobial peptides in innate host defences. *Trends in Microbiology*. 8:402-410.
- Hancock, R.E., and M.G. Scott. 2000. The role of antimicrobial peptides in animal defenses. *Proceedings of the National Academy of Sciences* 97:8856-8861.
- Hay, S., and G. Kannourakis. 2002. A time to kill: viral manipulation of the cell death program. *Journal of General Virology*. 83:1547-1564.
- He, Y., Y. Sun, and X. Zhang. 2017. Noncoding miRNAs bridge virusinfection and host autophagy in shrimpin vivo. *FASEB Journal*. 31:2854-2868.
- Hermann, A., and J.A. Cox. 1995. Sarcoplasmic calcium-binding protein. *Comparative Biochemistry and Physiology Part B: Biochemistry and Molecular Biology*. 111:337-345.
- Hernandez-Perez, A., J.A. Zamora-Briseno, E. Ruiz-May, A. Pereira-Santana, J.M. Elizalde-Contreras, S. Pozos-Gonzalez, E. Torres-Irineo, J. Hernandez-Lopez, M.G. Gaxiola-Cortes, and R. Rodriguez-Canul. 2019. Proteomic profiling of the white shrimp *Litopenaeus vannamei* (Boone, 1931) hemocytes infected with white spot syndrome virus reveals the induction of allergy-related proteins. *Developmental & Comparative Immunology*. 91:37-49.
- Huang, T., Y. Cui, and X. Zhang. 2014. Involvement of viral microRNA in the regulation of antiviral apoptosis in shrimp. *Journal of Virology*. 88:2544-2554.

- Huang, T., D. Xu, and X. Zhang. 2012. Characterization of host microRNAs that respond to DNA virus infection in a crustacean. *BMC genomics*. 13:1.
- Huang, X.D., Z.X. Yin, X.T. Jia, J.P. Liang, H.S. Ai, L.S. Yang, X. Liu, P.H. Wang, S.D. Li, S.P. Weng, X.Q. Yu, and J.G. He. 2010. Identification and functional study of a shrimp Dorsal homologue. *Developmental & Comparative Immunology*. 34:107-113.
- Hussain, M., and S. Asgari. 2010. Functional analysis of a cellular microRNA in insect host-ascovirus interaction. *Journal of Virology*. 84:612-620.
- Hussain, M., R.J. Taft, and S. Asgari. 2008. An insect virus-encoded microRNA regulates viral replication. *Journal of Virology*. 82:9164-9170.
- Hussain, M., S. Torres, E. Schnettler, A. Funk, A. Grundhoff, G.P. Pijlman, A.A. Khromykh, and S. Asgari. 2012. West Nile virus encodes a microRNA-like small RNA in the 3' untranslated region which up-regulates GATA4 mRNA and facilitates virus replication in mosquito cells. *Nucleic Acids Research*. 40:2210-2223.
- Hutvagner, G., and P.D. Zamore. 2002. A microRNA in a multiple-turnover RNAi enzyme complex. *Science*. 297:2056-2060.
- Ikura, M. (1996). Calcium binding and conformational response in EF-hand proteins. *Trends in biochemical sciences*. 21:14-17.
- Iwasaki, Y. W., Siomi. M.C., and Siomi H. 2015. PIWI-interacting RNA: its biogenesis and functions. *Annual review of biochemistry*. 84:405-433.
- Janeway, C.A., Jr. 1989. Approaching the asymptote? Evolution and revolution in immunology. *Cold Spring Harbor Symposia on Quantitative Biology*. 54 Pt 1:1-13.
- Jaree, P., C. Wongdontri, and K. Somboonwivat. 2018. White spot syndrome virus-induced shrimp miR-315 attenuates prophenoloxidase activation via PPAE3 gene suppression. *Frontiers in Immunology*. 9:2184-2199.
- Jayachandran, B., M. Hussain, and S. Asgari. 2013. Regulation of *Helicoverpa armigera*

- ecdysone receptor by miR-14 and its potential link to baculovirus infection. *Journal of Invertebrate Pathology*. 114:151-157.
- Jearaphunt, M., P. Amparyup, P. Sangsuriya, W. Charoensapsri, S. Senapin, and A. Tassanakajon. 2015. Shrimp serine proteinase homologues PmMasSPH-1 and -2 play a role in the activation of the prophenoloxidase system. *PLoS One*. 10:e0121073.
- Jiravanichpaisal, P., B.L. Lee, and K. Soderhall. 2006. Cell-mediated immunity in arthropods: hematopoiesis, coagulation, melanization and opsonization. *Immunobiology*. 211:213-236.
- Jopling, C.L., K.L. Norman, and P. Sarnow. 2006. Positive and negative modulation of viral and cellular mRNAs by liver-specific microRNA miR-122. *Cold Spring Harbor Symposia on Quantitative Biology*. 71:369-376.
- Kaewkascholkul, N., K. Somboonwiwat, S. Asakawa, I. Hirono, A. Tassanakajon, and K. Somboonwiwat. 2016. Shrimp miRNAs regulate innate immune response against white spot syndrome virus infection. *Developmental & Comparative Immunology*. 60:191-201.
- Kaplan, G. 1977. Differences in the mode of phagocytosis with Fc and C3 receptors in macrophages. *Scandinavian Journal of Immunology*. 6:797-807.
- Keezhedath, J., P.P. Kurcheti, M.K. Pathan, G.P. Babu, G. Tripathi, A. Sudhagar, and S.P. Rao. 2013. Expression profile of *Penaeus monodon* ubiquitin conjugating enzyme (PmUbc) at protein level in *white spot syndrome virus* challenged shrimp. *Indian Journal of Virology*. 24:48-53.
- Kim, C.S., Z. Kosuke, Y.K. Nam, S.K. Kim, and K.H. Kim. 2007. Protection of shrimp (*Penaeus chinensis*) against white spot syndrome virus (WSSV) challenge by double-stranded RNA. *Fish & Shellfish Immunology*. 23:242-246.
- Koyama, A.H., T. Fukumori, M. Fujita, H. Irie, and A. Adachi. 2000. Physiological

- significance of apoptosis in animal virus infection. *Microbes and Infection*. 2:1111-1117.
- Krem, M.M., and E. Di Cera. 2002. Evolution of enzyme cascades from embryonic development to blood coagulation. *Trends in Biochemical Sciences*. 27:67-74.
- Lee, Y., M. Kim, J.J. Han, K.H. Yeom, S. Lee, S.H. Baek, and V.N. Kim. 2004. MicroRNA genes are transcribed by RNA polymerase II. *EMBO Journal*. 23:4051-4060.
- Leu, J.H., S.J. Lin, J.Y. Huang, T.C. Chen, and C.F. Lo. 2013. A model for apoptotic interaction between white spot syndrome virus and shrimp. *Fish & Shellfish Immunology*. 34:1011-1017.
- Leu, J.H., H.C. Wang, G.H. Kou, and C.F. Lo. 2008. *Penaeus monodon* caspase is targeted by a white spot syndrome virus anti-apoptosis protein. *Developmental & Comparative Immunology*. 32:476-486.
- Li, C., Y.X. Chen, S. Zhang, L. Lu, Y.H. Chen, J. Chai, S. Weng, Y.G. Chen, J. He, and X. Xu. 2012. Identification, characterization, and function analysis of the Cactus gene from *Litopenaeus vannamei*. *PLoS One*. 7:e49711.
- Li, F., and J. Xiang. 2013. Recent advances in researches on the innate immunity of shrimp in China. *Developmental & Comparative Immunology*. 39:11-26.
- Liu, H., P. Jiravanichpaisal, I. Soderhall, L. Cerenius, and K. Soderhall. 2006. Antilipopopolysaccharide factor interferes with white spot syndrome virus replication *in vitro* and *in vivo* in the crayfish *Pacifastacus leniusculus*. *Journal of Virology*. 80:10365-10371.
- Lo, C.F., J.H. Leu, C.H. Ho, C.H. Chen, S.E. Peng, Y.T. Chen, C.M. Chou, P.Y. Yeh, C.J. Huang, H.Y. Chou, C.H. Wang, and G.H. Kou. 1996. Detection of baculovirus associated with white spot syndrome (WSBV) in penaeid shrimps using polymerase chain reaction. *Diseases of Aquatic Organisms*. 25:133-141.
- Martinez, J., and T. Tuschl. 2004. RISC is a 5' phosphomonoester-producing RNA

- endonuclease. *Genes & Development*. 18:975-980.
- May, C., F. Brosseron, P. Chartowski, C. Schumbrutzki, B. Schoenebeck, and K. Marcus. 2011. Instruments and methods in proteomics. *In Data Mining in Proteomics*. Springer. 3-26.
- McManus, M.T., and P.A. Sharp. 2002. Gene silencing in mammals by small interfering RNAs. *Nature Reviews Genetics*. 3:737-747.
- Mohan, C.V., K.M. Shankar, S. Kulkarni, and P.M. Sudha. 1998. Histopathology of cultured shrimp showing gross signs of yellow head syndrome and white spot syndrome during 1994 Indian epizootics. *Diseases of Aquatic Organisms*. 34:9-12.
- Moretti, F., R. Thermann, and M.W. Hentze. 2010. Mechanism of translational regulation by miR-2 from sites in the 5' untranslated region or the open reading frame. *RNA*. 16:2493-2502.
- Mussabekova, A., Daeffler. L., and Imler. J. L. 2017. Innate and intrinsic antiviral immunity in *Drosophila*. *Cellular and Molecular Life Sciences*. 74(11):2039-2054.
- Naitza, S., and P. Ligoxygakis. 2004. Antimicrobial defences in *Drosophila*: the story so far. *Molecular Immunology*. 40:887-896.
- Nils Kautsky, P.R., Michael Tedengren,, and M. Troell. 2000. Ecosystem perspectives on management of disease in shrimp pond farming. *Aquaculture*. 191:145-161
- Noda, N.N., T. Kobayashi, W. Adachi, Y. Fujioka, Y. Ohsumi, and F. Inagaki. 2012. Structure of the novel C-terminal domain of vacuolar protein sorting 30/autophagy-related protein 6 and its specific role in autophagy. *Journal of Biological Chemistry*. 287:16256-16266.
- Ongvarrasopone, C., Y. Roshorm, and S. Panyim. 2007. A Simple and Cost Effective Method to Generate dsRNA for RNAi Studies in Invertebrates. *ScienceAsia*. 33.
- Orrenius, S., B. Zhivotovsky, and P. Nicotera, 2003. Calcium: Regulation of cell death: the calcium–apoptosis link. *Nature reviews Molecular cell biology*. 4:552-565.

- Patil, K.S., I. Basak, R. Pal, H.-P. Ho, G. Alves, E.J. Chang, J.P. Larsen, and S.G. Møller. 2015. A proteomics approach to investigate miR-153-3p and miR-205-5p targets in neuroblastoma cells. *PLoS One*. 10:e0143969.
- Pfeffer, S., M. Zavolan, F.A. Grasser, M. Chien, J.J. Russo, J. Ju, B. John, A.J. Enright, D. Marks, C. Sander, and T. Tuschl. 2004. Identification of virus-encoded microRNAs. *Science*. 304:734-736.
- Pinton, P., D. Ferrari, P. Magalhães, K. Schulze-Osthoff, F. Di Virgilio, T. Pozzan, and R. Rizzuto. 2000. Reduced loading of intracellular Ca^{2+} stores and downregulation of capacitative Ca^{2+} influx in Bcl-2-overexpressing cells. *The Journal of Cell Biology*. 148:857-862.
- Ponprateep, S., S. Tharntada, K. Somboonwiwat, and A. Tassanakajon. 2012. Gene silencing reveals a crucial role for anti-lipoplysaccharide factors from *Penaeus monodon* in the protection against microbial infections. *Fish & Shellfish Immunology*. 32:26-34.
- Rabah, G., R. Popescu, J.A. Cox, Y. Engelborghs, and C.T. Craescu. 2005. Solution structure and internal dynamics of NSCP, a compact calcium-binding protein. *The FEBS Journal*. 272:2022-2036.
- Ramos-Carreño, S., R. Valencia-Yáñez, F. Correa-Sandoval, N. Ruíz-García, F. Díaz-Herrera, and I. Giffard-Mena. 2014. White spot syndrome virus (WSSV) infection in shrimp (*Litopenaeus vannamei*) exposed to low and high salinity. *Archives of Virology*. 159:2213-2222.
- Rolland, J.L., M. Abdelouahab, J. Dupont, F. Lefevre, E. Bachere, and B. Romestand. 2010. Stylicins, a new family of antimicrobial peptides from the Pacific blue shrimp *Litopenaeus stylirostris*. *Molecular Immunology*. 47:1269-1277.
- Ruan, L., X. Bian, Y. Ji, M. Li, F. Li, and X. Yan. 2011. Isolation and identification of novel microRNAs from *Marsupenaeus japonicus*. *Fish & shellfish immunology*. 31:334-

340.

- Scherp, P., G. Ku, L. Coleman, and I. Kheterpal. 2011. Gel-based and gel-free proteomic technologies. *In Adipose-Derived Stem Cells*. Springer. 163-190.
- Shi, Y.-Y., H.-J. Zheng, Q.-Z. Pan, Z.-L. Wang, and Z.-J. Zeng. 2015. Differentially expressed microRNAs between queen and worker larvae of the honey bee (*Apis mellifera*). *Apidologie*. 46:35-45.
- Shin, C., J.W. Nam, K.K. Farh, H.R. Chiang, A. Shkumatava, and D.P. Bartel. 2010. Expanding the microRNA targeting code: functional sites with centered pairing. *Molecular Cell*. 38:789-802.
- Shu, L., C. Li, and X. Zhang. 2016. The role of shrimp miR-965 in virus infection. *Fish & Shellfish Immunology*. 54:427-434.
- Shu, L., and X. Zhang. 2017. Shrimp miR-12 suppresses white spot syndrome virus infection by synchronously triggering antiviral phagocytosis and apoptosis pathways. *Frontiers in Immunology*. 8:855-897.
- Singh, C.P., J. Singh, and J. Nagaraju. 2012. A baculovirus-encoded microRNA (miRNA) suppresses its host miRNA biogenesis by regulating the exportin-5 cofactor Ran. *Journal of Virology*. 86:7867-7879.
- Singh, C.P., J. Singh, and J. Nagaraju. 2014. bmnvp-miR-3 facilitates BmNPV infection by modulating the expression of viral P6.9 and other late genes in *Bombyx mori*. *Insect Biochemistry and Molecular Biology*. 49:59-69.
- Skalsky, R.L., and B.R. Cullen. 2010. Viruses, microRNAs, and host interactions. *Annual review of microbiology*. 64:123-141.
- Sodeik, B. 2000. Mechanisms of viral transport in the cytoplasm. *Trends in Microbiology*. 8:465-472.
- Somboonwiwat, K., V. Chaikerasitak, H.C. Wang, C.F. Lo, and A. Tassanakajon. 2010. Proteomic analysis of differentially expressed proteins in *Penaeus monodon*

- hemocytes after *Vibrio harveyi* infection. *Proteome science*. 8:39-49.
- Sun, Y., and X. Zhang. 2019. Role of DCP1-DCP2 complex regulated by viral and host microRNAs in DNA virus infection. *Fish & shellfish immunology*. 92:21-30.
- Suwansa-Ard, S., W. Kankuan, T. Thongbuakaew, J. Saetan, N. Kornthong, T. Kruangkum, K. Khornchatri, S.F. Cummins, C. Isidoro, and P. Sobhon. 2016. Transcriptomic analysis of the autophagy machinery in crustaceans. *BMC Genomics*. 17:587-600.
- Takashi, T.K., K. 1984. Amino acid sequence of α chain of sarcoplasmic calcium binding protein obtained from shrimp tail muscle. *The Journal of Biochemistry*. 95:1603-1615.
- Tang, X., J. Wu, J. Sivaraman, and C.L. Hew. 2007. Crystal structures of major envelope proteins VP26 and VP28 from white spot syndrome virus shed light on their evolutionary relationship. *Journal of Virology*. 81:6709-6717.
- Tanji, T., and Y.T. Ip. 2005. Regulators of the Toll and Imd pathways in the *Drosophila* innate immune response. *Trends in Immunology*. 26:193-198.
- Tassanakajon, A., K. Somboonwiwat, P. Supungul, and S. Tang. 2013. Discovery of immune molecules and their crucial functions in shrimp immunity. *Fish & Shellfish Immunology*. 34:954-967.
- Thammasorn, T., P. Sangsuriya, W. Meemetta, S. Senapin, S. Jitrakorn, T. Rattanarojpong and V. Saksmerprome. 2015. Large-scale production and antiviral efficacy of multi-target double-stranded RNA for the prevention of white spot syndrome virus (WSSV) in shrimp. *BMC biotechnology*. 15:110-116.
- Tharntada, S., S. Ponprateep, K. Somboonwiwat, H. Liu, I. Soderhall, K. Soderhall, and A. Tassanakajon. 2009a. Role of anti-lipopolysaccharide factor from the black tiger shrimp, *Penaeus monodon*, in protection from white spot syndrome virus infection. *Journal of General Virology*. 90:1491-1498.
- Tharntada, S., S. Ponprateep, K. Somboonwiwat, H. Liu, I. Soderhall, K. Soderhall, and A.

- Tassanakajon. 2009b. Role of anti-lipopolysaccharide factor from the black tiger shrimp, *Penaeus monodon*, in protection from white spot syndrome virus infection. *J Gen Virol.* 90:1491-1498.
- Thitamadee, S., A. Prachumwat, J. Srisala, P. Jaroenlak, P.V. Salachan, K. Sritunyalucksana, T.W. Flegel, and O. Itsathitphaisarn. 2016. Review of current disease threats for cultivated penaeid shrimp in Asia. *Aquaculture.* 452:69-87.
- Thomson, D.W., C.P. Bracken, and G.J. Goodall. 2011. Experimental strategies for microRNA target identification. *Nucleic acids research.* 39:6845-6853.
- Tossi, A., and L. Sandri. 2002. Molecular diversity in gene-encoded, cationic antimicrobial polypeptides. *Current Pharmaceutical Design.* 8:743-761.
- Treiber, T., N. Treiber, and G. Meister. 2012. Regulation of microRNA biogenesis and function. *Thrombosis and Haemostasis.* 107:605-610.
- Tsai, J.M., H.C. Wang, J.H. Leu, A.H. Wang, Y. Zhuang, P.J. Walker, G.H. Kou, and C.F. Lo. 2006. Identification of the nucleocapsid, tegument, and envelope proteins of the shrimp white spot syndrome virus virion. *Journal of Virology.* 80:3021-3029.
- Umbach, J.L., and B.R. Cullen. 2009. The role of RNAi and microRNAs in animal virus replication and antiviral immunity. *Genes & development.* 23:1151-1164.
- van Hulten, M.C., J. Witteveldt, S. Peters, N. Kloosterboer, R. Tarchini, M. Fiers, H. Sandbrink, R.K. Lankhorst, and J.M. Vlak. 2001. The white spot syndrome virus DNA genome sequence. *Virology.* 286:7-22.
- Verma, A.K., S. Gupta, S.P. Singh, and N.S. Nagpure. 2017. An update on mechanism of entry of white spot syndrome virus into shrimps. *Fish & Shellfish Immunology.* 67:141-146.
- Wang, H.-C., A.-T. Lin, D.-M. Yii, Y.-S. Chang, G.-H. Kou, and C.-F. Lo. 2004. DNA microarrays of the white spot syndrome virus genome: genes expressed in the gills of infected shrimp. *Marine Biotechnology.* 6:S106-111.

- Wang, H.C., H.C. Wang, J.H. Leu, G.H. Kou, A.H. Wang, and C.F. Lo. 2007. Protein expression profiling of the shrimp cellular response to white spot syndrome virus infection. *Developmental & Comparative Immunology*. 31:672-686.
- Wang, L., B. Zhi, W. Wu, and X. Zhang. 2008. Requirement for shrimp caspase in apoptosis against virus infection. *Developmental & Comparative Immunology*. 32:706-715.
- Wang, P.H., Z.H. Gu, D.H. Wan, B.D. Liu, X.D. Huang, S.P. Weng, X.Q. Yu, and J.G. He. 2013. The shrimp IKK-NF-kappaB signaling pathway regulates antimicrobial peptide expression and may be subverted by white spot syndrome virus to facilitate viral gene expression. *Cellular & Molecular Immunology*. 10:423-436.
- Wang, P.H., T. Huang, X. Zhang, and J.G. He. 2014. Antiviral defense in shrimp: from innate immunity to viral infection. *Antiviral Research*. 108:129-141.
- Wang, X.W., and J.X. Wang. 2013. Pattern recognition receptors acting in innate immune system of shrimp against pathogen infections. *Fish & Shellfish Immunology*. 34:981-989.
- Waterhouse, P.M., M.-B. Wang, and E.J. Finnegan. 2001. Role of short RNAs in gene silencing. *Trends in Plant Science*. 6:297-301.
- Wongprasert, K., P. Sangsuriya, A. Phongdara, and S. Senapin. 2007. Cloning and characterization of a caspase gene from black tiger shrimp (*Penaeus monodon*)-infected with white spot syndrome virus (WSSV). *Journal of Biotechnology*. 131:9-19.
- Wongteerasupaya, C., P. Pungchai, B. Withyachumnarnkul, V. Boonsaeng, S. Panyim, T.W. Flegel, and P.J. Walker. 2003. High variation in repetitive DNA fragment length for white spot syndrome virus (WSSV) isolates in Thailand. *Diseases of Aquatic Organisms*. 54:253-257.
- Woramongkolchai, N., P. Supungul, and A. Tassanakajon. 2011. The possible role of

- penaeidin5 from the black tiger shrimp, *Penaeus monodon*, in protection against viral infection. *Developmental & Comparative Immunology*. 35:530-536.
- Wu, W., L. Wang, and X. Zhang. 2005. Identification of white spot syndrome virus (WSSV) envelope proteins involved in shrimp infection. *Virology*. 332:578-583.
- Xie, X., and F. Yang. 2005. Interaction of white spot syndrome virus VP26 protein with actin. *Virology*. 336:93-99.
- Xu, P., S.Y. Vernooy, M. Guo, and B.A. Hay. 2003. The *Drosophila* microRNA Mir-14 suppresses cell death and is required for normal fat metabolism. *Current Biology*. 13:790-795.
- Xue, S., W. Yang, and J. Sun. 2013. Role of chymotrypsin-like serine proteinase in white spot syndrome virus infection in *Fenneropenaeus chinensis*. *Fish & Shellfish Immunology*. 34:403-409.
- Yang, G., Y. Gong, Q. Wang, L. Wang, and X. Zhang. 2017. miR-100 antagonism triggers apoptosis by inhibiting ubiquitination-mediated p53 degradation. *Oncogene*. 36:1023-1037.
- Yang, L., S. Niu, J. Gao, H. Zuo, J. Yuan, S. Weng, J. He, and X. Xu. 2018. A single WAP domain (SWD)-containing protein with antiviral activity from Pacific white shrimp *Litopenaeus vannamei*. *Fish & Shellfish Immunology*. 73:167-174.
- Yun, C., and R. Dasgupta. 2014. Luciferase reporter assay in *Drosophila* and mammalian tissue culture cells. *Current Protocols in Chemical Biology*. 6:7-23.
- Zhan, S., J.J. Aweya, F. Wang, D. Yao, M. Zhong, J. Chen, and Y. Zhang. 2019. *Litopenaeus vannamei* attenuates white spot syndrome virus replication by specific antiviral peptides generated from hemocyanin. *Developmental & Comparative Immunology*. 91:50-61.
- Zhao, F., G. Xu, Y. Zhou, L. Wang, J. Xie, S. Ren, S. Liu, and Y. Zhu. 2014. MicroRNA-26b inhibits hepatitis B virus transcription and replication by targeting the host factor

- CHORDC1 protein. *Journal of Biological Chemistry*. 289:35029-35041.
- Zhou, Y., T.K. Frey, and J.J. Yang. 2009. Viral calciomics: interplays between Ca²⁺ and virus. *Cell Calcium*. 46:1-17.
- Zhou, Y., Y. Liu, H. Yan, Y. Li, H. Zhang, J. Xu, S. Puthiyakunnon, and X. Chen. 2014. miR-281, an abundant midgut-specific miRNA of the vector mosquito *Aedes albopictus* enhances dengue virus replication. *Parasit Vectors*. 7:488-458.
- Zhu, F., Z. Wang, and B.-Z. Sun. 2016. Differential expression of microRNAs in shrimp *Marsupenaeus japonicus* in response to *Vibrio alginolyticus* infection. *Developmental & Comparative Immunology*. 55:76-79.
- Zhu, L., Y.H. Chang, J. Xing, X.Q. Tang, X.Z. Sheng, and W.B. Zhan. 2018a. Comparative proteomic analysis between two haemocyte subpopulations in shrimp *Fenneropenaeus chinensis*. *Fish & Shellfish Immunology*. 72:325-333.
- Zhu, L., X. Tang, J. Xing, X. Sheng, and W. Zhan. 2018b. Differential proteome of haemocyte subpopulations responded to white spot syndrome virus infection in Chinese shrimp *Fenneropenaeus chinensis*. *Developmental & Comparative Immunology*. 84:82-93.

VITA

NAME Nichaphat Kanoksinwuttipong

DATE OF BIRTH 6 Dec 1992

PLACE OF BIRTH Bangkok

HOME ADDRESS 2/187 Baan Klang Muang The Paris Rama 9 Ramkamhaeng, Krungthep Kreetha 7, Huamark, Bangkok, 10240

PUBLICATION Kanoksinwuttipong, N., Wongdontri, C., Somboonwiwat, K., Expression analysis of miRNAs involved in pathogen challenge in shrimp. The 22nd Biological Sciences Graduate Congress (BSGC2017). 19-21 December 2017, National University of Singapore, Singapore (Poster presentation).

Kanoksinwuttipong, N., Somboonwiwat, K., Functional characterization of a pathogen responsive microRNA in black tiger shrimp *Penaeus monodon*. The 44th Congress on Science and Technology of Thailand (STT44). 29-31 October 2018, Bangkok International Trade & Exhibition Centre (BITEC), Thailand (Proceeding).